Role of Aqp1, Sm51 and GATA6 in Differentiation and Migration of Bone Marrow Derived Mesenchymal Stem Cells

MENG, Fanbiao

A Thesis Submitted in Partial fulfillments

of the requirements for the Degree of

Doctor of Philosophy

in

Orthopaedics and Traumatology

The Chinese University of Hong Kong

July 2013

Declaration

I hereby declare that the work within the thesis is completed by myself from September 2010 to July 2013 in the Department of Orthopaedics and Trauma of the Chinese University of Hong Kong.

MENG, Fanbiao

Acknowledgements

I would like to sincerely thank

Professor Gang Li for his constructive supervision and offering me as much help as possible to let me overcome the difficulties encountered in the whole study period.

Doctor Liangliang Xu for his kind help in plasmids construction and transfection methods and advices on the project.

Mr Shuang Huang for the technical support on establishment of femoral fracture model and mechanical testing.

Mr Jimmy Cheung for his time, his patience and readily available for lab instructions.

Doctor Wayne Lee for the technical support of blood collection from rat.

Doctor Yunfeng Rui for the technical support on on establishment of tibial fracture model.

Ms Yang Liu for the patient guidance on micro-CT analysis.

Abstract

Role of Aqp1, Sm51 and GATA6 in differentiation and migration of bone marrow derived mesenchymal stem cells

Introduction: Bone marrow derived mesenchymal stem cells (BM-MSCs) have high migration and multiple differentiation potentials. Enhanced migration and osteogenic ability of BM-MSCs may be beneficial for promoting bone formation. Our laboratory once compared rat BM-MSCs and rat peripheral blood derived MSCs (PB-MSCs) by microarray and found many differential genes, Aquaporin 1 (Aqp1), small nuclear ribonucleoprotein polypeptide N clone sm51 (Sm51) and GATA-binding factor 6 (GATA6), were differentially expressed in the PB-MSCs. The precise roles of Aqp1, Sm51 and GATA6 in MSCs have not been studied clearly yet. Given that their high differential expression in PB-MSCs, we hypothesize that manipulating expression level of Aqp1, Sm51 and GATA6 will be beneficial for migration and differentiation of MSCs.

Methods: Aqp1, Sm51 and GATA6 overexpressing and knocking down stable MSCs cell lines were established by lentiviral transfection. The migration ability of Aqp1 modified MSCs were assessed through transwell and wound healing assays *in vitro* and administrated systemically in rats with experimental tibial fracture in *vivo*. Aqp1 overexpressing rat were then administrated into femora fracture rat intracardiaclly, and the outcome of bone healing were assessed by mechanical testing and micro-CT. The osteogenic potentials of rat Sm51 and GATA6 modified MSCs were assessed using standard osteogenic induction assays in vitro and ectopic bone formation by implanting into nude mouse with HA/TCP scaffolds *in vivo*.

Results: Knocking down Aqp1 had no effects on osteogenesis, adipogenesis, chondrogenesis and proliferation of MSCs. Overexpression of Aqp1 promoted MSCs migration, while knocking down Aqp1 impaired MSCs migration *in vitro*. Higher numbers of GFP-MSCs were found at the

fracture site in the Aqp1-MSCs treated group compared to the DsRed-MSCs group. The level of beta-catenin and focal adhesion kinase (FAK) increased in the Aqp1-MSCs, and decreased in the Aqp1 knocking down MSCs. Beta-catenin and FAK were co-immunoprecipitated with Aqp1, and the co-localization of FAK and Aqp1 was confirmed by confocal images.

Administration of Aqp1 overexpressing MSCs enhanced the outcome of bone fracture healing in terms of bone stiffness and bone density, while the structure and morphology of callus had no significant difference when compared to DsRed-MSCs group.

Overexpression of Sm51 accelerated osteogenic differentiation of MSCs by enhancing the bone mineralization rate and alkaline phosphatase (ALP) activities. Ectopic bone formation data showed Sm51-MSCs induced more osteoid bone formation than that of DsRed-MSCs control. The expressions of osteogenic markers such as Runx2, Osteocalcin (OCN), Osteopontin (OPN), alkaline phosphatase (ALP), type I collagen increased after overexpressing Sm51 with or without osteogenic induction on mRNA level. In addition, we proved that Sm51 up-regulated expression of Runx2 on protein level, and Sm51 bound to Runx2 RNA precursor directly and specifically, no bounding was seen with other osteogenic genes such as OCN, OPN; adipogenic gene like peroxisome proliferator-activated receptors gamma (PPARγ) and CCAAT-enhancer-binding proteins (C/EBPs). Finally, knockdown of Runx2 abolished Sm51 effects on osteogenesis of MSCs.

Overexpression of GATA6 enhanced the mineralization of osteogenic differentiation of rat and human BM-MSCs. Depletion of GATA6 in human BM-MSCs led to the reduction of Runx2. In addition, GATA6 was capable of interacting with Runx2 physically demonstrated by co-immunoprecipitation.

Conclusions: The studies demonstrate that Aqp1 enhances MSCs migration ability by affecting expression of beta-catenin and FAK. Aqp1 empowers MSCs move faster to reach the fracture site, which contributes to the better healing outcome. Sm51 promotes osteogenic differentiation of MSCs by modulate the splicing of Runx2, while GATA6 enhances osteogenic differentiation of MSCs by interaction with Runx2.

摘要

Aqp1, Sm51 和 GATA6 在骨髓干细胞分化与迁移中的作用

引言：骨髓间充质干细胞 (BM-MSCs) 具有高的迁移与多向分化的潜力。提高 BM-MSCs 的迁移与成骨分化能力有益于促进骨的形成。通过芯片技术，我们实验室鉴别出外周血间充质干细胞(PB-MSCs)与 BM-MSCs 的差异表达基因：水通道蛋白 1 (Aqp1), 小核糖蛋白多肽 N 克隆 Sm51 (Sm51)和 GATA 结合蛋白 6 (GATA6). Aqp1, Sm51 and GATA6 在 MSCs 中的功能尚不清楚。考虑到它们在 PB-MSCs 高的差异性表达， 我们假设改变 Aqp1,Sm51 和 GATA6 的表达水平有益于 MSCs 的分化与迁移。

方法：使用慢病毒建立 Aqp1, Sm51 and GATA6 过表达与沉默的稳定的 MSCs 细胞系。Aqp1 的迁移能力在体外通过 transwell 和损伤修复实验进行检测，通过系统移植到大鼠胫骨骨折模型检测体内迁移能力。Aqp1 过表达的 MSCs 移植到股骨骨折的大鼠体内，并用力学仪器与 mico-CT 检测骨折愈合情况。使用标准的成骨分化方法检测在体外转染 Sm51 和 GATA6 后 MSCs 的成骨分化能力，通过与 HA/TCP 联合种植裸鼠检测体内异位成骨能力。

结果：沉默 Aqp1 的表达不影响 MSCs 的成骨，成脂，成软骨和增殖能力。在体外过表达 Aqp1 促进 MSCs 的迁移，而沉默 Aqp1 降低了 MSCs 的迁移。在骨折部位的 Aqp1-MSCs 数量显著比 DsRed-MSCs 多。Beta-catenin 与 focal adhesion kinase (FAK)的水平在体外过表达 Aqp1 的 MSCs 升高，而在沉默 Aqp1 的 MSCs 降低。Beta-catenin 与 FAK 可与 Aqp1 共沉淀，而共聚焦技术显示 FAK 与 Aqp1 共定位。

移植过表达 Aqp1 过表达的 MSCs 增强骨折愈合后骨的韧性和骨密度，但骨痂的形态与结构与对照组比没有区别。

过表达 Sm51 通过提高骨钙化速率与碱性磷酸酶活性促进的成骨分化。Sm51-MSCs 比 DsRed-MSCs 具有显著高的异位成骨能力。无论有没有成骨诱导，过表达 Sm51 后 MSCs 的成骨分化的标记物 Runx2, Osteocalcin (OCN), Osteopontin (OPN), alkaline phosphatase (ALP), type I collagen 的 mRNA 水平上调。同时，我们证明在蛋白水平 Sm51 上调 Runx2 表达，并且 Sm51 能特异的直接结合 Runx2 的 RNA 前体，而不是其它的成骨基因像 OCN, OPN， 或是成脂的基因例如 peroxisome proliferator-activated receptors gamma (PPARγ) and CCAAT-enhancer-binding proteins (C/EBPs)。最后，沉默 Runx2 后抵消了 Sm51 在 MSCs 成骨分化中的作用。

过表达 GATA6 增强了大鼠与人的 MSCs 钙化速率。沉默 GATA6 导致 Runx2 表达水平下降。更进一步，通过共沉淀检测 GATA6 能够与 Runx2 结合。

结论：这项研究表明 Aqp1 通过影响 beta-catenin 与 FAK MSCs 的表达来提高的迁移能力。Aqp1 使得 MSCs 更快到达骨折位点并增强骨折的愈合。Sm51 通过调节 Runx2 的剪切提高 MSCs 的分化，而 GATA6 通过结合 Runx2 来提高 MSCs 的分化。

Abbreviation

ALP	alkaline phosphatase
α-MEM	MEM alpha medium
Aqp1	aquaporin 1
BMD	bone density
BM-MSCs	bone marrow mesenchymal stem cells
BV	total bone volume
CD	cell differentiation
C/EBPs	CCAAT-enhancer-binding proteins
CFU-Fs	colony-forming units-fibroblastic
Co-IP	co-immunoprecipitation
DMEM	dulbecco's modified eagle medium
ES	embryonic stem cells
FAK	focal adhesion kinase
FITC	fluorescein isothiocyanate
GATA6	GATA-binding factor 6
GM-CSF	granulocyte monocyte colony stimulating factor
iPS	induced pluripotential stem cells
OCN	osteocalcin
OPN	osteopontin
OVX	ovariectomised
PB-MSCs	peripheral blood mesenchymal stem cells
PE	phycoerithrine
PPARγ	peroxisome proliferator-activated receptors gamma
PWS	prader willi syndrome

RIPA	radio-immunoprecipitation assay
Runx2	runt-related transcription factor 2
SD	sprague dawley
SmB/B’	small nuclear ribonucleoprotein-associated polypeptide B/B’
Sm51	small nuclear ribonucleoprotein polypeptide N clone sm51
TV	total tissue volume

Contents

Chapter 1

Introduction

Stem cells known for couple of decades, even for non-academic people, are magic for their high proliferation, multiple differentiation potential and self-renewal capacity. Based on the cell origin, stem cells are categorized into embryonic stem cells (ES), induced pluripotential stem cells (iPS) and adult stem cells. Using stem cells for replacement of damage tissues or organs, exciting as it is, captivate so many biomedical researchers for so many years study. Due to the pluripotency, ES cells as well as iPS can be induced into all cell types (Drews et al., 2012; Ho et al., 2012). However, some disadvantages of ES or iPS cells, such as malignant transformation and low differentiation ratio limit their application in regeneration medicine. In contrast, adult stem cells, though limited differentiation potential, are much safer and useful for application.

Hence, rather than cover all of the work in this field, here we mainly tell a story of one type of adult stem cells─mesenchymal stem cells from peripheral blood and bone marrow.

1.1 The origin and biology character of PB-MSCs

Mesenchymal stem cells (MSCs), first known as colony-forming units-fibroblastic (CFU-F), were isolated from bone marrow by Friedenstein and colleagues in 1980s (Friedenstein et al., 1976). In their study, adherent spindle shaped cells appeared as colonies after discarding the nonadherent cells, most of hematopoietic cells, in plastic dishes after 4 days, and began to replicate rapidly after short quiescent period. The cells could then differentiated into osteoblast like cells with small deposit of bone or cartilage. Following this study, many laboratories further demonstrated these multiple differentiation potentials into connective tissue of these osteogenic cells at a clonal level (Dennis et al., 1999), providing an evidence of concept of a mesenchymal stem cell (Caplan, 1994). Apart of bone marrow origin, MSCs or MSC-like cells isolated from skeletal muscle (Williams et al., 1999), adipose tissue (Zuk et al., 2001), umbilical cord (Erices et al., 2000), and amniotic fluid (in `t Anker et al., 2003) as well as fetal blood and

lung(Campagnoli et al., 2001; Fan et al.). The varied tissue sources and methodologies of cell preparation raise the question of whether the reported MSCs were similar for direct comparison of biological properties and experimental data from different labs, especially in the context of cell therapy. In order to address this, the Mesenchymal and Tissue Stem Cell Committee of the ISCT proposed an minimal standards to identify human MSC, which were listed in table 1(Dominici et al., 2006).

1 Adherence to plastic in standard culture conditions		
2 Phenotype	Positive (>95%.)	Negative (<2%)
	CD105	CD45
	CD73	CD34
	CD90	CD14 or CD11b
		CD79a or CD19
		HLA-DR
3 In vitro differentiation: osteoblasts, adipocytes, chondroblasts		
(demonstrated by staining of *in vitro* cell culture)		

Table 1.1. Summary of criteria to identify MSC

Adopted from *Dominici et al Cytotherapy (2006) 8, 315-317*

1.1.1 Definition of PB-MSCs

Besides the sources mentioned above, MSCs are successfully isolated from peripheral blood and possessed similar biological characters with other tissues derived MSCs. PB-MSCs, the concept proposed by He in recent years (He et al., 2007), were initially referred as PB CFU-F, the fibroblast-like cells transformed from blood leukocytes(Stirling and Kakkar, 1969). Moreover, blood-borne fibroblast like cells are not a contamination of connective tissue fragment when obtained by the cardiac route, as number of the fibroblastic colonies have no change regardless of how many times of heart punctures are performed(Luria et al., 1971). However, the efficiency of successful culture of PB-MSCs is low, negative results are also reported. Wexler and colleagues were unable to isolate MSC from the peripheral blood of healthy individuals. This was determined by characterization of hematopoietic surface markers on the isolated cell population (CD45 and CD14) and their non-mesenchymal phenotype(Wexler et al., 2003). In the contrast, Zvaifler and colleagues found that non-mobilized human blood possessed mesenchymal potential irrespective of the elimination of CD34, CD3 or CD14 cells. It has also been proposed that circulating mesenchymal precursors may be present in pathological conditions. Fernandez isolated stromal cells from the blood of breast cancer patients given granulocyte monocyte colony stimulating factor (GM-CSF) following chemotherapy. In other independent studies, PB CFU-Fs were also defined as “circulating skeletal stem cells” or “Circulating Osteoblast-Lineage Cells” (Eghbali-Fatourechi et al., 2005; Kuznetsov et al., 2001), because of their osteogenic potential. Based on the biology character in regard of morphology and multipotent differentiation potential, described in detail in next section, PB CFU-Fs are recently substituted by PB-MSCs, which is adopted in this project.

1.1.2 Biological character of PB-MSCs

In morphology, PB-MSCs, similar with BM-MSCs, have plastic adherence property with spindle fibroblast like shape. From whole blood from mice, guinea pigs, and rabbits, Kuznetsov and his colleague isolated clonogenic adherent cells, though varied in colony forming efficiency, which were similar among species and from different individual donors. The majority of the colonies contained cells with fibroblastic morphology, while some of colonies were consisted of cells with a distinctive polygonal shape. According to the criteria of MSCs mentioned above, a panel of cell surface markers was detected. The expression of hematopoietic (CD45, CD14), endothelial (endoglin, CD34, Factor VIII–related antigen, Muc-18, PAL-E, EN4) markers was low, but the expression of osteogenic makers (OPN), collagen types I and III, fibronectin, osteonectin, α-smooth muscle actin, CD44, VCAM-1, and the β1 integrin subunit was consistent from various sources (Kuznetsov et al., 2001). Similar approach on human blood also detected circulating osteoblast lineage cells, positive for osteocalcin and bone alkaline phosphatase, which adhered plastic dishes after sorting. The notable point proposed in this study is that it provides clear evidence that osteoblast-lineage cells are present in the human circulation in significant numbers, and that the percentage of circulating osteocalcin-positive cells is higher during the adolescent growth spurt, which is associated with a marked stimulation of bone formation, than in adulthood(Eghbali-Fatourechi et al., 2005). In another study, plastic adherent MSCs, positive for CD73, CD105, CD90 and negative for CD45 and CD14, were found in peripheral blood from 22% of hip fracture patients, 46% of younger fracture patient(Alm et al., 2010). Taken together, circulating PB-MSCs, though isolated by various methods, is stringent consistent with the first two criteria.

The trilineage differentiation potential is critical for PB-MSCs, as one of adult stem cells, to generate different cell types for clinical application. The osteogenic potential of PB-MSCs was

intensively studied on various species including normal human individual and fracture patients. Using similar osteogenic differentiation protocol of BM-MSCs, PB-MSCs also could be induced to differentiate with positive staining for ALP and calcium deposits in vitro. When implanted with a ceramic based carrier in subcutaneous mouse, PB-MSCs were able to form bone. Besides of osteogenic potential, PB-MSCs are also capable of acquiring an adipogenic phenotype with lipid accumulation when cultured in rabbit serum (Khosla and Eghbali-Fatourechi, 2006) or well-established adipogenic medium with 0.5mM methyl-isobutylxanthine, 10 μg/ml insulin, 100mM indomethacin, and 1 μM dexamethasone. In regard to chondrogenic differentiation, similar with BM-MSCs, PB-MSCs was induced into chondrocyte like cells with expression of cartilage glycosaminoglycans in chondrogenic medium with low-glucose DMEM containing 1 mM dexamethasone, 1 mM sodium pyruvate, 1×insulin-transferrin-selenium, 17 mM ascorbic acid, 35 mM proline, and 10 ng/ml transforming growth factor β1 (Raghunath et al., 2010; Rochefort et al., 2006).

1.1.3 Relationship of BM-MSCs and PB-MSCs

Given their similar morphology, proliferation character and differentiation potential, there are some links between BM-MSCs and PB-MSCs. In bone marrow, hematopoietic stem cells (HSCs), responsible for blood production in vivo, co-localize with BM-MSCs, and their interaction conducted by β_1-integrin was shown to be crucial for the interaction of HSCs within the bone marrow microenvironment(Gottschling et al., 2007). Moreover, spindle-shaped N-cadherin$^+$ CD45$^-$osteoblastic (SNO) cells, lining the bone surface, attached to long-term HSCs, providing a specific niche for HSCs(Zhang et al., 2003). As HSCs can be mobilized from endosteal osteoblastic niche in bone marrow to peripheral blood by stimulation factors like granulocyte colony-stimulating factor (G-CSF), it is reasonable to speculate that such

mobilization is applicable for BM-MSCs, which implying PB-MSCs may be derived from BM-MSCs. To examine this, Li and colleagues found that fluorescently labeled MSCs administrated into a remote tibia bone marrow cavity 48 h after the osteotomy was found in the callus tissues, between Groups C and A, indicating the labeled bone marrow cells were capable of migrating to the fracture sites from the remote bone marrow cavity (Shirley et al., 2005). This investigation supports the hypothesis that some osteoblasts involved in fracture healing were systemically mobilized and recruited to the fracture from remote bone marrow sites. Although it is hard to identify exactly what factors triggered this mobilization, some inflammation factors in fracture, cancer or hip arthroplasty was reported to be involved in this process. In addition, Rochefort and colleagues found PB-MSC dramatically increased (by almost 15-fold) when animals are exposed to chronic hypoxia (Rochefort et al., 2006). The BM-MSCs could be exported to the circulation, thus became PB-MSCs, by means of sinusoids adjacent to the bone trabeculae. The number of PB-MSCs increased during pubertal growth, which further demonstrated the special interaction of bone modeling activity and PB-MSCs. Although PB-MSCs and BM-MSCs were similar with each other in most respects, there were still some difference like small population of CD34 (range 7.9–14.3%) among PB-MSCs(Alm et al., 2010).

1.2 Osteogenesis and fracture

MSCs, no matter from bone marrow or peripheral blood, are capable to be induced to osteogenesis, adipogenesis, chondrogenesis, *et al*. Some studies showed that MSCs could transdifferentiate into neural cells and epithelial cells in kidney or lung. However, the differentiation efficiency was low, and the results were confused and controversial (Lu et al., 2004; Ortiz et al., 2003). Because of its mesoderm origin, it is much easier to induce MSCs into osteoblast and adipocyte, even spontaneously in some time, both in cell culture or ectopic bone

formation. In native circumstance, MSCs from bone marrow was destined to differentiation into osteoblast, which contributes to bone formation. Dysfunction of differentiation of MSCs, such as differentiation into adipocyte, at some point leads to rapid bone loss in osteoporosis patients.

1.2.1 Osteogenesis

The osteogenesis of MSCs induced by cocktail factors like dexamethasone, ascorbic acid and β-glycerophosphate is easy to perform *in vitro*, while it is regulated by lots of extracellular signals and intracellular factors *in vivo*. In this section, we briefly introduce an overview of regulation of osteogenesis of MSCs.

MSCs differentiate into preosteoblasts, then to mature osteoblasts, the block of bone, via either intramembranous ossification for certain parts of the skull or endochondral ossification for rest of the skeleton. The differentiation of osteoblast from MSCs requires the coordination of a bunch of transcription factors. Each or combined transcription factor represent specific differentiation stage of MSCs (Figure 1.1)(Long, 2012).

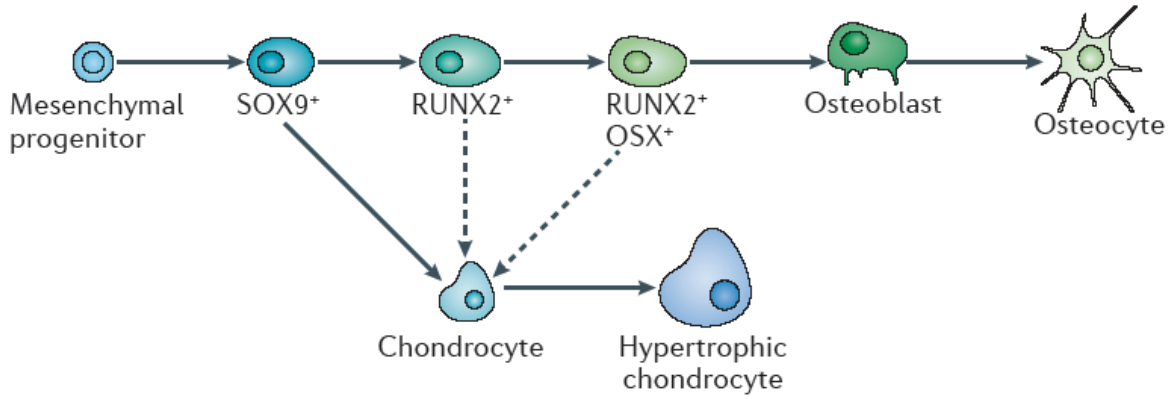

Figure 1.1 The different stages of osteoblast lineage cell differentiation

Adopted from *Long, F Nat Rev Mol Cell Biol (2012)13, 27-38.*

The master transcription factor in osteogenesis is Runx2, loss of which in the mouse results in absence of a mineralized skeleton and perinatal lethality. As a runt domain transcription factor, Runx2 expression occurs at an early stage of developing embryo by E9.5 prior to bone formation (Romero-Prado et al., 2006). Mutation of Runx2 in mice had a defect in intramembranous ossification that resembles cleidocranial dysplasia in humans(Otto et al., 1997). Located near nuclear matrix, Runx2 is an organizing hub for gene expression, integrating with exracelluar signals like parathyroid hormone (PTH), BMP/transforming growth factor-β (TGFβ), FGF/EGF, Hedgehog, Notch, Wnt and co-activators like TAZ, p300 CBP, MOZ(Schroeder et al., 2005). Target genes of Runx2 in osteogenesis includes but not limited Osteocalcin (OC), TGF-b receptor-1 (TGFb R1), human vitamin D receptor (hVDR), estrogen receptor α,collagenase 3, prolactin, collagen, osteopontin (OPN), bone sialo protein (BSP), alkaline phosphatase (ALP), osteoprotegrin (OPG), RANKL, C/EBP, Runx2, dentin sialo protein (DSP), Galectin-3,*et al*(Stein et al., 2004). Downstream of Runx2 in osteoblast differentiation is another transcription factor OSX, containing three C2H2-type zinc-fingers, which was discovered as a BMP-induced gene in C2C12 cells (Nakashima et al., 2002). In contrast to RUNX2 deletion, loss of Osx results in ectopic cartilage formation beneath a thickened perichondrium at the diaphysis (where a bone collar normally forms), presumably owing to a fate switch of progenitors to chondrocytes instead of osteoblasts. Several factors regulate osteoblast differentiation through Osx, such as p53 (Wang et al., 2006) and NFATC1 (nuclear factor of activated T cells, cytoplasmic 1), a calcium-sensitive transcription factor that stimulates osteoblast differentiation by enhancing OSX transcriptional activity(Koga et al., 2005). Besides of the above transcription factors, some other nuclear factors involved in regulation of osteoblast differentiation was demonstrated to interact

with Runx2, including MAF(Nishikawa et al., 2010), SATB2(Dobreva et al., 2006), MSX2(Satokata et al., 2000), Twist(Bialek et al., 2004), STAT1(Kim et al., 2003b), Schnurri 3(Jones et al., 2006) and so on.

Besides transcription factors in regulation of osteoblast differentiation, signal pathways are involved in this process. Hedgehog (HH) proteins, one of the developmental signals, binds to the receptor Patched homologue 1 (Ptch1) through the seven-pass transmembrane protein Smoothened (Smo) to regulate gene transcription through both derepression and activation of the GLI family of transcription factors(Oury et al., 2011). Mice deficient in IHH completely lack of osteoblast in endochondral ossification process(St-Jacques et al., 1999), as the perichondrial progenitors failed to express Runx2,discussed above, which is the master gene in osteogenesis. However, the role of IHH in osteoblast differentiation during postnatal in life is still poor understood.

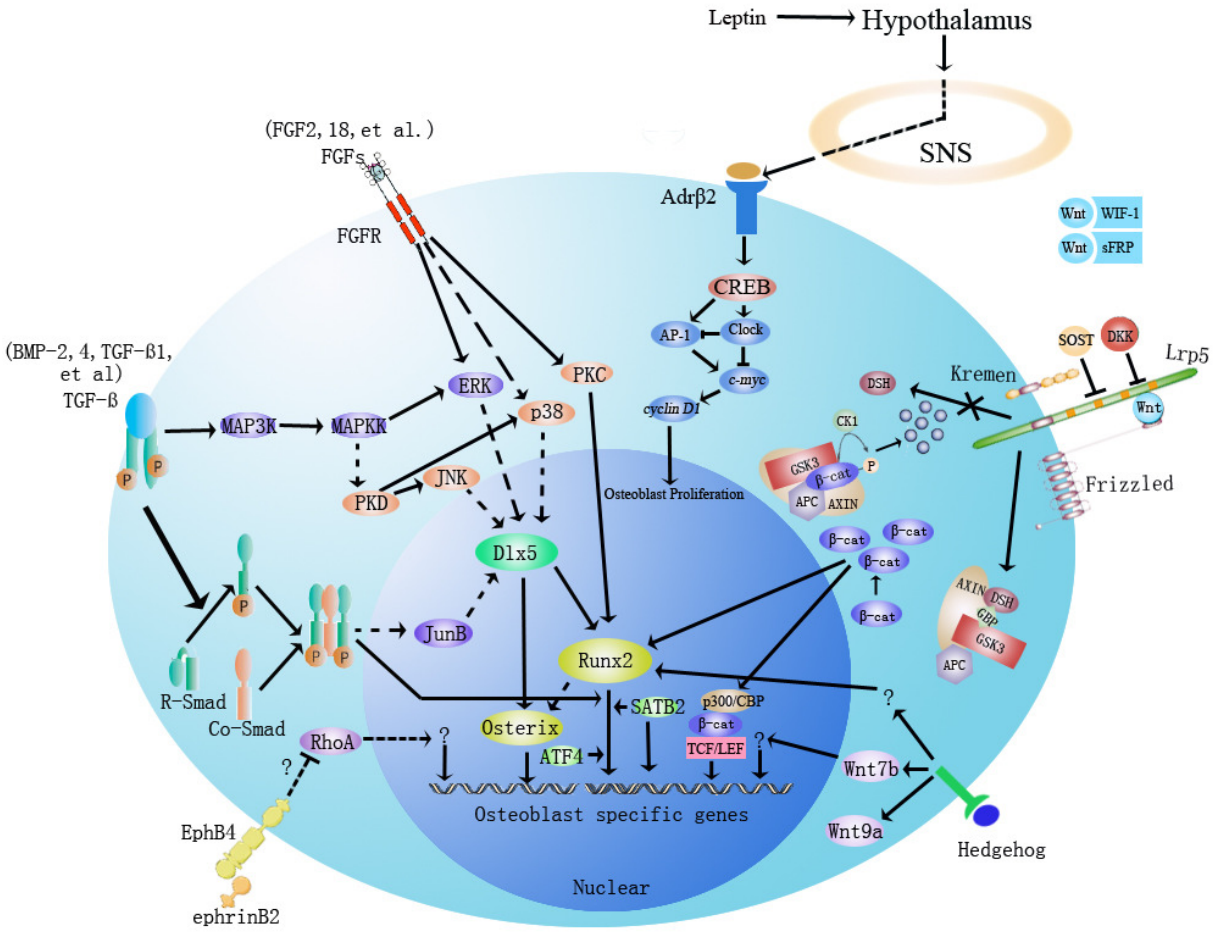

Figure 1.2 Role of Runx2 in signaling pathway network of osteogenesis

Adopted from *Huang W et al Front Biosci. 2007 May 1;12:3068-92.*

Another pathway in osteoblast differentiation is Wnt signaling, which is further categorized into dependent or independent on β−catenin. In β‑catenin-dependent WNT signaling, Wnt binds to Frizzled receptors and their co-receptors low-density lipoprotein receptor-related protein 5 (LRP5) or LRP6 to stabilize cytosolic β−catenin. β−catenin then enters the nucleus and stimulates the transcription of Wnt target genes by interacting with lymphoid enhancer-binding factor 1 (LEF1), T cell factor 1 (TCF1), TCF3 and TCF4. Genetic mutation of Wnt co-receptor

LRP5 caused osteoporosis pseudoglioma syndrome (Gong et al., 2001), a form of juvenile-onset osteoporosis. Furthermore, in mice, mutation of Lrp5 or Wnt10b reduced bone mass postnatally, and Lrp6 haploinsufficiency further decreases bone mass in LRP5−null mice(Holmen et al., 2004). Further studies proposed that Lrp5 had an effect on bone mass postnatally rather than in embryo. In contrast, genetic deletion of β−catenin in embryonic mesenchymal progenitors abolishes mature osteoblast generation. Specifically, β−catenin is required for the progression from the $Runx2^{+}$ stage to the $Runx2^{+}Osx^{+}$ stage and from $Runx2^{+}Osx^{+}$ cells to mature osteoblasts (Figure 1.1)(Hu et al., 2005). Nevertheless, β−catenin independent Wnt pathway was also found to exert a role in osteoblast differentiation. For instance, deletion of Frizzled 9 decreased bone mass in part through downregulation of Isg15, a ubiquitin-like protein modifier, without obvious effects on β−catenin signaling (Albers et al., 2011).

Bone morphogenetic proteins (BMPs), multifunctional growth factors within the transforming growth factor b (TGF-b) super family, possess a wide range of biological roles. First identified by their ability to initiate ectopic bone formation in adult animals(Wozney et al., 1988), BMPs is used for standard practice in spine fusion surgeries and tibial fracture healing. Like other TGF-b superfamily members, BMPs bind to two major types of membrane-bound serine/threonine kinase receptors, the type-I and type-II receptors(Massagué, 1998). Activated type I BMP receptors propagate BMP signals by phosphorylating BMP-specific R-Smads 1, 5 and 8. These R-Smads complex with Smad4, translocate into the nucleus and act as activators and repressors of transcription of osteogenic genes. Depletion of BMP2 in limb mesenchyme formed bone during embryogenesis exhibited a clear defect in bone mineral density shortly after birth, resulting in frequent fractures that failed to heal(Tsuji et al., 2006). On a molecular level, skeletal

progenitor cells from mice lacking BMP2 have reduced levels of osterix, Wnt1, Lrp5, Fzd1, Axin1 and Axin 2 (Figure 1.2).

1.2.2 Structure of Runx2

Due to the indispensable role in osteogenesis, Runx2 is studied intensively in gene structure, posttranslational modification and location. Another Runt domain containing family member Runx1 and Runx3, responsible for hematopoiesis and neurogenesis respectively, have similar gene structure with Runx2. They all are regulated by two separate promotors P2 (proximal) that is embedded in particular abundant CpG island (Bangsow et al., 2001), and P1 (distal) without no obvious CpG island (Figure 1.2) (Ghozi et al., 1996; Levanon et al., 2001). The bio-promotor systems of Runx genes reflects various alternative mRNA splicing isoforms are expressed in diverse cell types in different development stages.

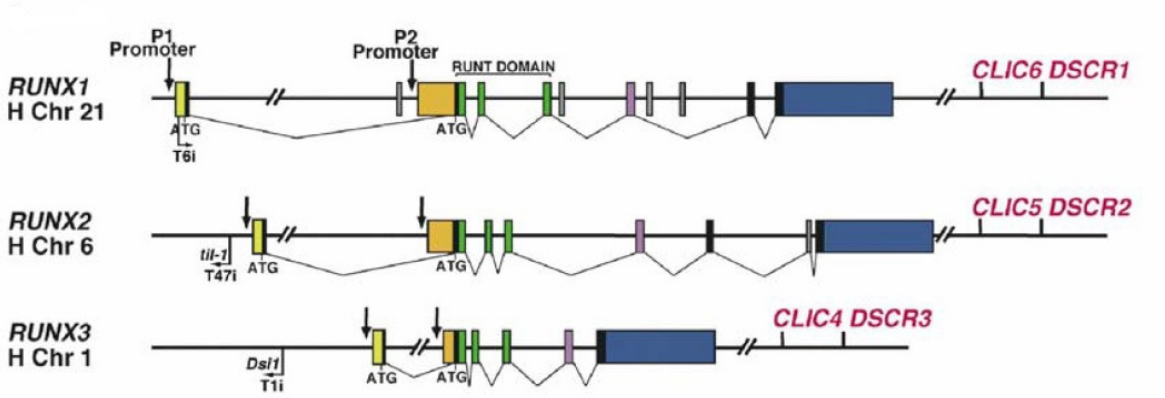

Figure 1.3 Gene structure and elements of Runx

Adopted from *Levanon et al Oncogene (2004) 23, 4211–4219*

Several in vivo functional studies of P1 promoter of Runx2, spanning from nucleotides -92 to -78, unraveled some responsive elements in this region, including vitamin D response element (VDRE) (Drissi et al., 2000), selective estrogen receptor modulators (SERMS) (Tou et al., 2001) and binding sites for NF1 and AP1(Zambotti et al., 2002). Both the P1 and P2 promoters have Runx binding sites, indicating the auto-regulation of Runx. Hypomethylation of the promoters of Runx2 was observed in chondrogenesis and adipogenesis(Ezura et al., 2009). The hypomethylation level of Runx2 did not change during osteogenesis (Kang et al., 2007).

The Runx2 gene is consisted with 8 exons and give rise to various isoforms by alternative splicing process, two of which such as type I isoform, type II isoform are mainly expressed at different levels in osteoprogenitor. There are several functional domain reside in Runx2 sequences, for instance, runt domain which has 128-amino acid and binds conserved DNA sequences 5'-PuACCPuCA-3' (Kamachi et al., 1990). Elements for Runx2 location in nuclear include the nuclear localization signal (NLS), a short nine amino acids, and the nuclear matrix targeting signal (NMTS), a 31 amino acids near the carboxy terminus of Runx2(Kanno et al., 1998). They are both required for precise distribution of Runx2 and normal function of runx2 by combining multiple partners as a regulating hub in osteogenic gene expression.

1.2.3 Bone fracture healing and stem cells therapy

Bone fracture is a prevalent disease, and the healing is a unique repair process in which the events of endochondral and intramembranous bone formation follow a specific time sequence. Normally, fracture healing is complex process involved with many cell types cortical bone, the periosteum, undifferentiated fascial tissue surrounding the fracture, and the bone marrow itself, which are constituted with four stages: inflammation, soft callus (fibrocartilage) formation, hard

callus formation and bone remodeling(Schindeler et al., 2008). In inflammation stage, first 7 to 10 days after fracture in rat, macrophages, and other inflammatory cells (granulocytes, lymphocytes, and monocytes) infiltrate the hematoma between the fractured fragments and combat infection, secrete cytokines and growth factors, and advance clotting into a fibrinous thrombus(Gerstenfeld et al., 2003). Next stage is soft callus (fibrocartilage) formation, properly around 14 days after fracture in rat, which is characterized by chondrocytes and fibroblasts, albeit with various relative proportions between fractures. The third stage is hard callus formation, day 21 in rat or about 4 or 5 weeks in a human, which becomes a target for chondroclasts, multinucleated cells specialized in the resorption of calcified tissues. The last bone remodeling stage, approximately 28 to 35 days in rat or about 6 to 7 weeks in the patient, encompasses the remodeling of the woven bone hard callus into the original intact trabecular bone structure. Regulation of fracture healing process in signaling factors can be categorized into the pro-inflammatory cytokines, the transforming growth factor-beta (TGF-β) superfamily and other growth factors, and the angiogenic factors. Inflammatory factors secreted by macrophage or cell of mesenchymal origin in the first stage of fracture healing process include interleukin-1 (IL-1) and interleukin-6 (IL-6) as well as tumour necrosis factor-alpha (TNF-α), which play roles in initiating the repair cascade. Other growth and differentiation factors including BMP2 and other TGF-β superfamily factors for intramembranous and endochondral bone ossification, and Fibroblast growth factor (FGFs), Insulin-like growth factors (IGFs) and VEGFs for cell matrix formation and angiogenesis.

Current therapy of fracture, apart from surgery procedure, employs hormones PTH and Growth hormone (GH) for systemic enhancement of fracture healing. Stem cell based therapy of fracture, especially by MSCs, the progenitor for osteoblast differentiation, has attracted much attention in

recent years. Systemic administration of MSCs targets to fracture sites is time, dose, and CXCR4-dependent way, and improves the fracture healing by increasing the material toughness of the callus and causing it to be less brittle (Granero-Moltó et al., 2009). The mechanism of MSCs therapy of fracture may be that MSCs modulate inflammatory reaction, differentiate into osteoblasts, or through a paracrine action. However, it is required for further study.

1.3 MSCs migration

Cell migration is a basic cell behavior as well as cell metabolism, proliferation, cell death and so on, starting from fertilization and embryonic development of various tissues to routine renewal of skin and intestine in postnatal life. Cell migration is also involved in pathology process. For instance, leukocytes migrate into the injured site for phagocytic and immune functions, and tumor cells migrate from initiating source into circulating systems and find new sites in metastasis. Stem cell migration, particular for MSCs, is required to reach damaged tissue for repair, and allow HSCs to mobilize into circulating system.

1.3.1 Basic biology of cell migration

Though seems differently, cell migration from various cell types including leukocytes, fibroblasts, and neurons do share some general characters. According to a model raised by Ridley and colleagues, cell migration can be usefully conceptualized as a cyclic process(Ridley et al., 2003)(Figure 1.2). The initial response of a cell to a migration-promoting agent is to polarize and extend protrusions including lamellipodia and filopodia in the direction of migration. Lamellipodia are broad, flat, sheet-like structures whereas filopodia are thin, cylindrical, needle-like projections. The elongated actin filament against the leading edge provides the driving force for protrusion. Actin polarization, inside of lamellipodia, was mediated Arp2/3 complex, which

is localized by WASP/WAVE family members (Welch and Mullins, 2002). While in Filopodial protrusion, it is thought to occur by a filament treadmilling mechanism, in which actin filaments within a bundle elongate at their barbed ends and release actin monomers from their pointed ends. On the molecular regulation, rho family proteins Rac, Cdc42, and RhoG are required for protrusion of lamellipodia and filopodia, which further targets WASP/WAVE family of Arp2/3 complex activators(Cory and Ridley, 2002). To facilitate migration, the polarity of cells allows

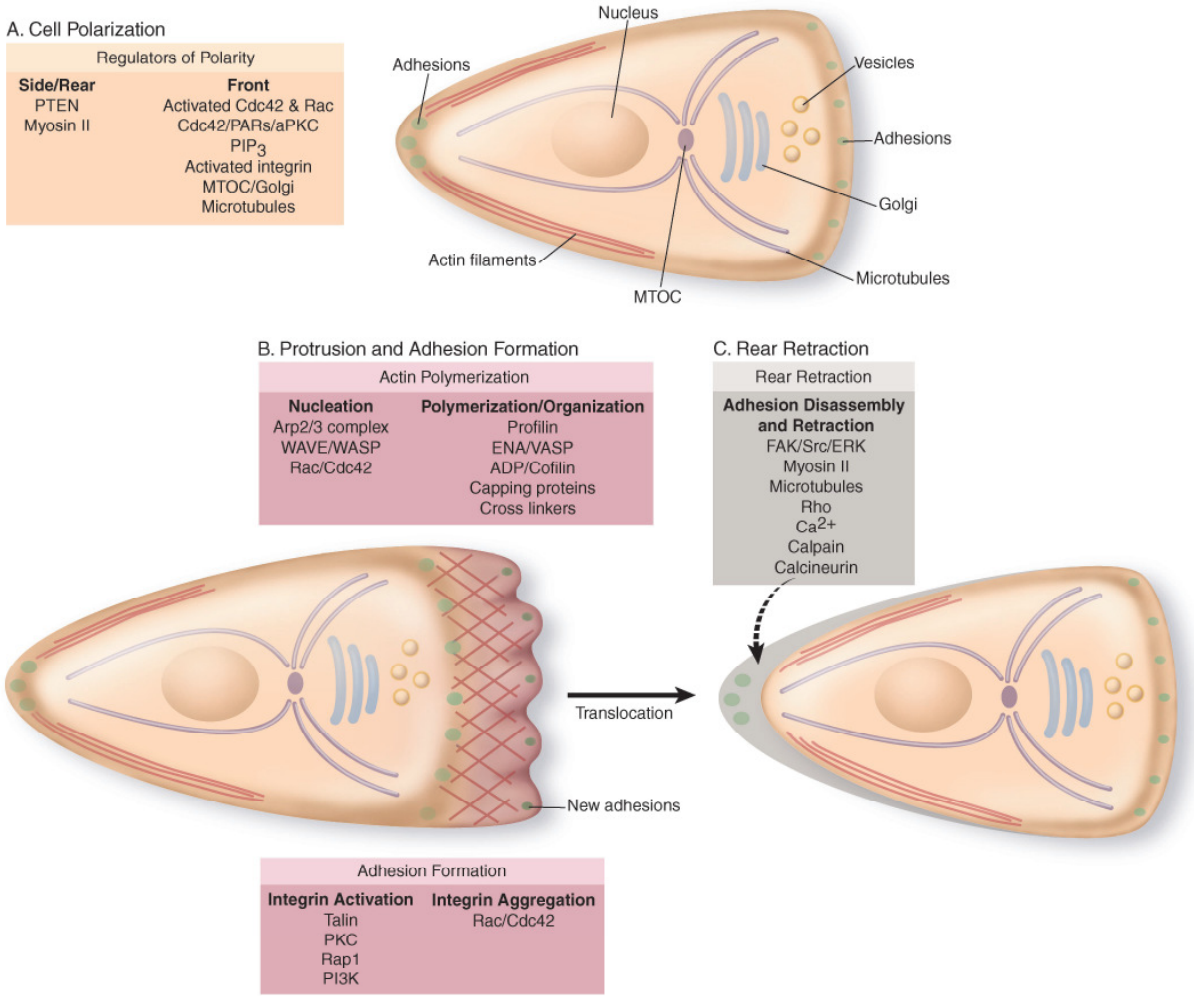

Figure 1.4 Steps in cell migration

Adopted from *Ridley, A.J Science(2003): 302,1704-1709.*

cell to sense the direction, with the high activity of Cdc42 in the front, and thus the downstream Pak1 and PIP3.

After polarization, a protrusion or adhesion complex at the leading edge form including integrins and extracellular matrix (ECM). Cell–substratum attachments subsequently remain fixed to the substratum as the cell moves forward effectively serve to remove adhesion molecules from the leading lamella. Integrins, with α and β chains, became clustering when bind ligands to the extracellular portion by conformational changes in the receptors by changing interactions(Emsley et al., 2000). This combination of occupancy and clustering of integrins conveys signals into intracellular tyrosine kinase, activation of small GTPases like Rap1 or PKC, the organization and dynamics of the cytoskeleton, and cell polarity during migration(Kim et al., 2003a).

In the last stage of cell migration, adhesion in the rear of cell should disassemble. The high tension in the rearmost adhesions sufficient to physically break the linkage between integrin and the actin cytoskeleton, with the result that integrin is left behind while the rest of the cell moves on. FAK, Src and other regulators seems to be involve in the rear turnover(Lee et al., 1999).

1.3.2 β-Catenin and cell migration

β-catenin is first identified as one of several proteins that were tightly bound to the C-terminus of classical cadherins (Ozawa et al., 1989), which consists of an N-terminal region of approximately 130 amino acids, a central region of 550 amino acids, and a C-terminal region of 100 amino acids(Akiyama, 2000). The N-terminal region contains consensus phosphorylation sites for GSK-β, while the C-terminal region possesses the transactivator function required for activation of target genes, and 12 armadillo repeats in the central region are required for the

interaction with various proteins, including cadherins, APC and TCF/LEF. The functions of β-catenin are, namely, maintaining cell-to-cell adhesion and mediating the Wnt/β-catenin signal transduction pathway, which plays pivotal roles in embryogenesis and in malignant transformation of cells. In the conventional Wnt signaling, β-catenin accumulates in the cytoplasm and translocates into the nucleus where it acts as a transcriptional coactivator through its binding with the members of the T cell factor/lymphoid enhancer factor (TCF/LEF) transcription factor family(Harris and Peifer, 2005). In the absence of Wnt signaling, β-Catenin is targeted for ubiquitination and degradation by paired phosphorylation through the serine/threonine kinases casein kinase I (CKI) and glycogen synthase-3 (GSK-3) bound to a scaffolding complex of axin and adenomatous polyposis coli (APC) protein(Polakis, 2000).

β-catenin plays pivotal role in cell adhesion, which is tightly related to cell migration. By attaching cadherin and α-catenin, β-catenin links the complex to the actin cytoskeleton and recruits actin-remodeling agents. These actions initiate cell contact by linking adhesion proteins to the propulsive force of actin polymerization(Vasioukhin et al., 2000), which is beneficial for cell migration (see above section). In addition, Müller and colleague found ectopic expression of β-catenin activated growth factor-induced epithelial cell probably through downstream target genes of the β-catenin signaling pathway (Baron and Kneissel, 2013; Müller et al., 2002). Further studies demonstrated that tyrosine phosphorylation of β -catenin may lead to disruption of the contact between E-cadherin and the cytoskeleton thus to facilitate migration, and to an increased pool of free β-catenin(Müller et al., 1999). Although β-catenin has multipotent functions in many aspects of cell behavior, the precise role of β-catenin in cell migration in regard of its downstream target genes was not yet fully understood.

1.3.3 Focal adhesion kinase and cell migration

FAK is a ubiquitously expressed non-receptor protein tyrosine kinase (PTK), with a central kinase domain, an N-terminal FERM domain and a C-terminal FAT domain. In, the FAT domain provide a direct link of FAK and focal adhesion complex (Müller et al., 1999), containing a paxillin-binding site. Through FERM domain, FAK binds directly to the intracellular domain of the β1-integrin subunit (Schaller et al., 1995)and to a sort of membrane receptors, such as hepatocyte growth factor (HGF), EGF-receptor, PDGF receptor, and vascular endothelial growth factor (VEGF) and c-Met(Chen and Chen, 2006; Garces et al., 2006; Golubovskaya et al., 2002; Sieg et al., 2000). Thus, FAK is a major player in mediating signaling that is initiated at sites of cell–ECM attachment. In other aspects, FAK is also involved in cancers survival and metastasis, endothelial cell proliferation, migration, as well as tumor angiogenesis (Lechertier and Hodivala-Dilke, 2012). As a part of a cytoskeleton-associated network of signaling proteins, FAK conveys integrin and growth factors signals to stimulate cell migration.

1.3.4 MSCs migration

The migration of MSCs, especially in vivo, is precious important to target injured tissues and systemic delivery in clinical therapy. In order to migrate into specific tissue, Firstly, MSCs should receive signal from target tissue, probably mediating by bunch of chemokines. The migration of other types of progenitor cells was mediated by chemokines. In particular, CXCL12 (also called stromal cell-derived factor-1) and its receptor CXCR4 are dispensable for bone marrow homeostasis, mobilization, and homing of hematopoietic stem cells(Lévesque et al., 2003). Although there were no definite chemokine/receptor pattern for MSCs, a variety of chemokine receptors were found in MSCs. Wynn and colleagues found the expression of CXCR4 on hMSCs was present on less than 1% cells, albeit high levels (83%–98%) of

intracellular CXCR4 expression were detected (Wynn et al., 2004). In contrast, Von Lüttichau and colleagues reported expression of CCR1, CCR4, CCR7, CXCR5, and CCR10 rather than CXCR4, which were functional in MSC migration(Von Lüttichau et al., 2005). Other reports have demonstrated functional expression of CXCR4(Kortesidis et al., 2005), CXCR6, CCR1, CCR7 and CX3CR1 on MSCs (Lee et al., 2006; Sordi et al., 2005). Various receptor expression patterns may reflect multiple roles of MSCs and different target tissues.

Next, It is necessary for MSCs to attach ECM substratum or endothelial cells to counteract blood shear force during migration. Some adhesion molecules like P-selectin rather than E- and L-selectins and various integrin molecules, such as α1, α 2, α 3, α 4, α 5, α v, β1, β 3, and β 4, are expressed on MSCs. In additon, other adhesion molecules, such as ALCAM, ICAM-3, VCAM-1, ICAM-1, and CD105 are expressed on MSCs (Krampera et al., 2006). Approximately 50% of hMSCs are thought to express the integrin very late antigen (VLA)-4 (α4β1, CD49d), providing the firm adherence of MSCs to endothelial cells in a VLA-4 dependent manner under conditions of shear flow (Rüster et al., 2006).

Last, to engraft target tissue, MSCs need migrate across basement membrane or secrete proteinase to degrade extracellular matrix. Matrix metalloproteinase 2 (MMP2), as well as MT1-MMP and TIMP-2, were shown to enhance transendothelial migration of MSCs (De Becker et al., 2007), which were further confirmed by Ries et al., who also showed that chemotactic invasion of MSCs through human ECM-coated transwell chambers could be hindered by inhibition of the proteases (Ries et al., 2007).

1.4 Biology character of Aqp1

1.4.1 Aquaporin family

Water transport across cell membrane through specific pore, so called water channel, was found from amphibian skin by Ussing and colleagues(Ussing, 1965). The first protein of water channel, Aqp1, was identified in 1991, while the other 12 members (Aqp0, AQP2–12) have been cloned in humans subsequently. Based on the primary sequences, they are subdivided into three subgroups: water selective AQPs (AQP0, 1, 2, 4, 5, 6, 8), aquaglyceroporins (AQP3, 7, 9, 10) permeable to small neutral solutes, such as glycerol and urea, as well as water, and superaquaporins (AQP11, 12)(Ishibashi et al., 2009; Juuti-Uusitalo et al., 2013). The heterogeneous Aqp family implies the various tissue distribution and physical functions. Aqp0 is essential for maintaining lens transparency and contributes to 60% of lens membrane protein (Engel et al., 2008). Aqp1 is wildly expressed in most tissue and will be discussed in detail in next section. Known a vasopressin-sensitive water channel, Aqp2 is expressed at the apical membrane of principal cells of the collecting duct (Taguchi et al., 2007). It was also found in the rete testis, efferent ducts, and epididymis, suggesting that Aqp2 plays an active role in the homeostasis of the endolymph. Aqp3 is shown to be expressed at the basolateral membrane of the principal cell from the collecting duct to be beneficial for water exportation and urine concentration (Roudier et al., 2002). Analysis of Aqp3 null mice revealed a role of Aqp3 in urine concentration and skin moisture, which was exerted by glycerol transport (Hara-Chikuma and Verkman, 2005). In the study of bib of flies, Aqp4 was found to express at glia cells in the brain, and null mutants of bib failed to suppress the differentiation of glia cells into neurons, resulting in a big brain. On the other hand, Aqp4 is expressed at myocytes and gastric parietal cells. Although there were no obvious abnormalities of Aqp4 null, a very mild urine concentration defect was noted (Lu et al., 2008). The main distribution of AQP5 were the exocrine portions of the pancreas, lacrimal, lung pneumocyte type I cells and salivary glands probably to export water

to the proteinaceous secretions (Nielsen et al., 1997). As a homolog of Aqp2, Aqp6 is found in the cerebellum [48] and at synaptic vesicles [49]. In regard of the distribution, Aqp6 is detected at the intercalated cell of the collecting duct. Aqp7 was expressed in the testis and adipose tissue. Because of Aqp7 the lower plasma glycerol concentration in Aqp7 null mice than wild-type mice, the Aqp7 mice had a lower glycemia and a higher plasma glycerol than wild-type mice after fasting (Maeda et al., 2004). The main distribution of Aqp8, unique to transport H_2O_2, is pancreatic acinar cells and the liver, except other tissues of the digestive tract (Bienert et al., 2007; Ma et al., 1997). is Expressed in the liver , Aqp9 is proposed to be essential in glycerol uptake in gluconeogenesis process during fasting(Carbrey et al., 2003). However, AQP9 null mice had no obvious abnormity despite of the slight increase of blood glycerol (Rojek et al., 2007). Aqp10 was cloned independently as fully-spliced aquaglyceroporin (Ishibashi et al., 2002). The unspliced Aqp10 resided at the apical membrane of epithelial cells of submucosal capillaries of the duodenum, while the mature Aqp10 was expressed at the granular vesicles of enterochromaffin cells (Li et al., 2005). Therefore, the unspliced and mature forms of Aqp10 seem to localize at the different cells. The distribution of Aqp11 is wild such as kidney, liver and intestine. AQP11 knockout mice had an defect on kidneys, which grew slowly and kidney defects appear from 10 till 2 months (Morishita et al., 2005). Aqp12 is expressed in the pancreas by in situ hybridization, specifically, at the acinar cells (Itoh et al., 2005), as well as Aqp1 and Aqp8. However, the precise role of Aqp12 needs to be elucidated.

1.4.2 Structures and roles of Aqp1

Aqp1 was first discovered as the relative protein of red cell Rh blood group antigens and contained 28kD polypeptide (Agre et al., 1987). Because its molecular functions were unknown, it was temporarily used as ‘CHIP28’ for a ‘channel-like integral protein of 28 kD’. Agre and his

colleagues found that when injected with cRNA for the 28-kDa polypeptide, oocytes had remarkably high osmotic water permeability (Pf ~200×10^{-4} cm s^{-1}) and rapidly exploded in hypotonic buffer, whereas control exhibited less than one-tenth this permeability. The oocyte studies demonstrated that Aqp1 behaved like water channels in native cell membranes (Preston et al., 1992). Aqp1 have six transmembrane domains with five connecting loops assembled in membranes as tetramers, and both amino and carboxyl termini resided in the cytoplasm. The signature motif─asparagine–proline–alanine (NPA) motifs, clustered into the plasma membrane, are responsible for a pore selective to water and/or solutes (Figure 1.3).

Besides of the first well-known location in red cell, Aqp1 protein was further demonstrated to be expressed at high levels in the proximal convoluted tubules and descending thin limbs of kidney. This observation was further shown confirmed with polyclonal rabbit antiserum and was expressed in rat and human kidney with affinity-purified antibody specific for the N- and C-terminal domains of Aqp1 (Nielsen et al., 1993b). In addition, Aqp1 protein was also reported in other tissues with secretory roles including cholangiocytes (bile), choroid plexus (cerebrospinal fluid) and capillary endothelium like bronchial circulation of lung (Nielsen et al., 1993a).

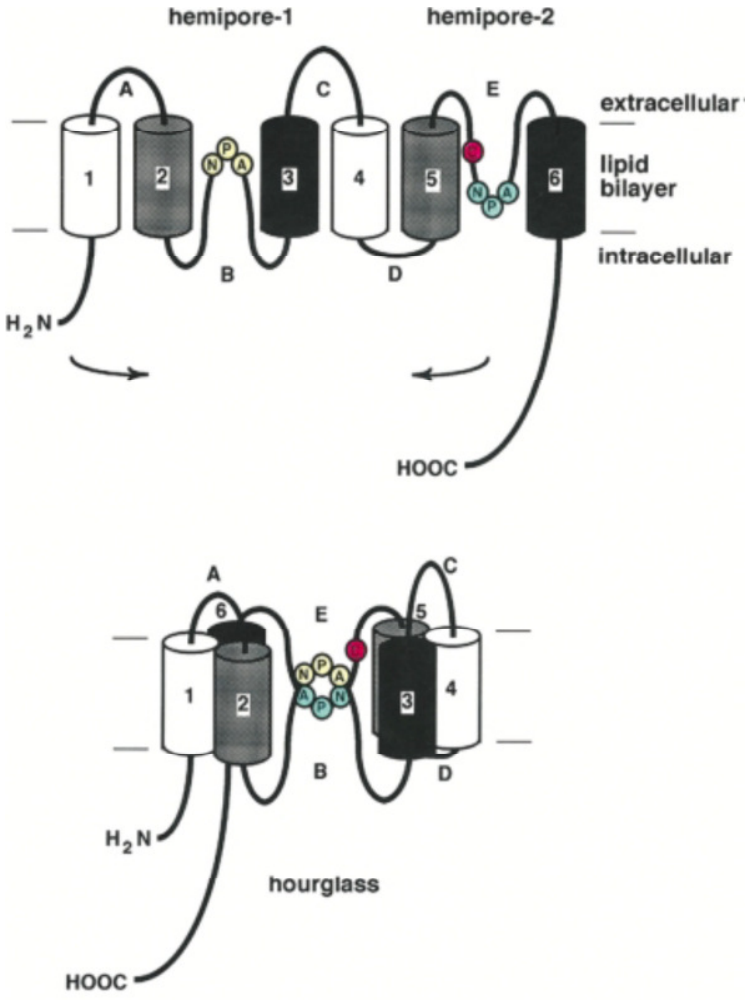

Figure 1.5 Hourglass model for Aqp1 topology

Adopted from *Carbrey, J.M. et al (2003) Proceedings of the National Academy of Sciences 100, 2945-2950*

Although Aqp1 was first discovered in erythrocytes, its role in erythrocytes is still unknown as Aqp1 null mice and null humans showed no obvious blood cell abnormalities. The main physiological role of Aqp1 is water transport in wild tissue, while Aqp1 was capable to transport some other small molecules like CO2 and Nitrate oxide (NO) in some circumstance(Herrera and Garvin, 2007). However, the function of Aqp1 in this process was not clarified. Recent studies

described a novel of Aqp1 role in tumor formation and angiogenesis, including glioma, cholangiocarcinoma, choroid plexus tumor and renal cell in human and rodent(Verkman et al., 2008). Another interesting observation was Aqp1 was re-expressed in tumor cell, in some cases, although it did not exist in corresponding normal tissue. The underlying mechanism was proposed Aqp1, expressed in most of endothelial cells, plays a key role in angiogenesis, which were demonstrated by in vitro matrix gel assay and in vivo tumor angiogenesis (Saadoun et al., 2005). Besides of angiogenesis, Aqp1 was involved in endothelial migration, which will be discussed in detail in next section.

1.4.3 Aqp1 and cell migration

Apart from the conventional role in water transport, recently, Aqp1 was reported in cell migration. Verkman and his colleague reported that tumor growth was significantly impaired in Aqp1 null mice compared to wild mice when implanted melanoma cells subcutaneously. In matrigel analysis *in vitro*, Aqp1 null endothelial cells had lower angiogenesis ability and slower movement, implying the critical role of Aqp1's role in migration of endothelial cells. Expression of Aqp1 in cells increase the osmotic water permeability to 6–8-fold compared to their correspondent control cells, while cell adhesion and cell growth were not affected. Moreover, under the microscope, Aqp1 was shown to present in the leading protrusion of cell membrane, which indicated that Aqp1 may contribute to local osmotic pressure to stimulate cell movement (Saadoun et al., 2005). Although there were no difference of kidney endothelial cells from Aqp1 null mice and wild type mice in appearance, growth and proliferation, the migration of Aqp1 null endothelial cells decreased >50% compared with wild-type cells. Moreover, Aqp1 null mice showed greater tubular injury compared with wild mice 3 to 5 d after ischemia-reperfusion, implying disability of endothelial cell caused by Aqp1 mutation impaired response of the

proximal tubule to injury (Hara-Chikuma and Verkman, 2006). Similar approaches were reached on gastric endothelial and melanoma cells, and β-catenin and Lin-7 were demonstrated to be downstream targets of Aqp1 in cell migration (Hayashi et al., 2009; Monzani et al., 2009).

1.5 RNA splicing and Sm51

1.5.1 Alternative splicing

The genetic information is stored in DNA but delivered by RNA, which is transcribed from template DNA and translated into proteins to exhibit routine cell metabolism. This RNA precursors need to eliminate introns and combine individual exons, so called alternative RNA splicing, and be reconstructed by adding a cap at 5' end and Ploy(A) at 3' end of sequence to produce mature RNA in cytoplasm. Alternative splicing contributes to the diversity of protein in metazoan species, accounting for more than 60% human gene products. Tight regulation of alternative splicing is essential for proper protein function under physiological condition, otherwise splicing defect results in human disease like cancer progression (Braunschweig et al., 2013; David and Manley, 2010). In most cases, RNA alternative splicing occurs in splicesome, a macromolecular particle which is consisted with pre-mRNA and the small nuclear ribonucleoproteins (snRNPs) U1, U2, U4, U5 and U6 as well as several auxiliary factors (Kornblihtt et al., 2013). Briefly, the 5' splice site is initially recognized by U1 snRNP via base pair between U1 snRNA and splice site sequence, while the 3' splice site is bound by a bunch of specific proteins like U2AF in some cases. The branch site is recognized by SF1 in mammal and BBP in yeast. In the first step of catalytic reaction, 2'OH group of a specifically adenosine from the branch consensus site attacks the phosphate of the 5′ splice site, give rising to a branched intermediate so called a lariat. The second transesterification step is that the phosphate at the 3'

end of the intron attacks on 3'OH of the detached exon, leading to fuse of two exons and elimination of intron (Black, 2003)(Figure 1.4).

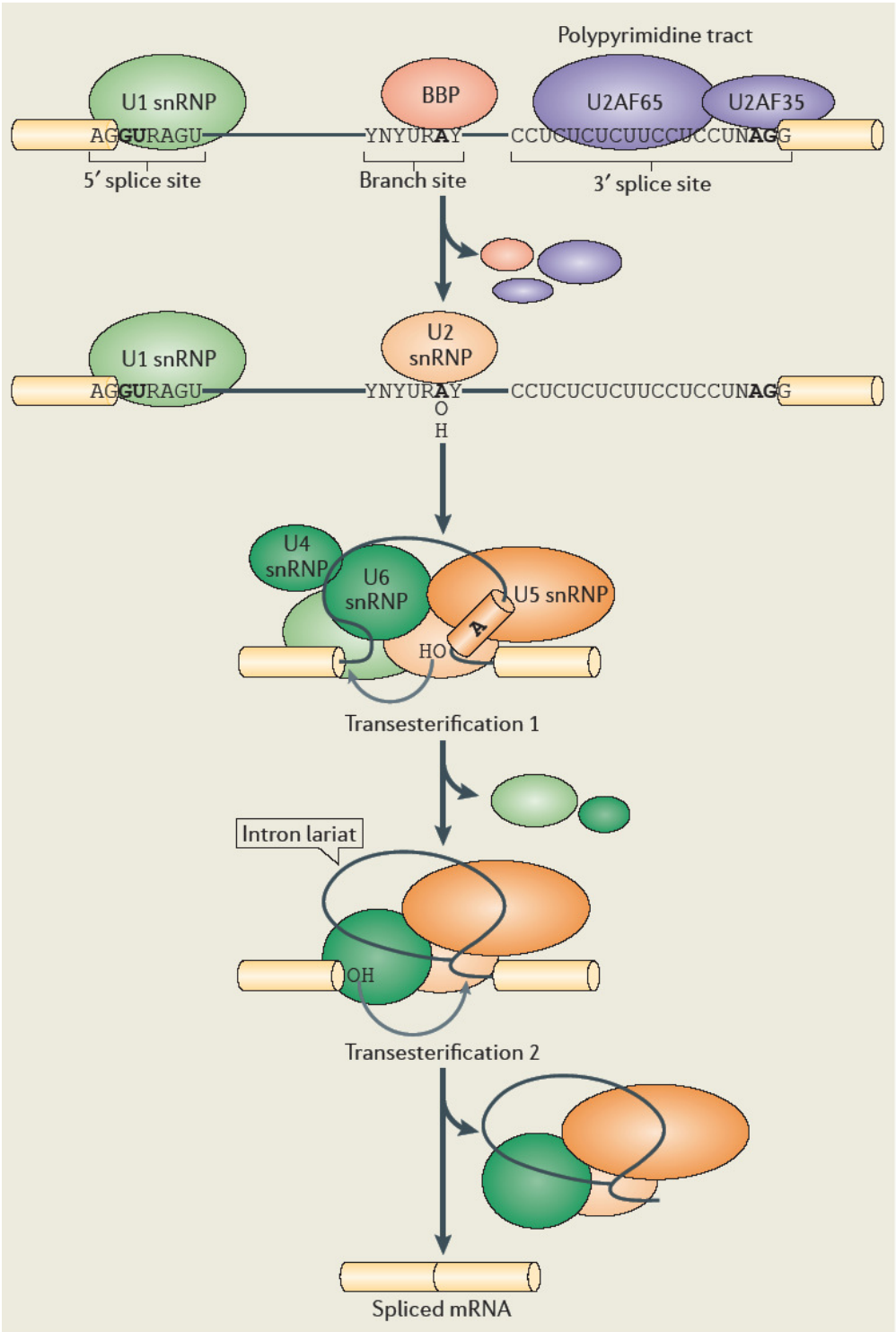

Figure 1.6 Basic procedure of alternative splicing

Adopted from *Kornblihtt et al Nat Rev Mol Cell Biol* 14, 153-165

In the splicing procedure, the splicesome recruited multiple auxiliary factors snRNPs U1, U2, U4, U5 and U6, which have common component termed SmB/B', D1, D2, D3, E, F and G, the nomenclature from Smith(Sm) antigen clarified from rheumatoid diseases. The seven Sm proteins assemble around Sm sites of snRNA into a ring structure, which constitute the structure core of all snRNPs except U6 snRNP (Lerner and Steitz, 1979). During biogenesis of snRNP, though intricate and segemented, snRNA were transcribed by RNA polymerase II, exported into cytoplasm and encircled by Sm proteins at Sm site. The trimethylguanosine (TMG) $m^{2,2,7}{}_3$G-cap are then generated subsequently by hypermethylation of the m^7G-cap, together with nuclear localization signal (NLS) at Sm core domain, allowing the processed snRNPs translocated to the nucleus (Fischer and Luhrmann, 1990; Hamm et al., 1990). Studies of the assembly of Sm proteins *in vitro* revealed a sequential and delicate process. First, Sm proteins are organized in hetero-oligomers form: B/B0–D3, D1–D2 and E–F–G instead of individual polypeptides. Next, D1–D2 and E–F–G join together as assembly intermediate to form a Sm subcore, while the none of individual hetero-oligomers contacts snRNA stably. Last, joining of B/B0–D3 tansforms the Sm subcore into mature Sm core (Raker et al., 1996). However, the mechanism of snRNP assembly in vivo, though discovered from another direction, seems much more complicated with the participation of the macromolecular SMN complex, which facilitates Sm proteins targeted to snRNA. Moreover, several *trans*-acting factors WD45, pICln, and protein arginine methyltransferase 5 (PRMT5), function as chaperone, are required to cooperate with SMN complex to direct snRNP assembly (Chari et al., 2008). However, the molecular mechanism of

site recognition and catalytic reaction performed by this macromolecular machine remains to clarify, due to the absence of high-resolution structure of snRNP.

1.5.2 Sm51

As an novel small nuclear ribonucleoprotein polypeptide N (Snrpn), Sm51 was first identified based on the autoantibodies of serum from systemic lupus erytiematosus (Lerner and Steitz, 1979). Sm51,29 kDa polypeptide, is very similar with SmB, but it was expressed restrictively in heart, brain, and embryonal carcinoma cell lines. Although Sm51 and SmB have 95% homology in amino acid sequence, they are encoded by two distinct genes. Unexpected, SmB and its very close SmB' presents at almost human tissue except for neuron where it is substituted by Sm51, but are absent in rodent tissue. Due to its tissue specific expression, Sm51was shown to be involve in alternative splicing calcitonin/CGRP transcript to generate CGRP mRNA, although the precise role of Sm51 in this process is controversial (Delsert and Rosenfeld, 1992). Besides of distinct tissue distribution with SmB, Sm51 was further demonstrated to exhibit disparate affinity with U1 snRNA and the U1 snRNP localization 3T3 mouse fibroblasts cell lines, PC12 cells and adult rat brain, while Sm51, unlike SmB, was excluded in U1 snRNP but associated with U2 snRNP in F9 and ND7 cells lines. Given F9 and ND7 cell lines were capable of splicing calcitonin/CGRP gene, Sm51 incorporated in U1 snRNP may affect the choice of 3' splicing site, thus determining the presence of exons in mRNA (Huntriss et al., 1993). Interestingly, analysis of Prader-Willi Syndrome (PWS) revealed a dysfunction of Sm51, which was either deleted paternally or duplication maternally. Further studies demonstrated Sm51 was imprinted maternally, and loss of Sm51 may conduce to PWS as depletion of snrpn in mice model led to Prader-Willi Syndrome like phenotype (Cattanach et al., 1992).

1.6 Biology character of GATA6

1.6.1 GATA Family

GATA transcription factors family are evolutionally conserved and play crucial roles in cardiac development, hematopoiesis and development of gastrointestinal epithelial cells. Six members (GATA1 to GATA6) ,with structurally similar zinc finger, are identified in vertebrate and shown to bind the consensus DNA sequence (A/T)GATA(A/G) in the promoter region of target genes (Orkin, 1992). Generally, GATA1, -2, and -3 seem to play a role in development of T lymphocytes and differentiation of erythroid and megakaryocyte and proliferation of hematopoietic stem cells, while GATA4, -5, and -6 are expressed in variety mesoderm and endoderm tissues and organs including heart, gut, pancreas and gonads (Molkentin, 2000).

All GATA factors share a common DNA zinc finger binding domain, thus have apparent similar property to target DNA sequence. The specificity is governed, at least in part, by cooperating with other tissue specific transcription factors. For instance, expressed in multipotential hematopoietic progenitor, GATA1 was upregulated during erythroid differentiation and cooperated with EpR to promote erythroid development in automatic positive feedback manner (Zon et al., 1991). In the development of heart, GATA-4 was shown to collaborate with the transcription factor Nkx2.5 to target promoters of cardiac genes like atrial natriuretic factor and cardiac α-actin (Durocher et al., 1997). GATA-4 was also involved in transcriptional regulation of Mullerian inhibiting substance by interacting directly with the nuclear receptor SF-1in Sertoli cells (Tremblay and Viger, 1999). The activity of GATA factors is further modulated by posttranslational modification like sumoylation, acetylation, and phosphorylation. In regard to sumoylation, for example, a highly conserved motif called PDSM (phosphorylation-dependent sumoylation motif) of GATA1 is responsible for sumoylation at a single lysine residue, which in turn led to transcription repression (Hietakangas et al., 2006). The acetylation of GATA2

performed by p300 and GCN5 contributed to their interaction and increase the transcription activity, while mutation of acetylating site impaired the interaction with p300 (Bresnick et al., 2012; Hayakawa et al., 2004). In contrast, acetylation of GATA3 at KRR (305-307) residues in T cells results in dysfunction of T cells homing to the systemic lymphnodes, and the survival of T cells after activation (Yamagata et al., 2000). The phosphorylation of GATA-1 in murinerythroleukemia (MEL) cells occurred on 6 serines near the amino terminus (serines 26, 49, 72, 142, 178, and 187) in uninduced MEL cells, and serine 310 near the DNA-binding domain was phosphorylated after inducing by exposure to dimethyl sulfoxid (Crossley and Orkin, 1994). Although phosphorylation of these serines residues did not influence DNA-binding affinity and bending, or transcriptional transactivation by GATA1, it was required for efficient degradation of GATA1 once cooperating with acetylation (Hernandez-Hernandez et al., 2006). GATA2 was also capable of to be phosphorylated by mitogen activated protein kinase (MAPK) when stimulated by interleukin 3 (IL3) after short time in COS cell (Towatari et al., 1995), implying a link between GATA2 and cytokines. While in preadipocytes, GATA2 was phosphorylated on serine 401 in a PI-3K/Akt–dependent manner induced by insulin, which further directed the differentiation of preadipocytes and prevented the inflammatory reaction (Menghini et al., 2005).

The gene null mouse model may help to uncover the precise role of GATA proteins *in vivo* by analysis of deficit phenotype. To assess GATA1 activity in vivo, Shimizu and the colleagues generated transgenic mice carrying the constructs of N-terminus, or an N- or C-terminal of GATA-1 and crossed to GATA1 germ line mutant mice. Only transgenic mice with N-terminus depleted can rescue definitive hematopoiesis instead of the other two mutants, implying GATA1 is indispensable for primitive and definitive erythroid (Shimizu et al., 2001). Haplo-insufficiency of GATA3 appear to cause human HDR syndrome (hypoparathyroidism, sensorineural deafness,

renal anomal) (Van Esch et al., 2000), while GATA3 null mice have unusual axonal projections of auditory neurons in the inner ear, implying that GATA3 is involved in the morphogenesis of inner ear (Karis et al., 2001; Mjösberg et al., 2012).

1.6.2 GATA6

GATA6, a 45 kDa polypeptide, is first cloned from rat heart cDNA library as well as GATA4 and possesses the common characters of GATA family proteins described in last section, however it still has several unique properties. In mammal, the primary structure of GATA6 contains a conserved zinc fingers (CVNC-X_{17}-CNAC)-X_{29}-(CXNC-X_{17}-CNAC) to bind conserved DNA sequence (G/A) GATA (A/T) and transcription activation domain.

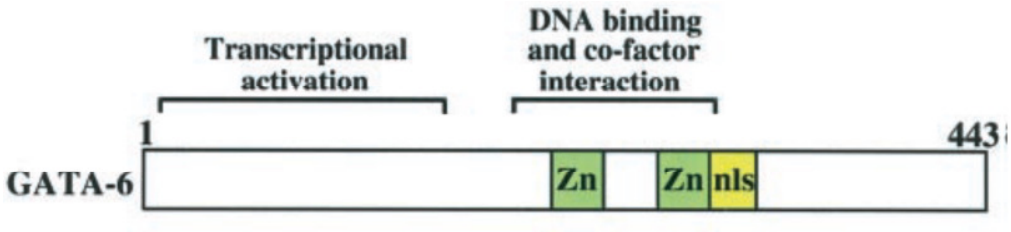

Figure 1.7 Structural domains and amino acid sequences of GATA6

Adopted from *Molkentin, J.D. (2003) Journal of Biological Chemistry 275, 38949-38952*

GATA6 has been demonstrated to play a role in regulating genes of epithelium of lung, specifically, by binding promoters of surfactant protein A and/ thyroid transcription factor-1 (TTF-1) (Bruno et al., 2000; Shaw-White et al., 1999). The role of GATA6 in determining lung development was from the observation that depletion of GATA6 in ES was not capable of differentiating into epithelium of lung (Keijzer et al., 2001). In the gut, GATA6 is implicated to bind the 5'-flanking region of trefoil factors family (TFF), TFF1 & TFF2 in stomach and TFF3

in intestine, to manipulate gut gene expression (Al-azzeh et al., 2000), and the exert a role in H^+/K^+-ATPase (Gao et al., 1998). In the pancreas development, GATA6 and GATA4 are expressed in early pancreatic progenitors, while GATA4 is further restrictively expressed in exocrine and GATA6 is limited to endocrine. In addition, GATA6 interacts directly with Nkx2.2, an indispensable transcription factor in pancreas specification (Decker et al., 2006). Studies of GATA6 null mice, died embryonic day (E) 6.5 and E7.5a, showed a specific defect in visceral endoderm differentiation as well as absence of GATA4 and HNF4 expression. Further studies demonstrated that GATA6 reside the upstream of HNF4 in the differentiation of the visceral endoderm as overexpression of GATA6 activated the expression of HNF4 in non-endoderm cells (Morrisey et al., 1998).

To modulate the target gene expression, GATA6 need cooperate with other regulators to activate gene transcription efficiently and specifically. Notably, the interaction of GATA6 and members from Nkx families in vertebrates has been illustrated recently with the finding that Nkx3.2 and GATA6 cooperated physically to activate smooth muscle genes: α_1 integrin, SM22α, and caldesmon (Nishida et al., 2002), resembling Nkx2.2 and GATA6 in pancreas development. Studies of calcium metabolism reveal a link with GATA6 in controlling differentiation of vascular smooth muscle cells (VSMCs) via smooth muscle–myosin heavy chain (Sm-MHC) gene. The level of calcium correlates with the differentiation status of skeletal muscle cells in a calcineurin dependent pathway, which in turn activates transcription of the nuclear factor of activated T cell (NFAT) family. At least four members of NFAT family NFATc (NFATc1), NFATp (NFATc2), NFAT3 (NFATc4), and NFAT4 (NFATc3) were identified with the conserved Rel homology domain, while NFATc1 appeared to physically interact with the zinc finger domain of GATA6 for activating Sm-MHC promoter (Wada et al., 2002).

1.7 Introduction to my PhD project

1.7.1 Hypothesis

In spite of higher similarity with BM-MSCs in regard of morphology and differentiation potential, PB-MSCs, mobilized from bone marrow into peripheral blood, should acquire some new property. So, what is the difference of PB-MSCs and BM-MSCs on molecular levels? To answer this, our lab once harvested the PB-MSCs and BM-MSCs from each individual and screened the differential genes by microarray, which were further confirmed by qPCR (Table1)(He et al., 2011).

Table 1. Difference in expression of selected genes between PB-MSCs and BM-MSCs determined by Microarray and real-time PCR

Gene name	PBMSCS vs BMMSCs	Microarray		Real-time PCR	
		Fold change	P value	Fold change	P value
Cellular retinol-binding protein 1	up	496.54	0.042	574.00	0.035
Cadherin 2		51.11	0.037	101.00	0.013
Bone morphogenetic protein 6		21.35	0.012	7.17	0.003
SRY-box containing gene 11		17.15	0.040	39.50	0.009
Chloride intracellular channel 5		10.68	0.007	3.07	0.023
Small nuclear ribonucleoparticle-associated protein (snRNP) mRNA, clone Sm51		10.35	0.007	3.89	0.000
Aquaporin 1	down	-94.01	0.048	-75.70	0.011
Arginine vasopressin receptor 1A		-15.31	0.030	-11.60	0.011
Prostaglandin E receptor 4 (subtype EP4)		-13.13	0.048	-4.56	0.000
Collagen, type XVIII, alpha 1		-10.23	0.000	-2.23	0.004

Table 1.2 Differential expression of genes from PB-MSCs compared to BM-MSCs

A group of genes is up-regualted including but not limited *cellular retinol binding protein 1(CRBP1)*, *bone morphogenetic protein 6 (BMP2), SRY-box containing gene 11(Sox11), chloride intracellular channel 5, small nuclear ribonucleoparticle-associated protein (snrpn)*

mRNA clone 51(Sm51), GATA binding protein 6, while another set of genes are down-regulated including *Aquaporin1 (Aqp1), Arginine vasopression 1A, Prostaglandin E receptor 4(subtype EP4), collagen XVIIIα1*. We hypothesize that manipulating the expression of these genes in BM-MSCs would have an impact on cell properties in regard of migration, proliferation and differentiation. In this project, we choose three genes Aqp1, Sm51 and GATA6 for further study, as they are expressed in these two cell types with a significant huge difference and their biological functions are seldom known in MSCs.

1.7.2 Experiment scheme

The project is comprised of the following 4 parts.

In the first part, PB-MSCs will be isolated from normal rat and analyzed their surface markers and differentiation potential. To examine the changes of PB-MSCs during fracture healing, $CD45^{-}CD90^{+}$ cells would be calculated using flow cytometry.

In the second part, Aqp1 depleted and overexpressing stable rat BM-MSCs will be established using lentiviral transfection method, and used for assays of migration and tri-lineage differentiation *in vitro*. Moreover, Aqp1 overexpressing MSCs will be administrated into rats with femora or tibia fracture, and the fracture healing outcome will be assessed.

In the third part, Sm51 overexpressing stable rat and human BM-MSCs will be established using lentiviral transfection method, and used for assays of migration and tri-lineage differentiation in vitro. Moreover, Sm51 overexpressing MSCs will be implanted with HA-TCP into nude for ectopic bone formation *in vivo*.

In the fourth part, GATA6 depleted and overexpressing stable rat and human BM-MSCs will be established using lentiviral transfection method, and used for assays of migration and tri-lineage differentiation in vitro. Moreover, GATA6 overexpressing rat MSCs will be implanted with HA-TCP into nude for ectopic bone formation *in vivo*.

Chapter 2

Characterization of PB-MSCs

The purpose of this chapter is to answer----

How to culture PB-MSCs from normal rat peripheral blood and what are their characters in vitro?

How do PB-MSCs change during fracture healing?

2.1 Chapter introduction

The disorder of fracture healing such as delayed union or non-union is still prevalent due to massively local tissue trauma and poor patient state especial for osteoporosis individuals (Dimitriou et al., 2011). Understanding more biological mechanism during fracture healing is beneficial for enhancing healing.

Fracture healing is a multiple stages, orchestrated biological events, and various growth factors, cytokines and cell types are involved in tissue repair and remodeling during this process (Einhorn, 2005). Osteoblast cells, differentiated from mesenchymal stem cells (MSCs) under the periosteum, commit to new bone formation during remodeling stage, while failure of osteoblast remodeling result in non-union morbidity in clinical trials (Doll et al., 2008). The treatment of non-union in clinical practice is usually to use autologous bone graft, which is quite limited by donor availability. Optional strategies in term of tissue engineering, bone substitutes, drugs inducement and gene therapy are under intense investigation, in order to surmount such hurdles. Previous studies showed that systemic and local MSCs transplantation could enhance fracture healing(Granero-Moltó et al., 2009; Quarto et al., 2001) Systemic delivery of MSCs preferred to engraft into fracture site and contribute to bone regeneration. The origin of MSCs during fracture healing process has not fully elucidated. Parabiotic animals study indicated circulating MSCs can specifically mobilize into fracture site(Kumagai et al., 2008). MSCs are not only adopted locally but also recruited from remote sites via peripheral circulation(Shirley et al., 2005).

Circulating MSCs has been successfully isolated and characterized in many species (Eghbali-Fatourechi et al., 2005; Kuznetsov et al., 2001). Due to dramatically increase in bone formation, the number of osteoblast-lineage cells was significant higher from adolescent boys compared to

adult man. Beside its role in bone development, circulating MSCs existed in circulation in fractured patients(Alm et al., 2010). It possessed similar characters with bone marrow derived MSCs. These studies indicated that circulating MSCs participate in fracture healing. However, the precise relationship between circulating MSCs and fracture healing is not studied completely.

We speculate that use of flow cytometry of primary antibodies specific for MSCs surface marker would monitor changes of circulating MSCs during fracture healing. Furthermore, circulating MSCs would be isolated and cultured from peripheral blood in vitro and examined their MSCs characters.

2.2 Methods

2.2.1Establishing rat closed fracture model and collecting peripheral blood

All animal surgery and sample collection were handled under an animal license issued by the Hong Kong SAR Government and local ethical committee. The study population constituted 14 male SD rats. Closed fracture model was established at the right femoral shaft of each rat by utilizing three-point bending apparatus following intramedullary insertion with a sterilized Kirschner wire(ϕ 1.2 mm, Stryker , Kalamazoo, USA) as reported (Leung et al., 2009). Fracture condition was assessed and confirmed by digital X-ray machine (Faxitron Bioptics, Lincolnshire, USA). Peripheral blood was harvested from fractured rat at 3 days before fracture surgery and 3,7,11,13,21,27 days after fracture surgery.

2.2.2Flow cytometry analysis of circulating MSCs from peripheral blood

Peripheral blood was incubated with PE conjugated mouse anti-rat CD90 antibody , PE-Cy™5 Mouse IgG1 κ Isotype Control, PE Mouse IgG1, κ Isotype Control and PE-Cy™5 conjugated

mouse anti-rat CD45 antibody (BD Biosciences, New Jersey, USA) for 30 min on ice. Blood erythrocytes were then lysed by lysing buffer following manufacturer's instruction (BD Biosciences, New Jersey, USA). Samples were analyzed by BD LSRFortessa flow cytometry with BD FACSDiva Software (BD Biosciences, New Jersey, USA). Fluorescence compensation was calculated with single staining of PE-CD90 and PE- Cy™5 antibody. Monocyte population was gated in a dot plot of forward versus side scatter. CD45-/CD90+ cells were further analyzed from monocytes population. The number of circulating MSCs was estimated by number of CD45-/CD90+ cells from monocyte per 10^5 mononuclear cells.

2.2.3 Isolation of PB- MSCs

Circulating MSCs was isolated modified previous report (Kuznetsov et al., 2001). Briefly, Peripheral blood was harvested from normal rats (SD, age 8 weeks) via heart puncture. Blood was diluted with equal volume α-MEM media and coated on Ficoll lymphocyte separation medium (Axis-Shield PoC AS, oslo, Norway). Mononuclear cells were collected at the buffy interface and plated in 10 cm dish at the density of 2×10^5 /cm^2. Media was changed after culture in 37 ºC incubator with 5%CO_2 for 5 days.

2.2.4 Flow cytometry of cell surface markers

Cells from passage 3 or 4 were chosen and digested with 0.25% trypsin-EDTA (Gibco, Carlsbad, USA). Pellet was resuspended in PBS plus 1%FBS containing fluorescein isothiocyanate (FITC)-CD34(Santa Cruz), FITC-CD44, phycoerithrine (PE)-CD90 and PE-Cy5-CD45(BD). After incubation for 1h on ice, cells were resuspended in 1% paraformaldehyde for flow analysis. Fluorescence parameter was adjusted in LSR Fortessa flow cytometry (BD). Data was further analyzed by FACSDiva Software (BD).

2.2.5 Osteogenic differentiation of circulating MSCs

Culture media was changed to osteogenesis mediaum once MSCs was on confluence. Osteogenesis medium based on low glucose DMEM (Gibco) supplemented with 1nM Dexamethasone, 50uM Ascorbic acid and 20mM β -glycerolphosphate (Sigma–Aldrich, Shanghai, China). Media was changed twice one week. After culture for three weeks, cells were fixed with 70% ethanol for 10min and stained with Alizarin red S (Sigma).

2.2.6 Adipogenic differentiation of circulating MSCs

Cells were cultured in basal medium supplemented with 500nM Dexamethasone, 50uM Indomethacin, 0.5mM Isobutylmethylxanthine and 10ug/ml Insulin (Sigma). After culture for three weeks, cells were fixed with 70% ethanol for 10min and stained with oil red O (Sigma). Intracellular lipid droplet was observed under microscope.

2.3 Results

2.3.1 Rat fracture model and analysis of circulating MSCs

Rat closed fracture with internal fixation model was established and verified by X-ray radiography (Figure 2.1A, B). Peripheral blood was harvested for flow cytometry detection of circulating MSCs during fracture healing. Three populations were shown after lysing red blood cells in side scatter and forward scatter plot, which were lymphocytes, monocytes and granulocytes. These three populations were firstly gated during data collecting. Monocyte population was further gated for analysis. The expression of CD45 and CD90 of monocyte population were gated normalized to their counterpart isotype control. Circulating MSCs was defined as CD45-/CD90+ (Q1 zone, Figure 2.1C).

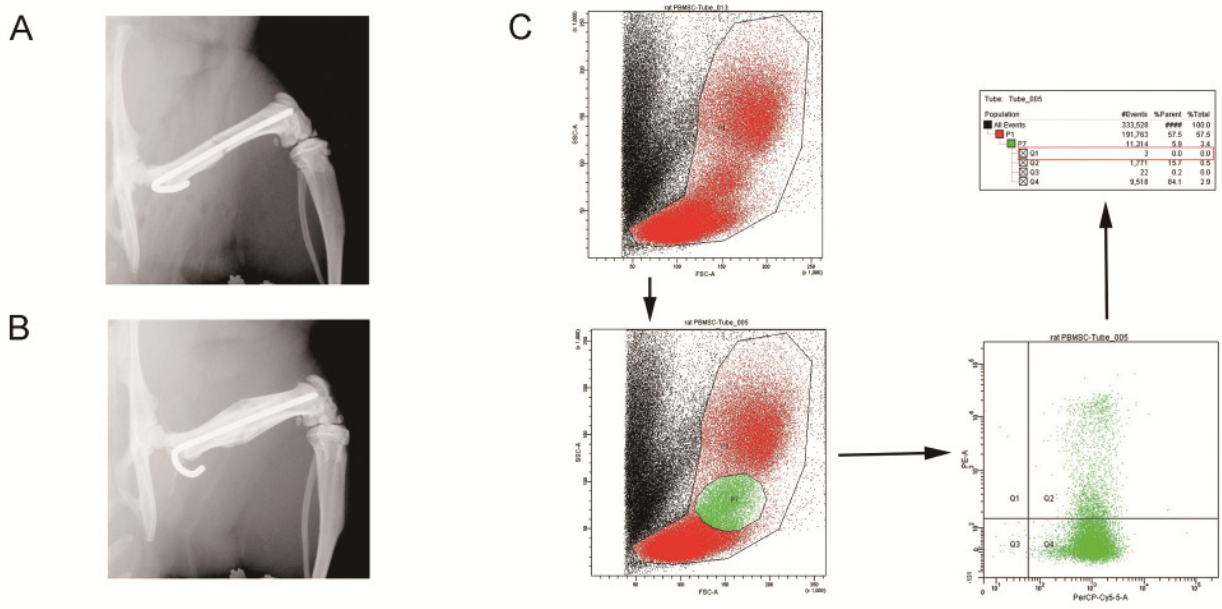

Figure 2.1 Rat fracture model and analysis of circulating MSCs.

A: Rat closed transverse fracture was created on right femoral shaft with Kirschner wire (φ1.2 mm) for internal fixation. **B:** Four weeks after fracture with visible callus formation. **C:** Blood from fractured rats were lysed for flow cytometry. Lysing blood were divided into three populations (red): granulocytes, monocytes and lymphocytes on side scatter versus forward scatter plot. Monocyte was further gated (green) and analyzed on PE-CD90 and PerCP-Cy5.5-CD45 scatter plot. Q1 zone present the number of CD45-/CD90+ cells (red frame).

2.3.2 Changes of circulating MSCs during fracture healing

The number of circulating MSCs was calculating from CD45-/CD90+ zone normalized per 10^5 mononuclear cells. It was shown to begin to increase 3 days after fracture compared to pre – fracture level. The number of circulating MSCs increased dramatically 11days after fracture and reached the peak at day 13. It then decreased from day 21 and returned to pre-fracture level (Figure 2.2). The number of circulating MSCs at day 13 was about 6 folds more than pre-fracture. There were no significant difference among day 21, day27 and pre-fracture.

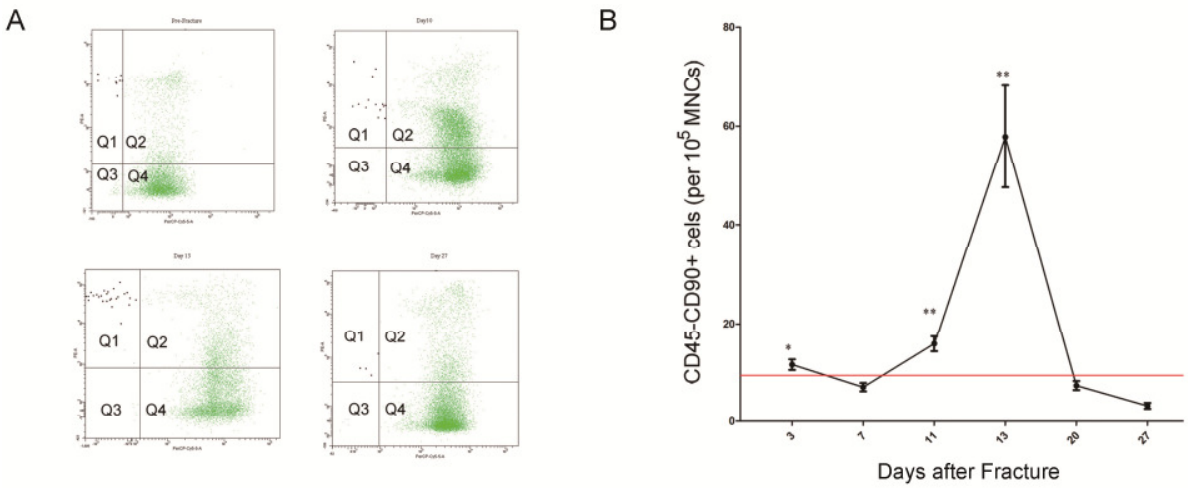

Figure 2.2. Changes circulating MSCs during fracture healing process

A: PE-CD90 and PerCP-Cy5.5-CD45 scatter plot show circulating MSCs at time point of 3 days pre-fracture and 11, 13, 27 days after fracture. Each dot or point represents an individual cell that has passed through the instrument. Cells from Q1 zone were shown using red dots. Much more cells were found at day11 and day13 compared to pre-fracture and day 27. **B:** The graph showed number of circulating MSCs (CD45-/CD90+) increased from day 3 and reached its acme at day13. Then it dropped sharply to pre-fracture level from day 21. Data were shown in Mean±SEM.

2.3.3 Isolation and culture of PB-MSCs

Circulating MSCs were isolated by their adherent characters. Some fibroblast like colonies appeared 8 days after primary culture (Figure 2.3A). They grew fast and became confluent at day11 (Figure 2.3B). Their morphology was very similar with bone marrow derived MSCs (Figure 2.3C). These MSCs were easily digested by trypsin. This character discriminate it to macrophage, which is common in blood culture and trypsin resistant. Their morphology and growth kinetics did not change even after 3 passages (Figure 2.3D). Cell surface CD markers of

expanded circulating MSCs were detected by flow cytometry with negative expression of CD31, CD45 and CD34 and positive expression of CD90 and CD44 (Figure 2.4).

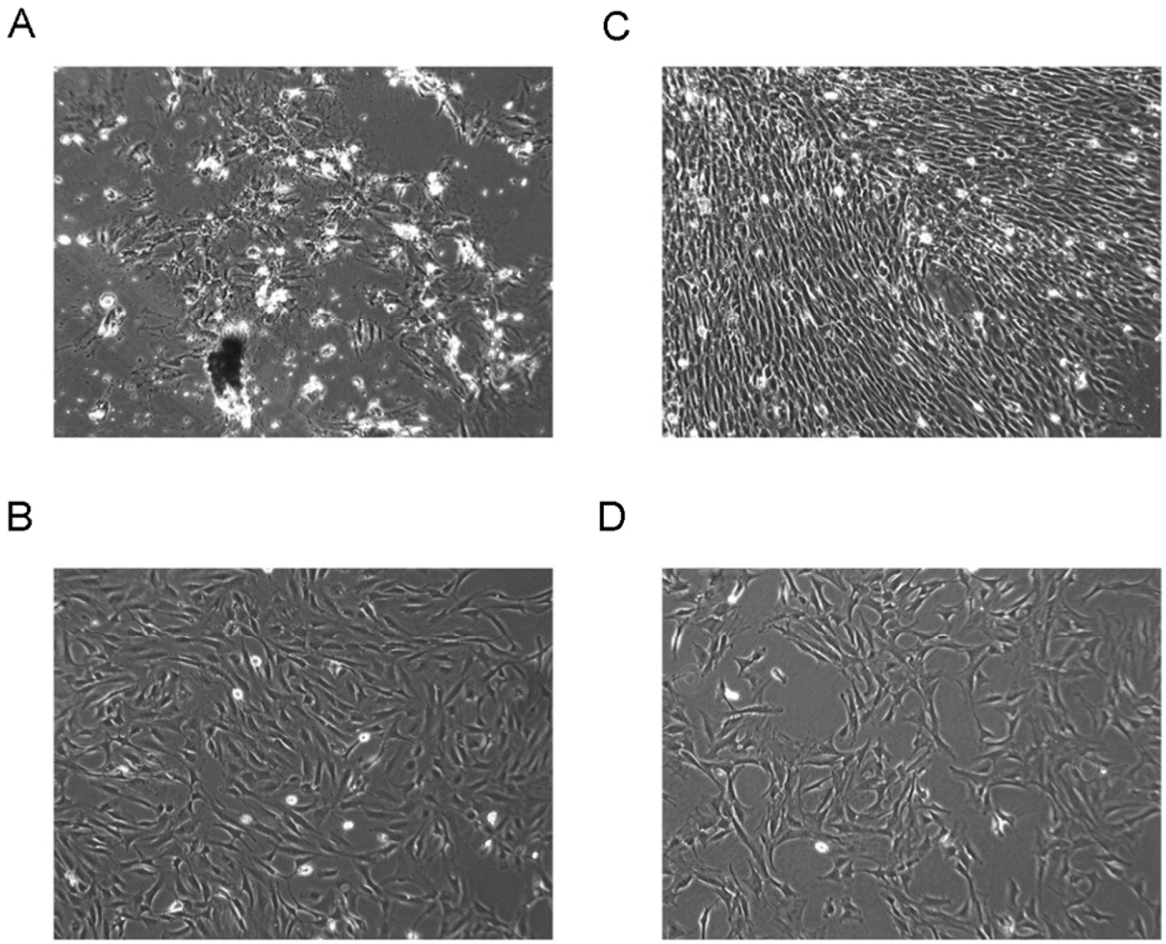

Figure 2.3.Culture of circulating MSCs

A: Fibroblast like colonies were found at day 8. **B:** cell became confluence at day11. **C:** 1st passage of PB-MSCs. **D:** 3rd passage of PB-MSCs.

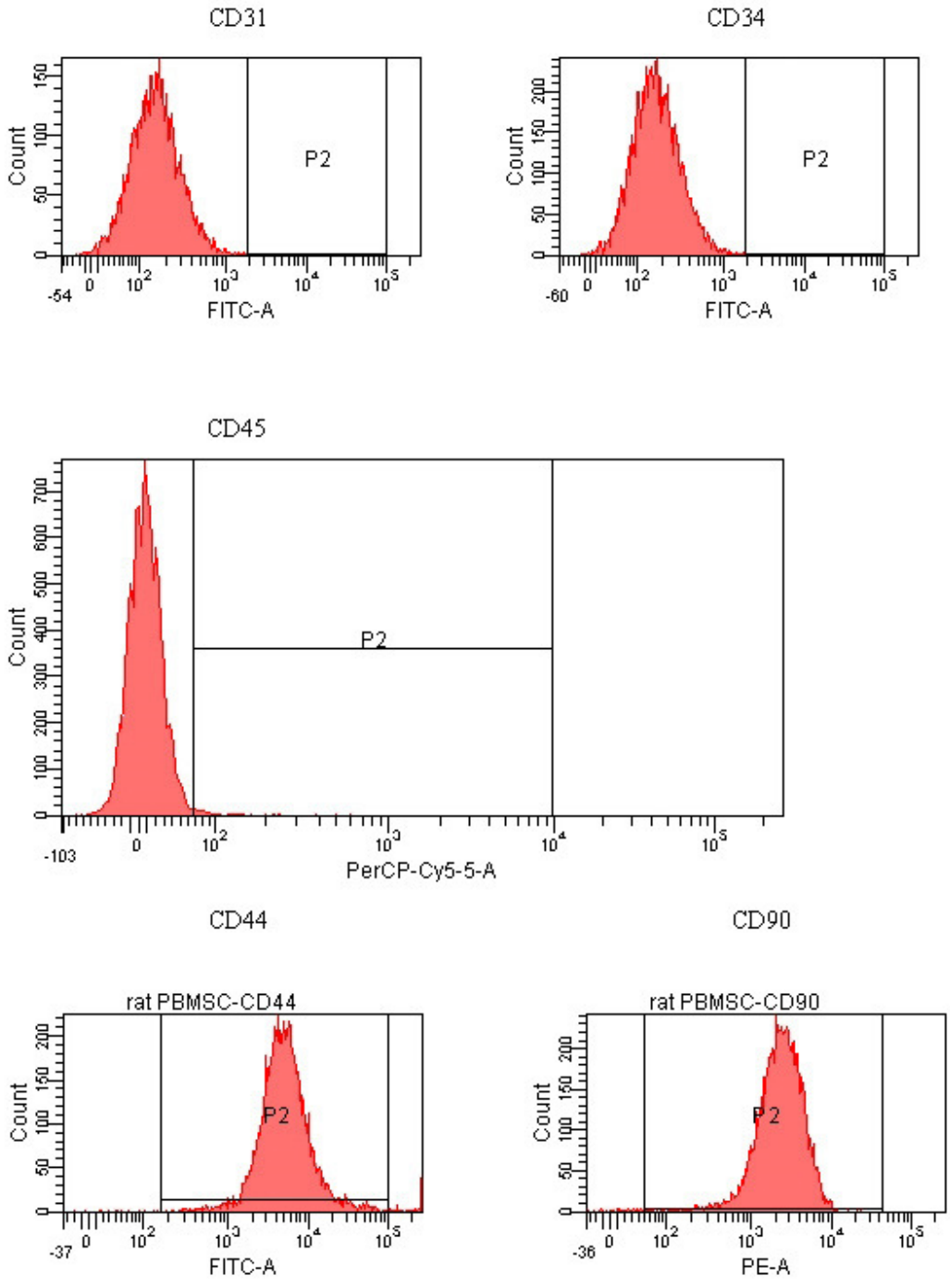

Figure 2.4.Flow cytometry detection of cultured circulating MSCs

Circulating MSCs after 3 or 4 passages were stained with PerCP-cy5.5-CD45, FITC-CD31, FITC-CD34, FITC-CD73, FITC-CD44 and PE-CD90 antibodies and detected by flow cytometry was negative for CD34, CD31, CD45 and positive for CD44, CD90. Gate (P2) was determined by isotype control.

2.3.4 Osteogenesis and adipogenesis of PB-MSCs

Passage 3 or 4 MSCs were used for osteogenic differentiation and adipogenic differentiation. After inducing for 3 weeks in osteogenic medium, calcium deposit appeared inside of PB-MSCs shown by alizarin red S (Figure 2.5A). In addition, PB-MSCs also had the ability of differentiate into adipocyte, which was shown accumulation of intercellular lipid droplets demonstrated by staining of oil red O (Figure 2.5B).

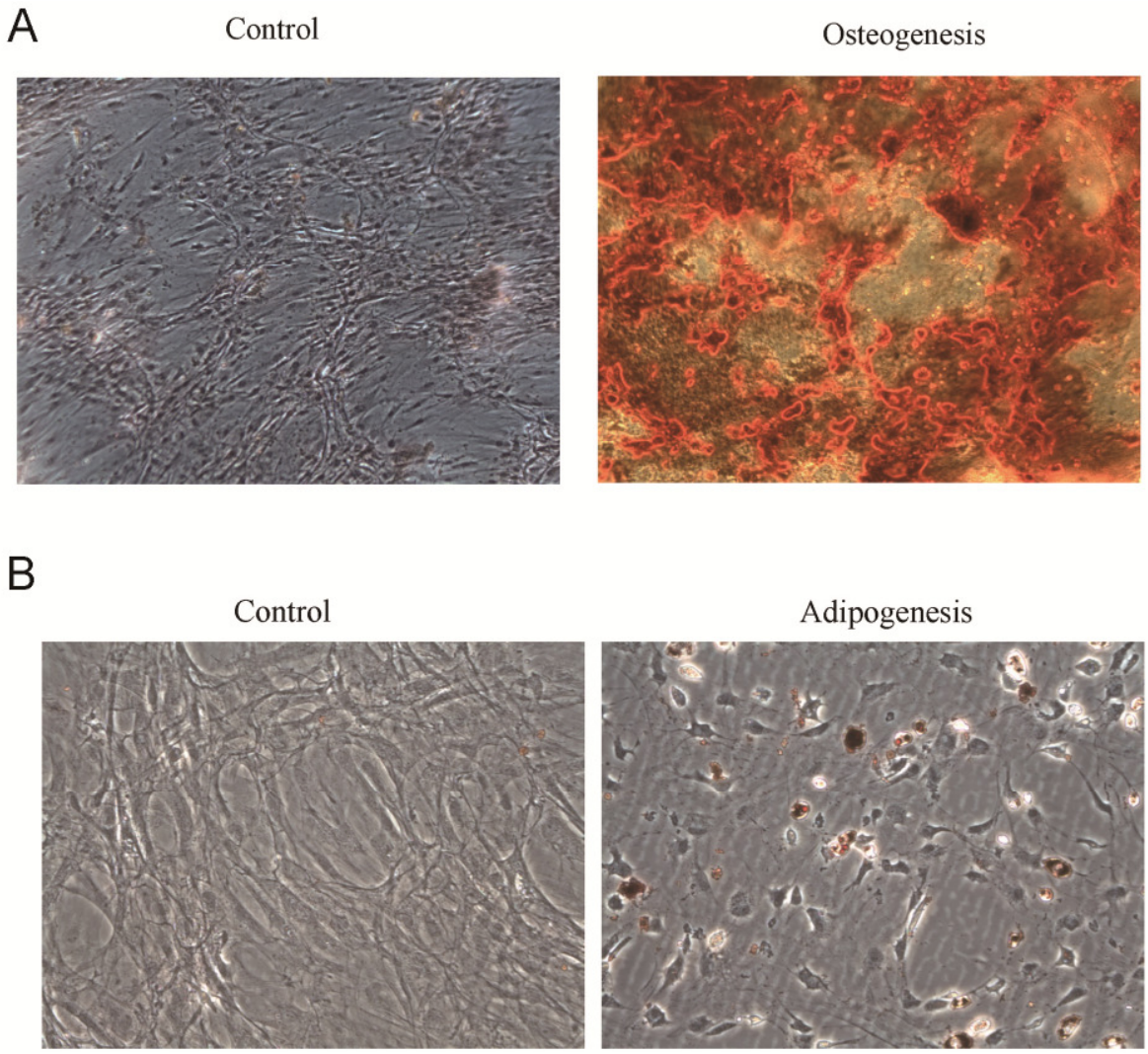

Figure 2.5 Osteogenesis and adipogenesis of circulating MSCs

A: Confluent MSCs were induced by osteogenic and adipogenic medium respectively. After 3 weeks osteogenic induction, many calcium deposits (arrow) were stained red by Alizarin Red S. **B:** Accumulation of lipid droplet (red dot, arrow) was shown by staining by oil red O after 3 weeks adipogenic induction (B).

2.4 Discussion

The major finding of this study suggests MSCs was systemically recruited during fracture healing. The recruitment began at the first stage of fracture trauma and ended with eventual formation of callus. The amount of circulating MSCs from different stages of fracture healing was quantified by flow cytometry. These results revealed the underlying relevant participation of circulating MSCs in fracture repair (Alm et al., 2010; Shirley et al., 2005).

MSCs was firstly characterized by Friedenstein and colleagues from bone marrow owing to its adherent properties, which can be easily distinguished from other hematopoietic lineage cells.(Friedenstein et al., 1976) MSCs from different tissues possesses similar cell surface marker expression pattern. Although none of known CD markers is specific for MSCs, it is generally thought rat MSCs do not express hematopoietic lineage markers CD45, CD34 and CD14. But they can express CD105, CD90, CD73 and CD44 (Chamberlain et al., 2007; Phinney and Prockop, 2007). Identification of circulating MSCs using all these markers by flow cytometry seems too complicated for future clinical application. Two bone specific proteins (osteocalcin and alkaline phosphatase) have been successfully utilized for characterizing circulating osteoblast-lineage cells(Eghbali-Fatourechi et al., 2005). We hypothesize combination of one negative marker-CD45 and one positive marker-CD90 is feasible for estimating or identifying circulating MSCs. In order to discriminate it from some CD45-/CD90+ lymphocytes, monocyte population was selected for analysis the number of circulating MSCs. Mesenchymal like cells was thought to reside within monocyte population. However, circulating MSCs could be easily distinguished from monocyte-derived multipotential cells (MOMC), which was positive for hematopoietic markers like CD45 and Cd34(Seta and Kuwana, 2007).

Fracture healing is multiple steps process, which undergoes inflammation, soft callus (fibrocartilage) formation, hard callus formation and bone remodeling stages (Schindeler et al.,

2008). Circulating MSCs started to increase at 3 days after fracture, which was corresponding to inflammation response. Dramatic increase of circulating MSCs was observed from day 10 after fracture, which was thought to be the time of chondrogenesis. The number of circulating MSCs reached maximal at 13 days after fracture with calcification of cartilage at fracture site. It declined rapidly and returned to normal level in following remodeling stages. Circulating MSCs participated fracture repair at early stages. In addition, it could be detected in human hip fracture at short period(Alm et al., 2010). This work support the hypothesis MSCs was systemically recruited druing fracture healing. However, fracture healing is the interplay of many growth factors, cell types, cytokines and extracellular matrix. The responsible factor for recruitment of circulating MSCs and the precise role in fracture site need to be elucidated further. We used flow cytometry technology to trace dynamic changes of circulating MSCs, which could be an indicator for fracture healing status and give some clues for monitoring healing process.

In order to prove the existence of circulating MSCs, we cultured it by plating peripheral blood from normal individual. It possessed similar cell morphology, cell surface marker expression pattern and lineage differentiation potential with canonical MSCs. The expression of CD45 was negative, while CD90 expression was positive. This was what we used in flow cytometry to identify it in circulation. However, it is still be hard to isolate circulating MSCs efficiently(He et al., 2007). Some other researchers once detected the nonadherent cells population in MSCs culture(Wan et al., 2006). It indicated that there existed at least a small amount of nonadherent MSCs. MSCs could be recruited from remote bone marrow to fracture site(Shirley et al., 2005). We also found circulating MSCs required much more time to form colony than canonical bone marrow derived MSCs. This maybe is due to its nonadherent characteristics. The relationship between bone marrow non adherent MSCs and circulating MSCs was not studied well.

In conclusion, we found circulating MSCs increased dramatically in early stage (within two weeks) after fracture and declined into normal level then. This study could be used to monitor fracture healing process. Unravel underlying mechanism of circulating MSCs changes will be beneficial for enhancing fracture healing in clinical application.

Chapter 3 Aqp1 promotes migration of BM-MSCs

The purpose of this chapter is to answer----

What is the role of Aqp1 in migration of BM-MSCs and bone healing?

3.1 Chapter introduction

Bone marrow derived mesenchymal stem cells (MSCs) has been characterized for decades (Friedenstein et al., 1976), and utilized extensively for improving/treatment of many disease conditions, such as bone defects (Yoshioka et al., 2007), myocardial infarction (Mirotsou et al., 2007; Ranganath et al., 2012), diabetes (Ezquer et al., 2008) etc. MSCs with low immunogenicity are relatively easy to obtain, culture (Phinney and Prockop, 2007). However, systemic administration of MSCs via circulation has some limitations, as only a few transplanting MSCs could reach injured tissue sites, most of which are trapped and dead within a short duration in small blood vessels in lung and other tissues (Song and Li, 2011). Therefore, enhancing MSCs migration capacity will allow them to migrate towards to injurious sites more efficiently, which will be beneficial for their clinical application.

Cell migration is complex process that orchestrates signal transduction, cytoskeleton rearrangement and morphogenesis. In canonical migration cycle, it is mainly comprised of three distinctive steps, including cell polarization, protrusion and adhesion formation, rear retraction (Ridley et al., 2003). Multiple regulators play roles in cell migration, among which focal adhesion kinase (FAK) mainly conveys signals from extracellular matrix (ECM) to the cell in adhesion complex (Provenzano and Keely, 2009). FAK is a ubiquitously non-receptor cytoplasmic protein tyrosine kinase (Lietha et al., 2007), which plays key roles in embryonic development and many human diseases, like cancer and cardiovascular disease (Schaller, 2010). In addition, FAK is crucial for MSCs migrating to injured sites, in response to stromal cell derived factor 1 (Gao et al., 2009; Song et al., 2010). Another important pathway in regulation of MSCs migration is stromal cell-derived factor (SDF) 1α and its receptor C-X-C chemokine receptor type 4 (CXCR-4) axis. Previous studies have shown that overexpression of CXCR4

accelerated MSCs mobilization and angiogenesis in the infarcted myocardium (Zhang et al., 2008).

The β-catenin is an important regulator in Wnt pathway, which regulates many aspects of cell behaviors, like fate decision, migration and cell differentiation (Davidson et al., 2012; Logan and Nusse, 2004). At cell surface, β-catenin binds α-catenin, which links the complex to the actin cytoskeleton and recruits actin-remodeling agents. After stimulation, β-catenin dissociates from E-cadherin/catenin cell membrane complex and translocates into cell nuclei where it acts as a transcriptional co-activator binding with the members of the T cell factor/lymphoid enhancer factor (TCF/LEF) transcription factor family (Polette et al., 2007). Target genes of TCF/LEF include matrix metalloproteinases (MMP), chemokines or cytoskeletal proteins, which regulate cell migration and cancer invasion (Brabletz et al., 1999; Gilles et al., 2003; Hatsell et al., 2003). Administration of MSCs has used wildly in regeneration medicine for decades including tissue repair and gene therapy, due to their low immunogenic reaction, higher proliferation, multiple differentiation capacity and high migration ability. Normally, injured tissue would secrete various chemokines or inflammatory factors, such as CXCL12/ SDF1 and IL6, to recruit MSCs through the circulating system. High migration ability of MSCs is indispensable, especially in vivo, for efficiently engrafting into target tissue in clinical application, although a large portion are trapped in lung and died in short period when administrated systemically. However, factors involved in migration of MSCs still are unclear. To test whether Aqp1 is capable of enhancing the migration of MSCs in vivo, we administrated systemically in tibia fracture rat and fond MSCs with Aqp1 overexpressed migrated much faster. Given that more MSCs will reach the fracture site in a given time, we hypothesize the fracture healing outcome should be better after administrating Aqp1 overexpressing MSCs systemically.

As one of the water channel molecules, Aquaporin 1 (Aqp1) transports water across cell membrane. The structure, distribution and biochemical properties of Aquaporin family have been studied extensively for decades (Borgnia et al., 1999). Recent evidences showed that Aqp1 promoted tumor angiogenesis and growth by modulating endothelial cell migration through Lin-7 and β -catenin. (Monzani et al., 2009; Saadoun et al., 2005). However, there was no study on the role of Aqp1 in MSCs migration. Here, we demonstrated that Aqp1 could promote MSCs migration through β-catenin and FAK pathways; overexpression of Aqp1 in MSCs could enable MSCs to migrate more efficiently to the fracture gap in rat fracture model.

What is the significance of Aqp1 in bone fracture healing? We design to administrate the Aqp1 overexpressing MSCs and control DsRed-MSCs into femoral fractured rat intracardiacly. One month after administration, the mechanical properties of fracture femora will be examined by 4-points bending mechanical testing, while the structure and bone density will be detected by histocheminstry and micro-CT analysis respectively. To trace the exogenous MSCs, the Aqp1-MSCs was labeled by GFP in vitro before administration and detected in fractured femora later by GFP antibody.

3.2 Methods

3.2.1 Isolation and characterization of MSCs

Male Spraque–Dauley (SD) rats were used under the animal license issued by the Hong Kong SAR Government and local ethical committee. Briefly, bone marrow was harvested from femora and layered onto Lymphoprep™ (1.077g/mL; AXIS-SHIELD, Norway) for centrifugation at 400 g, 25 min. The isolated mononuclear cells, were suspended in alpha essential eagle medium (αMEM) containing 10% fetal bovine serum (FBS), 1% Penicillin-Streptomycin-Neomycin

(PSN)(Life technologies, USA), seeded into T75 flasks (Corning, USA) at a density of 1×105 cells/cm2 and incubated at 37℃ in a humidified atmosphere with 5% CO2 /95% air. MSCs from passage 3 or 4 were used for flow cytometry analysis. The antibodies were as follows: PerCP-cy5.5-CD45, FITC-CD31, FITC-CD34, FITC-CD73, FITC-CD44 and PE-CD90 (BD Bioscience, USA). Expanded cultures of the MSC were analyzed for chondrogenic, osteogenic and adipogenic differentiation in vitro to determine multi-potency according to standard conditions as described previously (Chen et al., 2007).

3.2.2 Plasmids construction and lentiviral transfection

Rat Aqp1 gene (GeneBank number: NM_012778.1) was amplified from rat bone marrow MSCs cDNA, cloned into pLenti-MCS-DsRed vector between EcoRI and SalI sites. For Aqp1 and FAK depleted experiments, Aqp1-shRNA, FAK-shRNA and scramble control were designed following previous report (Splinter et al., 2003) and cloned into plentiLox3.7 vector. The correspondent sequences were: Aqp1-shRNA 5'-CTTCTCAAACCACTGGATT-3', Scramble-shRNA 5'-ACTTGCCATACATGACTCT-3', FAK-shRNA 5'-CTGTAGCATAGAGTCAGA-3'. Lentivirus carrying above vectors were produced in 293FT cell line by transient transfected with calcium phosphate transfection method as described before (Song and Li, 2011). Cell supernatants containing lentiviral particles were collected after transfection for 48h and 72h, filtered through 0.45 membrane (Millipore, USA) and subject to further concentration using PEG-it Virus Precipitation kit (System Biosciences, USA) following manufacturer's instructions. MSCs were immortalized by lentiviral transduction of Simian virus 40 plasmid and single colony was selected and amplified for the following experiments. For transduction, 1×10^5 MSCs were seeded into 6-well plate and incubated with lentiviruses together with 8μg/ml polybrene in the

incubator for 24 h. Stable transfected MSCs cell lines were then established in the presence of blasticidin (10μg/ml) for two weeks. The expression of Aqp1 in transfected stable cell lines was examined using quantitative PCR and western blot. In order to trace their fates *in vivo*, Aqp1 transfected MSCs and DsRed MSCs were further labeled with GFP (green fluorescent protein) gen by lentiviral transfection as described above.

3.2.3 Quantitative PCR assays

RNA was extracted using PureLink RNA Mini Kit (Ambion, USA), and contaminated genomic DNA was eliminated with DNAaseI treatment (Invitrogen, USA). The first-strand cDNA was synthesized by M-MLV reverse transcriptase (Promega, USA). Quantitative PCR of Aqp1 was performed using SYBR green PCR master mix (Applied Biosystems, USA), and the primers were as follows: Aqp1-forward: 5'-GCTCACCCGCAACTTCTCA-3' and Aqp1-reverse: 5'-CCTCTATTTGGGCTTCATCTCC-3'. β catenin-forward: 5'-CGAGGACTCAATACC ATTCC-3' and β catenin-reverse: 5'-AGCCGTTTCTTGTAGTCCTG-3'.The correct size of the amplified products was checked by electrophoresis.

3.2.4 Western blot

Western blot examination was carried out as described previously (Song and Li, 2011). In brief, cells at confluence were scraped and lysed in RIPA buffer (Invitrogen, USA). Total protein concentration was quantified by BCA method (Pierce, USA). Equal amount of proteins was ran on 10% SDS-PAGE. Proteins were then transferred from gel into PVDF membrane. After blocking in 5% milk, membranes were incubated with primary antibodies overnight at 4℃. After washing three times with TBST buffer, membranes were then incubated with secondary antibodies conjugated with horseradish peroxidase for 1h at room temperature. Proteins were

visualized with enhanced chemiluminescence (Pierce, USA). The following primary antibodies were used: Aqp1 (1:1000, Santa Cruz, USA), β-catenin (1:3000, BD Biosciences, USA), GAPDH (1:1000, Santa Cruz, USA), β-actin (1:1000, Santa Cruz, USA) and FAK (1:1000, Santa Cruz, USA).

3.2.5 Co-immunoprecipatation

Cells at confluence were washed in ice-cold PBS, scraped and re-suspended with 1ml lysis buffer containing 20 mM Tris-HCl (pH 8), 137 mM NaCl, 10% glycerol, 1% Nonidet P-40 (NP-40), 2 mM EDTA. Cell lysate was pre-cleared by incubated with 50µl protein G-agorose slurry (Invitrogen, USA) for 1h at 4℃. After brief centrifuge (2min at 14,000g at 4℃), supernatant was incubated with 1µg Aqp1 (Santa Cruz, USA) antibody and IgG (Epitomics, Inc., USA) overnight at 4℃, then 50µl protein G-agorose slurry for 4h. The immunoprecipitated samples were recovered after centrifugation, washed three times for 2 minutes at 14,000g at 4℃, each with lysing buffer. The immunoprecipitated samples were boiled 5 min and re-suspended with 2× Laemmli buffer (4% SDS, 10% 2-mercaptoehtanol, 20% glycerol, 0.004% bromophenol blue, 0.125 M Tris-HCl) for SDS/PAGE examination as described previously.

3.2.6 Immunocytochemistry

Cells were fixed with 4% paraformaldehyde for 20 min at room temperature. After washing with PBS, cells were permeated with 0.1% Triton×100 for 10min and blocked with 5% BSA for 30min at room temperature. Then, cells were incubated with primary antibodies Aqp1 (1:100, Santa Cruz, USA) and FAK (1:100, Santa Cruz, USA) over night at 4℃. After washing with PBS, cells were incubated with Fluorescein anti-mouse IgG (1:200, Vector Laboratories, USA)

and Texas Anti-goat IgG (1:200, Vector Laboratories, USA) for 1h at room temperature. Nuclear counterstaining was performed with DAPI Vectashield mounting medium (Vector Laboratories, USA). Immunostaining was observed under Olympus FV1000 confocal microscope.

3.2.7 Rat tibia fracture model and MSCs administration

Rat tibia fracture model was established as previously reported (Ozturan et al., 2011). SD rats (n=10) were used in this study and randomly into two groups. Under general anesthesia, soft tissues were carefully dissected and a transverse osteotomy was performed with a ring-cutter type saw at the mid-shaft of the tibia, which was fixed internally with 21G needle. Fracture quality and position were assessed and confirmed by digital X-ray machine (Faxitron Bioptics, USA). 2 days following fracture, 1×10^6 cells (Aqp1-MSCs and DsRed-MSCs) in 1 ml saline were administrated via tail vein into the fractured rats. All animals were terminated 5 days after the cell administration and the fractured tibia samples as well as other internal organs were harvested, prepared and embedded in paraffin for further examinations.

3.2.8 Cell migration assay

For transwell assay, cells (4×10^4 cells/cm^2) were inoculated into upper layer of transwell insert (BD Falcon, USA) in serum-free medium with 10% FBS contained medium at the bottom layer. After incubating for 10h at 37℃, MSCs at upper layer of membrane were scraped and MSCs at lower layer were stained with 0.05% crystal violet and photographed under microscope. The number of cells was quantified from randomly selected fields.

For wound healing assay, confluent MSCs was scraped by yellow plastic pipette tip. The width of the wound area was measured in triplicate wells under inverse phase contrast microscope.

3.2.9 Rat femora fracture model and MSCs administration

Rat femora fracture model was established and modified from previously report (Bonnarens and Einhorn, 1984). SD rats (n=10) were used in this study and randomly into two groups. Under general anaesthesia, a sterilized Kirschner wire (φ1.2 mm, Stryker, Kalamazoo, USA) was inserted into the medullary canal retrograde ly, following drilling with an 18 G needle. The K-wire was inseted into the proximal femora through the piriformis fossa, and the distal end was bent to prevent distal migration. The fracture was performed at the midshaft of the femora in a custom-designed 3-point-bending apparatus. Fracture quality and position were assessed and confirmed by digital X-ray machine (Faxitron Bioptics, Lincolnshire, USA). 2 days following fracture, 1×106 cells (Aqp1-MSCs and DsRed-MSCs) in 1 ml saline were administrated via tail vein into the fractured rats. All animals were terminated 5 days after the cell administration and the fractured tibia samples as well as other internal organs were harvested, prepared and embedded in paraffin for further examinations.

3.2.10 Mechanical testing of femora

The protocol of four-point bending mechanical testing of femora follows previous report with a few modification (Leung et al., 2009). Briefly, five rat femora from Aqp1-MSCs and DsRed-MSCs groups were harvest 4 weeks after cell administration to test immediately or stored in -20℃ with saline. After removing the Kirschner wire and dissecting soft tissues, the femora were loaded in the anterior-posterior position with the inner and outer range of the blades from 8 to 20 mm and the long axis of the femora perpendicular to the blades. The maximal force, the energy

and stiffness of each sample were recorded and analyzed by commercial software (QMAT Professional Material testing software. Hounsfield Test Equipment Ltd. Redhill, Surrey, UK).

3.2.11 Micro-CT analysis of femora

The protocol of Micro-CT analysis of femora follows previous report with a few modification (Leung et al., 2009). After removal of soft tissues, the femora (n=4 for each group) were scanned by micro-CT system (mCT-40, Scanco Medical, Bruttisellen, Switzerland) with the scope of 5 mm proximal and 5 mm distal to the fracture line at a resolution of 16 mm per voxel. Contoured region of interest (ROI) was chosen in two-dimensional (2D) CT images, while a low-pass Gaussian filter (Sigma=1.2, Support=2) was used for 3D reconstruction of mineralized tissue. To discriminate newly formed mineralized bone from old cortices, the low- and high-density mineralized tissues were set with distinct thresholds (high attenuation=325, low attenuation=120). The low- and high-density mineralized tissues were evaluated quantitatively from the mid 260 slices of the 2D images. Morphometric parameters were applied for evaluation of total tissue volume (TV), total bone volume (BV) and normalized percentage of the tissue volumes BV/TV.

3.2.12 Statistical analysis

Values were presented for each group as means ± SEM. The Student's t-test and one-way ANOVA were used for comparison of mean values between different groups. P value was calculated with SPSS16.0, and $P<0.05$ was considered be statistical significant.

3.3 Results

3.3.1 Establishment of stable Aqp1 depleted and overexpressing MSCs

MSCs were isolated from rat femora marrow and characterized by using flow cytometry analysis of CD45 (2%), CD31(1.5%), CD34 (2%), CD73 (80%), Cd44 (95%) and CD90 (95%)(Figure 3.1A), which were further verified by tri-lineages differentiation assay (data not shown). Considering the limited passage number of normal MSCs and variation of different batches of MSCs, we chose to use the immortalized MSCs by transfection of SV40 as described before (Hamada et al., 2005; Singer et al., 1987). These immortalized MSCs had similar cell surface markers expression pattern and tri-lineage differentiation potential (data not shown). All the following experiments were carried out using immortalized rat MSCs. We delivered Aqp1 specific shRNA and Aqp1 coding sequence by lentiviral transfection into MSCs and developed stable Aqp1 depleted MSCs and Aqp1 overexpressing cell lines designed as Aqp1-shRNA MSCs with Scramble-shRNA MSCs as control and Aqp1-MSCs with DsRed-MSCs as control respectively. The transfection efficiency of transduction was high without any apparent cell death and morphology change (Figure 3.1B and E). Aqp1 shRNA transduction depleted expression of Aqp1 both in mRNA and protein level (Figure 3.1 C and D). Similarly, Aqp1 transduction highly regulated expression of Aqp1 both in mRNA and protein level (Figure 3.1F and G). The expression status of Aqp1 did not change after successive passages. We also confirmed that depletion or overexpression of Aqp1 had no effect on MSCs tri-lineage differentiation (data not shown).

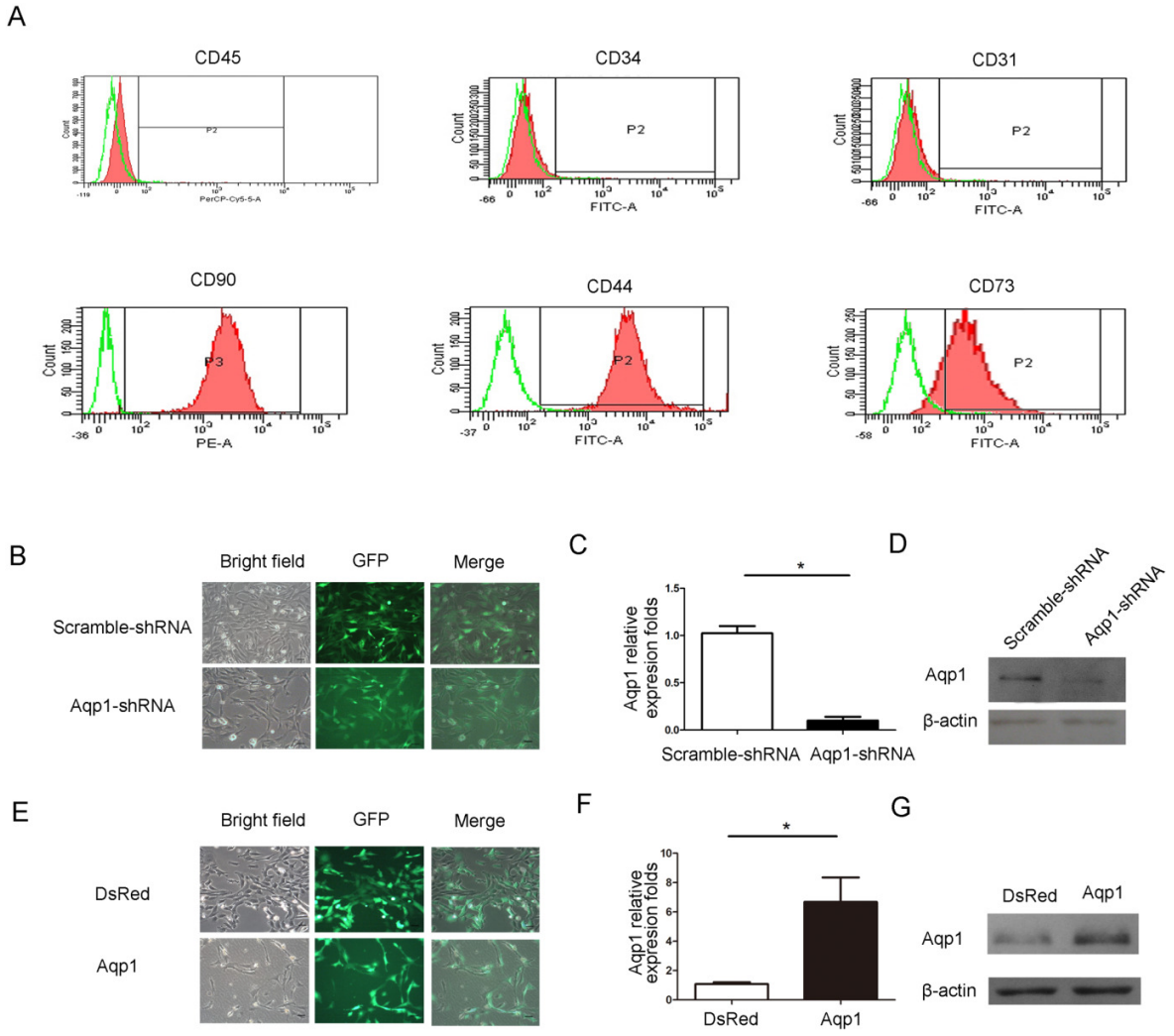

Figure 3.1 CD markers expression of MSCs and establishment of the stable Aqp1 overexpressed and depleted MSCs cell line.

A: MSCs from passage 3 or 4 were stained with PerCP-cy5.5-CD45, FITC-CD31, FITC-CD34, FITC-CD73, FITC-CD44 and PE-CD90 antibodies and detected by flow cytometry (red). Isotype IgG was used as negative control (green) to gate positive part of CD45 (2%), CD31(1.5%), CD34 (2%), CD73 (80%), CD44 (95%) and CD90 (95%)(P2). **B:** The immortalized MSCs were transduced with GFP labeling Aqp1-shRNA and control scramble-shRNA lentiviral vector, showing that the stable cell lines were established with high transfection efficiency. **C:** The expression of Aqp1 after transduction was quantified with real time PCR (B, n=3). **D:** Western Blot of Aqp1 after transfection of Aqp1-shRNA and Scramble-shRNA. **E:** Aqp1 overexpressing MSCs cell lines were established by

lentiviral transfection carrying Aqp1 coding sequence. **F**: The expression of Aqp1 after transduction was quantified with real time PCR (n=3). **G**: Western Blot of Aqp1 after transfection of Aqp1-shRNA and Scramble-shRNA. Scale bar: 100μm. All error bars represent SEM (* $p<0.05$).

3.3.2 Aqp1 augments MSCs migration *in vitro*

In order to assess the role of Aqp1 in MSCs migration, we examine the effect of Aqp1 depletion on MSCs migration in vitro. MSCs migration ability was evaluated by transwell assay. Migrated MSCs from lower layer of membrane were fixed and stained. MSCs from randomly selected fields were calculated and the number of Aqp1-shRNA MSCs in the lower layers of membrane was significant less than of control group (Figure 3.2A). In addition, wound healing assay was also performed by scraping the confluent cell layer. After 8 hours, the distances between the wound edges in Aqp1-shRNA MSCs were significantly wider than that of control cells (Figure 3.2C). Transwell assay indicated that overexpression of Aqp1 increased the number of trans-membrane MSCs compared to the control group (Figure 3.2B). Consistent with transwell results, the distances between the wound edges in Aqp1-MSCs were significantly smaller than that of control group (Figure 3.2D). Furthermore, we examined migration of ability of MSCs from primary culture after overexpression and knockdown of Aqp1 by transwell. The number of trans-membrane MSCs was quantified as described above. As expected, higher number of MSCs migrated across the membrane after overexpressing Aqp1, while lower number of MSCs migrated across the membrane after silencing Aqp1(Figure 3.2E and F). Taken together, the data revealed that Aqp1 enhanced MSCs migration ability *in vitro*.

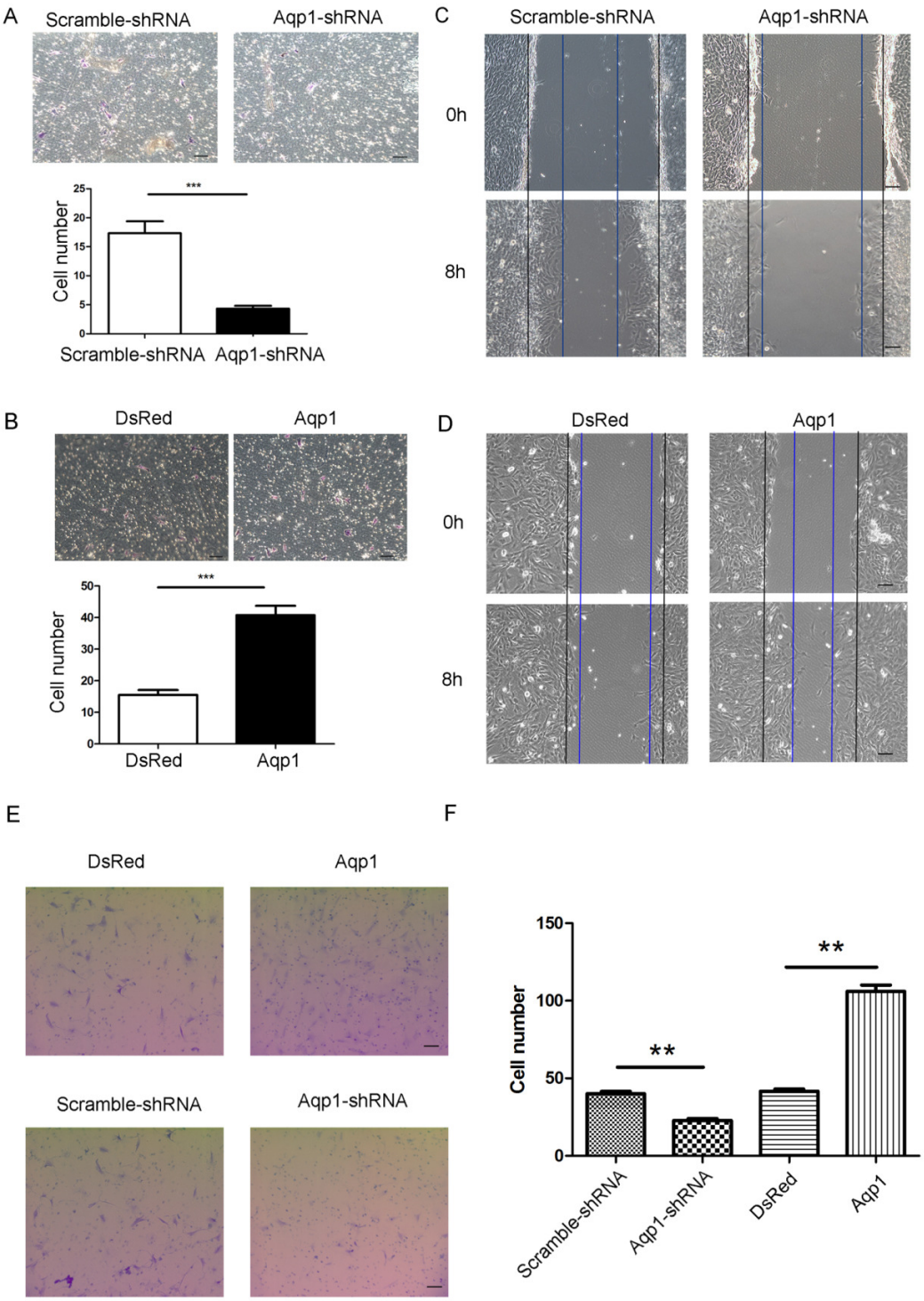

Figure 3.2 Migration assays of Aqp1 depleted and overexpressed MSCs.

A: Migrated Aqp1 depleted from transwell membrane were stained by crystal violet (purple) and quantified (n=5). **B:** Migrated overexpressed Aqp1 MSCs from transwell membrane were stained by crystal violet (purple) and quantified (n=5). **C**: Wound healing of Aqp1 depleted MSCs were recorded under contrast microscope with black and blue lines representing start and end (8h) positions of MSCs after scraping. **D**: Wound healing of overexpressed MSCs were recorded under contrast microscope with black and blue lines representing start and end (8h) positions of MSCs after scraping. **E:** Transwell migration assays were also performed on MSCs from primary culture after transfection of Aqp1 and Aqp1-shRNA. **F:** Migrated MSCs from bottom lower of the membrane were stained with crystal violet (purple) and quantified. Overexpressing Aqp-1 in MSCs has significantly enhanced their cell migration ability *in vitro*. Scale bar: 100μm. All error bars represent SEM (* $p<0.05$).

3.3.3 Aqp1 facilitates MSCs homing to bone fracture site

In order to test the effect of Aqp1 on MSCs migration in vivo, we administrated GFP labeled Aqp1-MSCs into rat with tibial fracture and observed the fate of MSCs. Established tibial fracture model was confirmed by X-ray image (Figure 3.3A). MSCs were administrated into fractured rat at 2 days following fracture (osteotomy surgery) via tail vein. After 5 days, all animals were terminated and the fractured tibiae harvested and prepare for paraffin histology. The GFP-positive cells at fracture site were detected using immunohistochemistry and quantified using imaging software. We found that most of MSCs resided in lung, GFP positive MSCs was not seen in contralateral tibia (Figure 3.4). Nonetheless, large number of MSCs was found at the cartilagious tissues at fracture site, (Figure 3.3B). The percentage of GFP positive cells at fracture site was calculated and compared among the Aqp1-MSCs and DsRed-MSCs groups, and there was significantly higher GFP positive cells in the Aqp1-MSCs treated group than that of the DsRed-MSCs treated group.

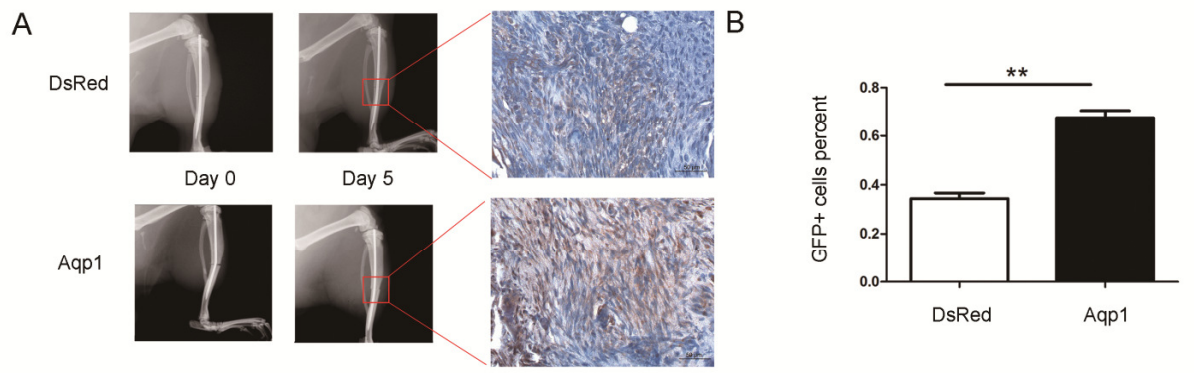

Figure 3.3 Immunohistochemistry of administrated MSCs at the fracture site

A: X-rays images depicted tibial fracture after surgery (left) and 5 days later (right). There was only soft callus in the fracture gap at 5 days after fracture and GFP positive cells were seen at the boxed areas, showing more GFP cells in the Aqp1-MSCs group. **B:** The percentage of GFP positive cells was quantified by the ratio of brown cells (GFP positive) to whole cells (blue cells plus brown cells) auto-selected by software image pro plus 6.0 in the randomly selected fields, showing that there was significantly more GFP-MSCs in the Aqp-1 MSCs group (n=5). Scale bar: 50μm. All error bars represent SEM (*p<0.05).

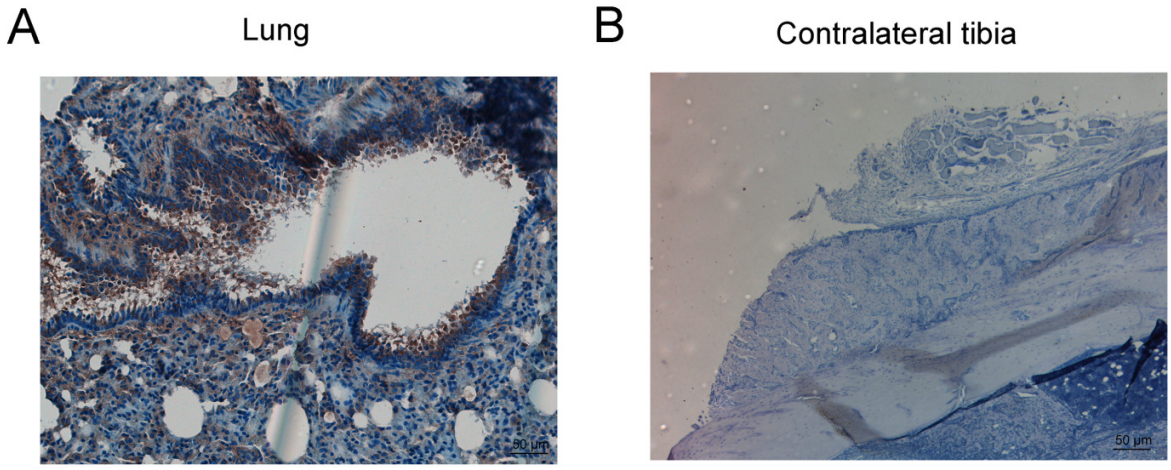

Figure 3.4 Immunohistochemistry of administrated MSCs of lung and contralateral tibia

A: Immunohistochemistry of GFP in lung of fractured rats **B:** Immunohistochemistry of GFP in in contralateral tibia of fractured rats. Scale bar: 100μm**.**

3.3.4 Beta-catenin is involved in Aqp1 mediated migration of MSCs

To explore underlying mechanism of Aqp1 in MSCs migration, we examine expression of β-catenin both in Aqp1-shRNA MSCs and Aqp1-MSCs. Depletion of Aqp1 in MSCs lead to degradation of β-catenin (Figure 3.5A). To address whether Aqp1 could contribute to stability of β-catenin, we overexpressed Aqp1 in MSCs and found overexpression of Aqp1 could upregulate expression of β-catenin (Figure 3.5B). This regulation was restricted on protein level, as overexpression of Aqp1 had no effects on mRNA level of β-catenin (Figure 3.6). Furthermore, we demonstrated that Aqp1 was co-immunoprecipitated with β-catenin, which implied their physical interaction was likely beneficial for β-catenin stability (Figure 3.5C and 3.8C).

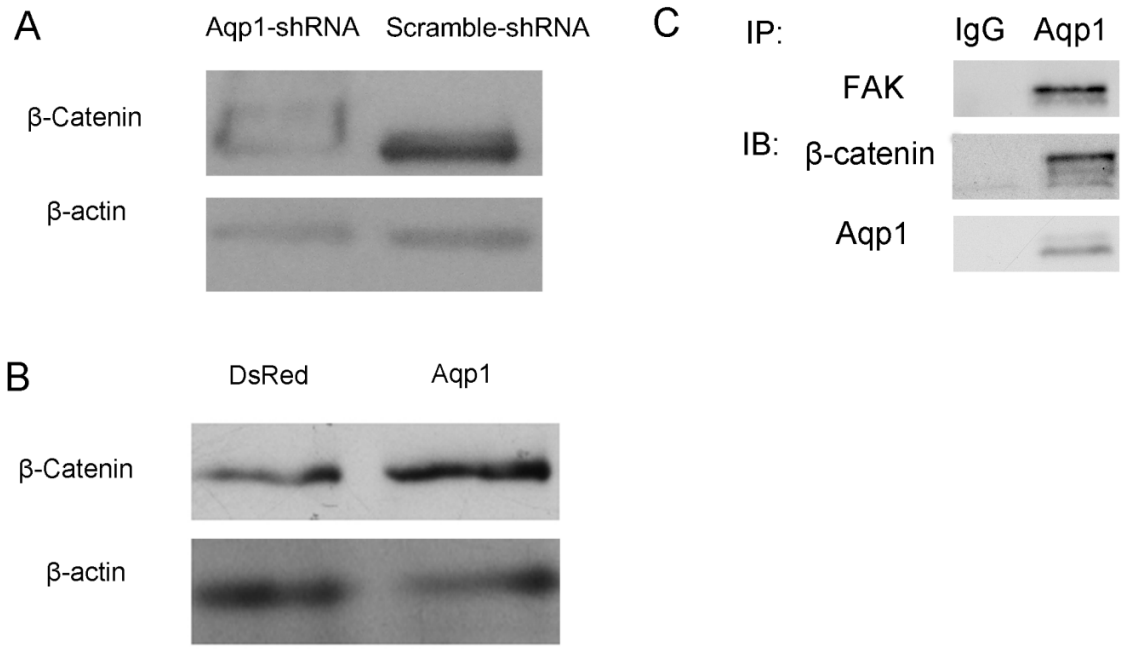

Figure 3.5 Aqp1 affects expression of β-catenin.

A: Western blot of β-catenin of in Aqp1 depleted MSCs **B:** Western blot of β-catenin of in Aqp1 overexpressing MSCs. **C:** Cell lysate was immunoprecipitated with Aqp1 antibody and blotted with β-catenin, FAK and Aqp1 antibodies.

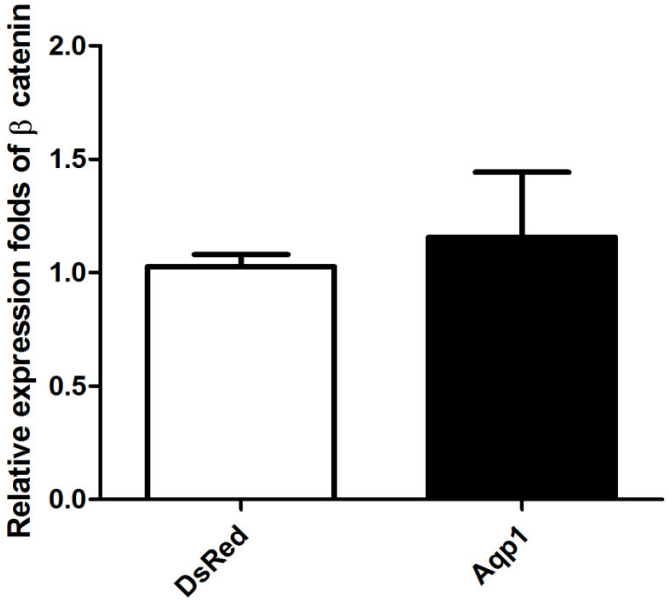

Figure 3.6. Real time PCR of β-catenin in aqp1 overexpressing MSCs.

The mRNA level of β-catenin was detected from Aqp1-MSCs and DsRed-MSCs by real time PCR. No significant difference was found.

3.3.5 Aqp1 regulates migration of MSCs through FAK not CXCR4

In addition to β-catenin, we also tested other pivotal regulators of cell migration like focal adhesion kinase (FAK) and CXCR4. The FAK level instead of CXCR4 increased when Aqp1 was overexpressed. Depletion of Aqp1 led to degradation of FAK rather than CXCR4 (Figure 3.7A and 3.7B). This meant that Aqp1 regulated expression of FAK instead of CXCR4. To

further explore the relationship between Aqp1 and FAK, we traced their location in cell by labeling with fluorescent antibody and demonstrated that Aqp1 was co-localized with FAK (Figure 3.7C), which was further confirmed by co-immunoprecipitation assay (Figure 3.5C and 3.8B).

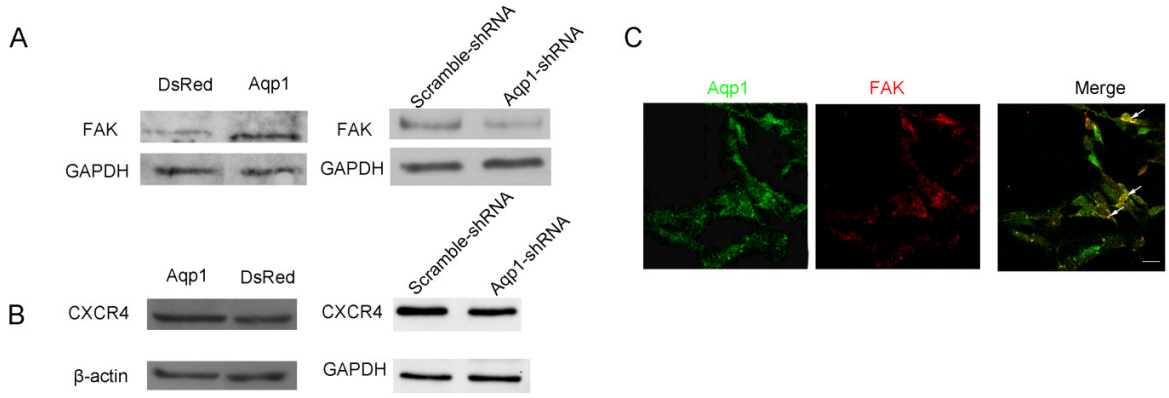

Figure 3.7 Relationships of FAK, CXCR4 and Aqp1.

A: Western blot of the expression FAK in Aqp1 depleted and overexpressing MSCs. **B**: Western blot of the expression CXCR4 in Aqp1 depleted and overexpressing MSCs. **C**: The localization of Aqp1 (green) and FAK (red) labeled with fluorescent antibodies was displayed by confocal microscope. Co-localization area of Aqp1 and FAK was highlighted (arrow). Scale bar: 100μm.

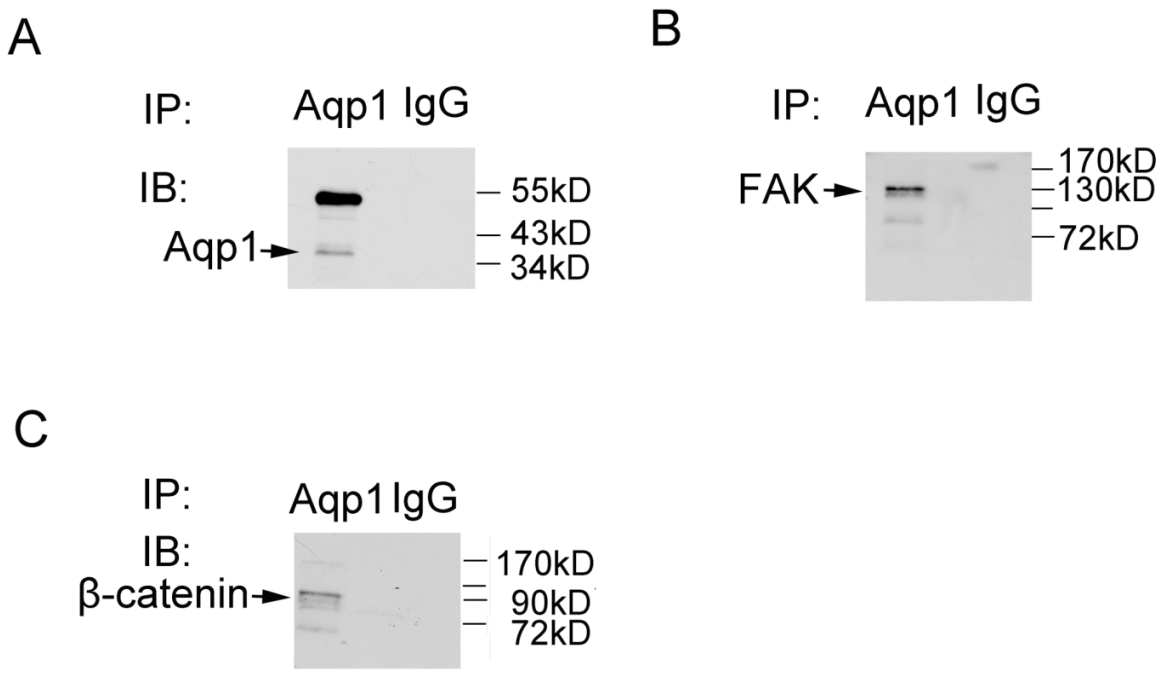

Figure 3.8 Immunoprecipitation data of Aqp1, β-catenin and FAK.

Total proteins of MSCs were collected and pull down by Aqp1 antibody and IgG control. **A:** The co-immunoprecipitation product was blot with Aqp1 antibody. **B:** The co-immunoprecipitation product was blot with FAK. **C:** The co-immunoprecipitation product was blot with β-catenin antibody.

3.3.6 Depletion of FAK abolished Aqp1 effects on MSCs migration

To uncover whether FAK was indispensable for Aqp1 mediating MSCs migration, we silenced FAK expression in Aqp1-MSCs by introducing lentiviral FAK-shRNA. The migration of MSCs was examined by transwell method and found that overexpression of Aqp1 enhanced MSCs migration, whereas depletion of FAK dramatically reduced migration ability of DsRed-MSCs and Aqp1-MSCs, which implied that depletion of FAK in Aqp1-MSCs counteracted Aqp1

enhancing effects on MSCs migration. The migration ability had no significant difference between DsRed-MSCs and Aqp1-MSCs after silencing expression of FAK, which further demonstrated that FAK was downstream of Aqp1 (Figure 3.9).

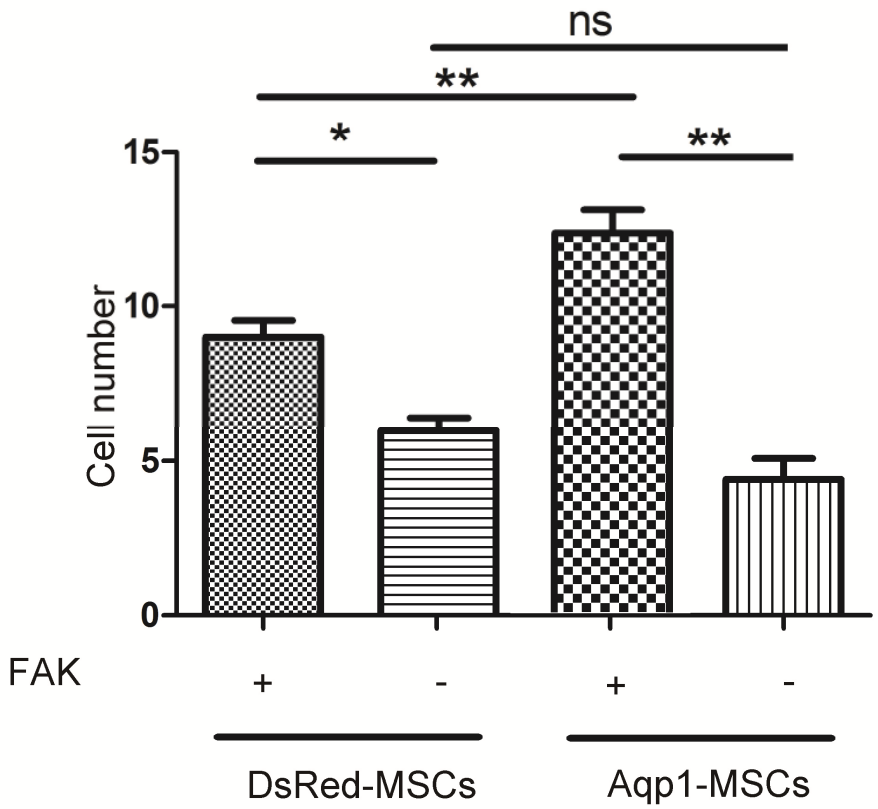

Figure 3.9 Transwell analysis of Aqp1-MSCs after depletion of FAK.

Migrating MSCs were assessed by transwell and quantified; the data showed that the deletion of FAK expression in MSCs diminished cell migration ability. FAK gene expression was silenced in Aqp1-MSCs by lentiviral transfection. All error bars represent SEM (n = 5, *p < 0.05, **p < 0.01, ns: none significance).

3.3.7 Establishment of femora fractured rat model

In this study, 10 SD rats (male, 8 weeks) for each group were used for femora fractured model as described above. The X-ray image of the femora from DsRed and Aqp1 groups after surgery and

4 weeks later showed obvious callus formation in both groups (Figure 4.1). However, it has not significant difference of both groups in callus size after 4 weeks.

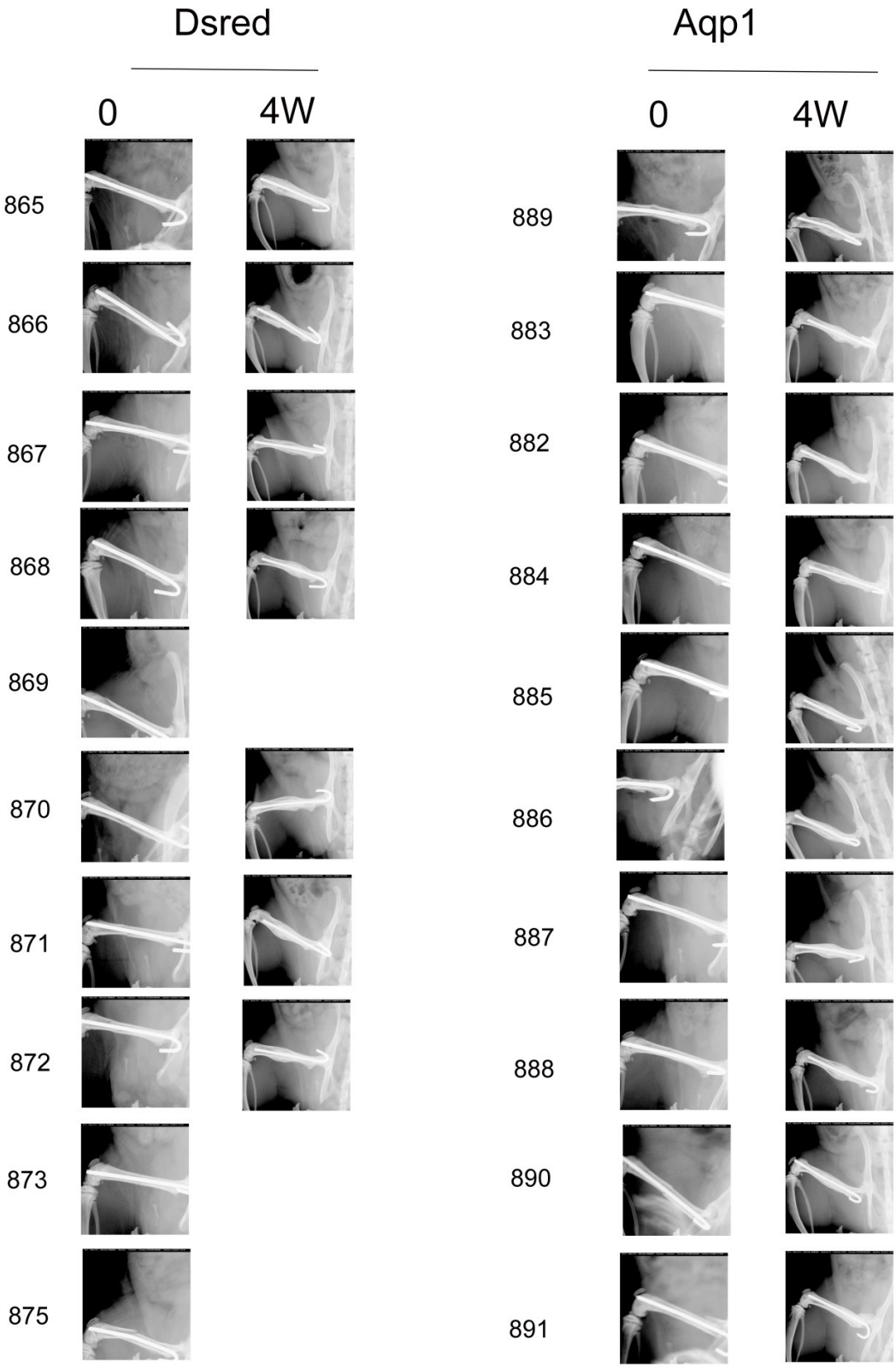

Figure 4.1 X-ray image of femora after surgery

Right femora fracture of each rat from Dsred (No.865-873, 875) and Aqp1 (No.882-891) groups was created using 3 points binding apparatus and observed under digital X-ray machine.

3.3.8 Histochemistry of fractured femora

To assess the bone healing outcome, fractured femora were subjected to histochemistry examination. In H&E staining, new woven bone was observed in fracture site from Dsred and Aqp1 groups 4 weeks after surgery, implying a typical bone remodeling. There was no significant difference between Dsred and Aqp1 groups in regard of the amount of mineralized tissue in callus (Figure 4.2A). When subject to GFP staining, samples from both groups had no GFP signal in callus (Figure 4.2B).

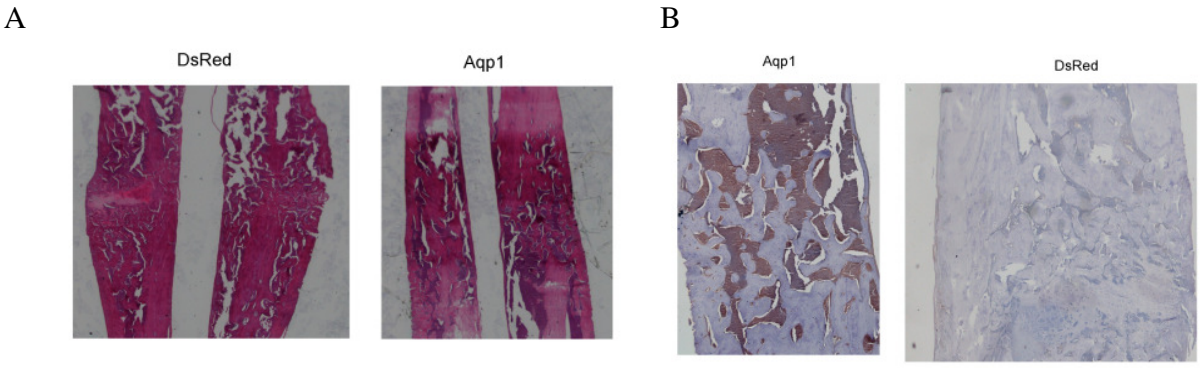

Figure 4.2 H&E staining and GFP immunohistochemistry of callus

A: Sections of fractured femora from both Dsred and Aqp1 groups (n=5) were stained with hematoxylin and eosin. **B**: Sections of fractured femora from both Dsred and Aqp1 groups (n=5) were stained GFP for immunohistochemistry.

3.3.9 Mechanical testing

As one type of functional analysis, mechanical testing is considered to be a gold standard for evaluation of bone healing outcome. The e-modulus parameter defined by the slant of force

/distance curve was higher in Aqp1 group than DsRed group, indicating femora from Aqp1 group had a higher stiffness (E-modulus) than Dsred group (Figure 4.3A). However, the maximal force and energy, representing the strength of bone, had no significant difference between these groups (Figure 4.3B, C).

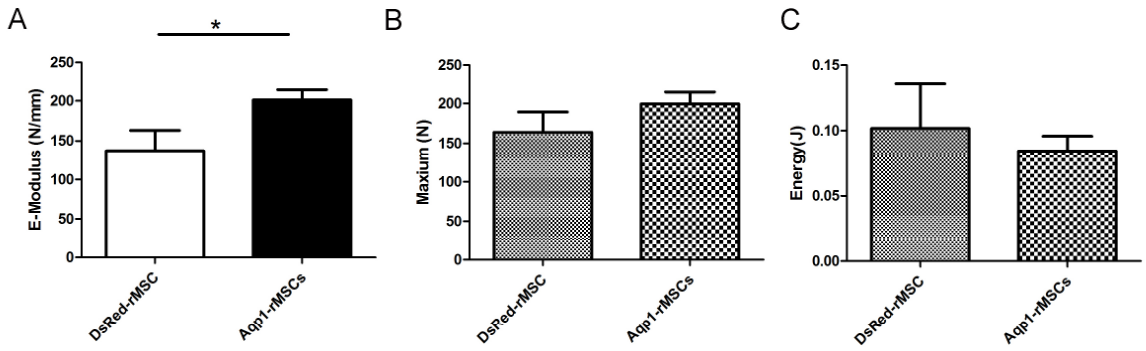

Figure 4.3 Mechanical testing of fractured femora

A: E-modulus of femora without fixation were bent in 4 points apparatus using 250N sensor. **B**: maximal force femora without fixation were bent in 4 points apparatus using 250N sensor. **C:** Energy of femora without fixation were bent in 4 points apparatus using 250N sensor. All the data were recorded by QMAT Professional Material testing software. The difference was calculated by *student t-test* n=5, * $P<0.05$.

3.3.10 Micro-CT analysis

The structure and bone density of fractured femora from Aqp1 group than DsRed group were further analyzed by micro-CT by scanning the area of callus. The callus bone density of femora from Aqp1 group represented by BMD parameter was significantly higher than femora from DsRed group, while the new bone formation represented by BV/TV parameter had no significant difference (Figure 4.4A and 4.4B). To examine the callus in more detail, we performed 3D

reconstruct based on the scanning data and found notable groove existed at the callus area in both Aqp1 and DsRed groups without obvious significant difference (Figure 4.4C).

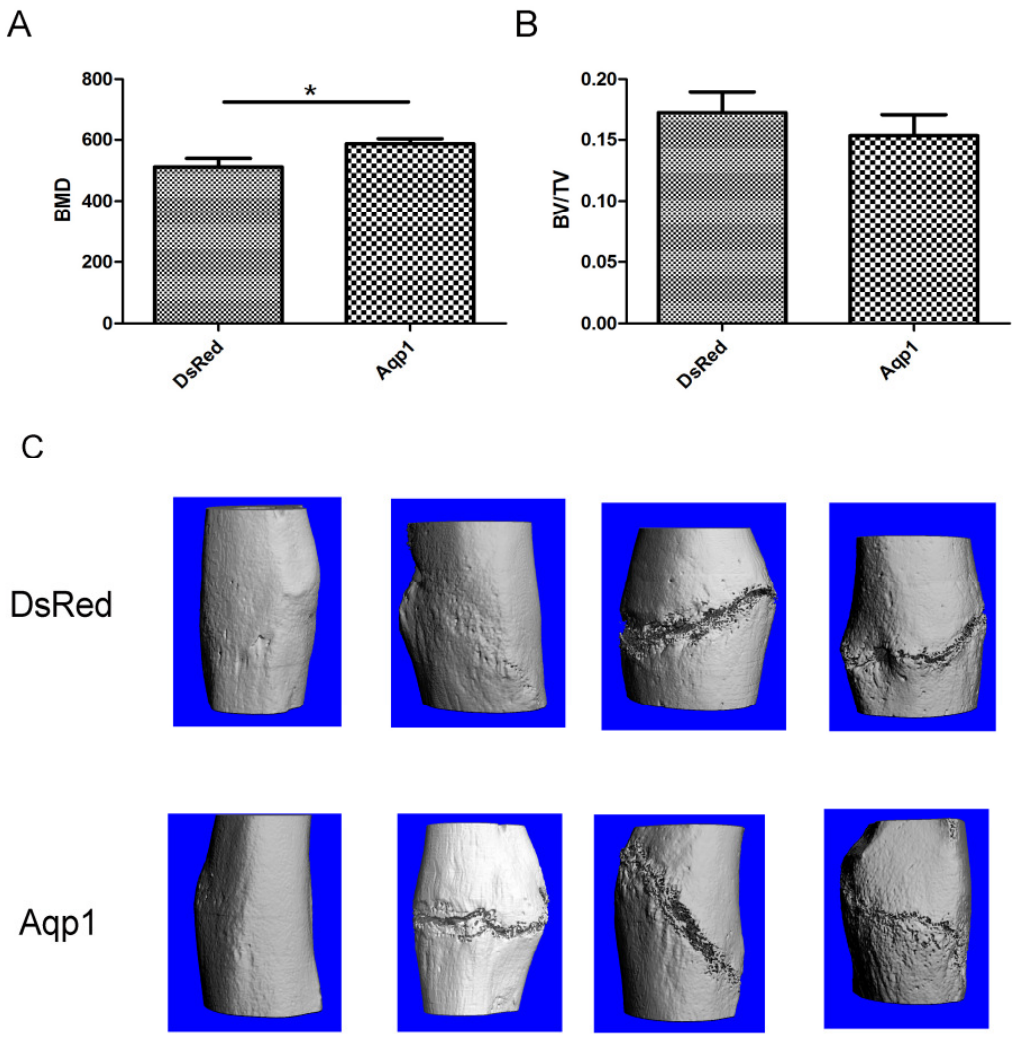

Figure 4.4 Micro-CT analysis of fractured femora

The areas of femora callus were scanned for 260 slices per sample by microCT. **A-C:** Bone density(BMD, **A**), new bone formation (BV/TV, **B**) and 3D reconstruction (**C**) were generated by software. The difference was calculated by *student t-test* n=5, * P<0.05.

3.4 Discussion

This study reports Aqp1 promotes MSCs migration by up-regulating expression of β-catenin and FAK. After administrating into rat, Aqp1-MSCs migrated much more efficiently into fracture site. Furthermore, our study also reveals Aqp1 interacted with FAK and β-catenin directly.

As one of water channel molecules, Aqp1 is also involved in endothelia cell migration and cancer invasion (Verkman et al., 2008). In our study, we reported that Apq1 contributed to MSCs migration. Overexpression of Aqp1 accelerated MSCs movement, while silencing Aqp1 reduced its migration ability. Moreover, we designed to test migration capacity in vivo by administrating the Apq1-MSCs into tibia fracture rat. Previous studies have shown that MSCs was recruited systemically in bone fracture healing (Shirley et al., 2005) and both systemic and local MSCs administration enhanced fracture healing (Granero-Moltó et al., 2009; Quarto et al., 2001). Based on these studies, we evaluated migration ability of MSCs by comparing the quantity of exogenous MSCs at fracture site. The results showed significant more MSCs at fracture site in Aqp1-MSCs treated group, suggesting Aqp-1-MSCs has enhanced tropism towards to wounded tissue areas in vivo.

Utilizing MSCs transplantation to enhance fracture healing has been reported before, and the MSCs retention ability at the fracture site is essential for enhancing healing process (Kumar and Ponnazhagan, 2012). In this study, we chose only one time point, which was 5 days after fracture (3 days after MSCs administration) to examine the cell migration ability differences

between the Aqp-1 MSCs and control MSCs, and confirmed that more MSCs homed to the fracture gap in the Aqp-1 MSCs group. One can assume that the fracture healing may be superior in the Aqp-1 MSCs group as more MSCs reached in this group. Since the primary aim of the current study was to test the migration ability of Aqp-1 MSCs in vivo, we did not purposely compare the fracture healing outcome, and this will be subjects for our future studies. Multiple factors have been identified to regulate MSCs migration, like CCR1, mi335, HIF-1alpha, and SDF/CXCR4 (Huang et al., 2010; Liu et al., 2012; Raheja et al., 2011; Tome et al., 2011). Among these factors, SDF/CXCR4 was an indispensable universal pathway to regulate migration of many cell types, which had been elucidated thoroughly in MSCs (Ghosh et al., 2012; Wendel et al., 2012; Yu et al., 2012). In the current study, we demonstrated Aqp1 could regulate MSCs migration independent of the SDF-1/CXCR4 pathway, indicating that Aqp1 may be a new factor controlling MSCs migration capacity that was not previously known.

The role of Aqp1 on cell migration is poor understood. One study led by Verkman proposed that aquaporins might provide the major pathway for water entry into lamellipodia drived by local osmotic gradient (Saadoun et al., 2005). The alternative mechanism may be that Aqp1 promoted cell migration through lin7 and β-catenin, which decreased when depletion Aqp1 in endothelial cells. The treatment of Aqp1 silenced cells with the proteasome inhibitor MG132 enhanced the recovery of β-catenin, which implies that lack of Aqp1 targets the Lin-7/beta-catenin complex to proteolytic degradation (Monzani et al., 2009). In this study, we found that β-catenin was downregulated after silencing Aqp1 and upregulated after overexpressing Aqp1 in MSCs. This implies that the existence of Aqp1 partially contributes to posttranslational level of β-catenin, as overexpression of Aqp1 did not affect β-catenin mRNA level. However, the precise relationship between Aqp1 and β-catenin still need further study.

Next, we found that Aqp1 also regulated expression of FAK, which was not known before. FAK binds directly to the intracellular domain of the β1-integrin subunit (Lechertier and Hodivala-Dilke, 2012). The mechanism of FAK-dependent cell migration is that FAK regulates the disassembly of focal adhesions as well as versatile regulators like Rac, Rho and N-WASP, etc (Wu et al., 2004; Yang and Kim, 2012). We showed that FAK physically interacted and co-localized with Aqp1, indicating there may be functional cross talking of FAK and Aqp1 in cell migration process. Our data showed that overexpression of Aqp1 increased expression of FAK, while silencing Aqp1 decreased expression of FAK. The regulation was only seen at translational level as overexpression of Aqp1 did not alter mRNA level of FAK, suggesting that Aqp1 may enhance the stability of FAK. Anchoring at focal adhesion site, FAK communicates with many other signal events like Ras, Src and the extracellular signal-regulated kinase-2 (ERK2)/mitogen-activated protein kinase (MAPK) cascade (Mitra et al., 2005), how Aqp1 interacts and activates FAK to elicit downstream signal events still remains largely unknown and warrants for the future studies.

Meanwhile, we demonstrate that Aqp1 overexpressing MSCs enhance the outcome of bone fracture healing in terms of bone stiffness and bone density, while the structure and morphology of callus have no significant difference when compared to DsRed group.

Bone fracture is a prevalent disease, and the healing is a unique repair process in which the events of endochondral and intramembranous bone formation follow a specific time sequence. While bone was formed by osteoblast differentiated from MSCs, administration of MSCs in fracture site either systemically or in situ was shown to be beneficial for fracture healing of mice model (Obermeyer et al., 2012). In above sections, we have demonstrated that overexpression of Aqp1 allow MSCs reached tibial fracture site much higher after administrating systemically. In

order to assess the outcome of bone healing, we choose the rat model with femora fracture as previous reports (Cheung et al., 2013). Undale and the colleagues reported bone marrow MSCs treated group had superior effects on biomechanical properties in the nonunion nude rat model (Undale et al., 2011). In our study, we found the higher stiffness of femora from Aqp1-MSCs treated group, though the maximal force and energy had minimal difference compared to DsRed control. The insights of the properties of fractured fermora come from the further analysis of callus areas by micro-CT. The bone density of femora from Aqp1 treated group was higher compared to control, while the 3D construction and BV/TV have no significant difference. This means higher mineralized tissue was formed in Aqp1-MSCs treated group. However, the callus from both groups was not obvious, and the GFP labeled MSCs was undetectable probably due to the last remodeling stage. In addition, the new woven bone from both Aqp1-MSCs treated and Dsred-MSCs treated group have no significant difference. Taken together, Aqp1 empowers MSCs move faster to reach the fracture site, which contribute to the better healing outcome.

Chapter4 Sm51 enhances osteogenic differentiation of MSCs

The purpose of this chapter is to answer----

What is the role of Sm51 in osteogenic differentiation of BM-MSCs?

4.1 Chapter introduction

Bone is formed through either intramembranous or endochondral ossification, which were mainly carried out by osteoblast(Harada and Rodan, 2003), the main cell type after osteogenic differentiation of bone marrow derived mesenchymal stem cells (MSCs). As the adult stem cells, MSCs is characterized for decades and applied for therapy of many diseases due to its multiple differentiation potential and low immunogenicity after transplantation (Chamberlain et al., 2007). Dysfunction of differentiation of MSCs, such as differentiation into adipocyte, at some point leads to rapid bone loss in osteoporosis patients.

The osteogenic differentiation of bone marrow mesenchymal stem cells was regulated by many molecules at different levels including extracellular signals and transcription factors. BMP2 and Wnt pathways play key role in inducing osteogenic differentiation of MSCs (Etheridge et al., 2004; Wan and Cao, 2005), which were further integrated with internal transcription factors to proceed to osteogenic differentiation. Meanwhile, lots of transcript factors were identified such as Runx2, Msx2, OSX, TAZ(Long, 2012), among which runx2 was the master regulator to orchestrate multiple signals and transcription factors (Schroeder et al., 2005). Runx2 expression occurs at an early stages of the mesenchymal stem cell lineage and is evident in the developing embryo by E9.5 prior to bone formation (Ducy et al., 1997). The importance of Runx2 is obvious as homozygous deletion of Runx2 totally impaired skeletal development in mice(Komori et al., 1997). Another new mechanism in regulating osteogenic differentiation of MSCs by histone demethylases KDM4B and KDM6B with regard to epigenetic events has been proposed recently(Ye et al., 2012). While significant progress has been made in understanding of molecular regulation of MSCs differentiation at transcription level, very little is known with regard to RNA splicing events that control MSCs commitment to bone.

Using microarray technology to screen differential gene expression profile between bone marrow derived MSCs and peripheral blood derived MSCs, Our lab characterized Sm51 gene. Identified as the tissue specific small nuclear ribonucleoprotein-associated polypeptide N (SNRPN), Sm51 mainly presents in the U-2 snRNP of RNA splicing complex (Huntriss et al., 1993; McAllister et al., 1988). Unlike ubiquitously expressed SmB/B', Sm51 was only detected in several tissues and responsible for splicing the calcitonin/CGRP transcript in the brain(Horn et al., 1992). Moreover, a lack of Sm51 resulted in a Prader-Willi-Syndrome(PWS) like phenotype in murine model (Cattanach et al., 1992) and human study, which was characterized by short hands and feet , low bone mineral density and so on (Butler et al., 2001; Kuslich et al., 1999). Considering the high conserved property of Sm51 in murine and human and its critical role in PWS disease, we hypothesize Sm51 may play a role in osteogenic differentiation of MSCs. In this study, we demonstrate that Sm51 promotes osteogenic differentiation of MSCs, providing a new understanding of osteogenesis and regulation of runx2 at RNA splicing level.

4.2 Methods

4.2.1 Plasmids construction and lentiviral transfection

Rat Sm51 gene (GeneBank number: NM_031117.1) was amplified from rat bone marrow MSCs cDNA, cloned into pLenti-MCS-DsRed vector between EcoRV and SalI sites. For Runx depleted experiments, 3 pairs of Runx2-shRNA and scramble control were designed and cloned into plentiLox3.7 vector. The correspondent sequences were: Runx2-sh-1 5'-GGACAGAGTCAGATTACAG-3', Runx2-sh-2 5'-GCTTGATGACTCTAAACCT-3' Runx2-sh-3 5'-GCACTATCCAGCCACC-3' Scramble-sh 5'-ACTTGCCATACATGACTCT-3', Lentivirus carrying above vectors were produced in 293FT cell line by transient transfected with

calcium phosphate transfection method as described before (Song and Li, 2011). Cell supernatants containing lentiviral particles were collected after transfection for 48h and 72h, filtered through 0.45 membrane (Millipore, Billerica, USA) and subject to further concentration using PEG-it Virus Precipitation kit (System Biosciences, Mountain View, USA) following manufacturer's instructions. Rat and human derived MSCs were immortalized by lentiviral transduction of Simian virus 40 plasmid and single colony was selected and amplified for the following experiments. As the amino acide sequence of human Sm51 gene is identical to rat Sm51 gene, we used rat Sm51 gene for human MSCs transduction. For transduction, 1×10^5 MSCs were seeded into 6-well plate and incubated with lentiviruses together with 8μg/ml polybrene in the incubator for 10 h. Stable transfected MSCs cell lines were then established in the presence of blasticidin (10μg/ml) for two weeks. The expression of Sm51 in transfected stable cell lines was examined using quantitative PCR and western blot.

4.2.2 Osteogenic differentiation

MSCs were seeded in 6-well plate at a concentration of 1×10^5 cells per well. After incubating in the α-MEM for two or three days, the medium was changed into osteogenic induction medium (OIM) containing 100 nmol/L dexamethasone, 10 mmol/L beta-glycerophosphate, and 0.05 mmol/L l-ascorbic acid-2-phosphate. The medium refreshed twice a week. The osteogenic differentiation was evaluated by real-time PCR and 2% alizarin red S staining (sigma, St. Louis, USA).

4.2.3 Quantitative PCR assays

RNA was extracted using PureLink RNA Mini Kit (Ambion, Guangzhou, China), and contaminated genomic DNA was eliminated with DNAase I treatment (Invitrogen, Grand Island,

USA). The first-strand cDNA was synthesized by M-MLV reverse transcriptase (Invitrogen, Grand Island, USA). Quantitative PCR of Aqp1 was performed using SYBR green PCR master mix (Applied Biosystems, Carlsbad, USA), and the primers were listed at table 1. Each experiment was performed three times independently. The correct size of the amplified products was checked by electrophoresis.

4.2.4 Western blot

Western blot examination was carried out as described previously (Song and Li, 2011). In brief, cells on confluence were scraped and lysed in RIPA buffer (Invitrogen, Grand Island, USA). Total protein concentration was quantified by BCA method (Pierce, Rockford, USA). Equal amount of proteins was run on 10% SDS-PAGE. Proteins were then transferred from gel into PVDF membrane. After blocking in 5% milk, membranes were incubated with primary antibodies overnight at 4℃. After washing three times with TBST buffer, membranes were then incubated with secondary antibodies conjugated with horseradish peroxidase for 1h at room temperature. Proteins were visualized with enhanced chemiluminescence (Pierce, Rockford, USA). The following primary antibodies were used: Runx2 (1:1000, Cell Signaling Technology, Danvers, USA), GAPDH (1:1000, Santa Cruz Biotechnology, Santa Cruz, USA).

4.2.5 RNA immunoprecipitation

Flag coding sequence was insert into vector pLenti-MCS-Sm51 to create Flag-Sm51 recombinant protein by transducing into rat MSCs. After selecting in blasticidin for 2 weeks, stable Flag-Sm51-MSCs cell line was established and used for RNA immunoprecipitation as described before(Peritz et al., 2006). Cells on confluence were washed in ice-cold PBS, scraped and re-suspended with 1ml RAPA buffer containing 20 mM Tris-HCl (pH 8), 137 mM NaCl, 10%

glycerol, 1% Nonidet P-40 (NP-40), 2 mM EDTA. After centrifuge 16,000g 15min, cell lysate was pre-cleared by incubated with 50µl protein G-agorose slurry (Invitrogen, USA) for 1h at 4℃. After brief centrifuge (2min at 14,000g at 4℃), supernatant was incubated with 1µg Flag (Sigma, St. Louis, USA) antibody and IgG (Epitomics, Burlingame, USA) overnight at 4℃, then 50µl protein G-agorose slurry for 4h. The immunoprecipitated samples were recovered after centrifugation, washed three times for 2 minutes at 14,000g at 4℃, each with lysing buffer. Beads was resuspenjd in 100 µl of lysis buffer with 0.1% SDS and 30µg proteinase K and incubated in a heating block at 50 °C for 30 min. RNA was extracted using PureLink RNA Mini Kit (Ambion, Guangzhou, China) following manufacturer instructions. Runx2, Osteocalcin (OCN), Osteopontin (OPN), type I collagen, Peroxisome proliferator-activated receptor *gamma* (*PPAR*-γ) and CCAAT-enhancer-binding proteins (C/EBP) were amplified using Taq polymeras (TAKARA, Shiga, Japan) with the following specific primers (table 2).

4.2.6 Ectopic bone formation

The protocol followed previous reports with little modification(Xu et al., 2012).Briefly, 1×10^6 MSCs overexpressing Sm51 or DsRed were loaded onto sterilized Skelite® resorbable HA-TCP bone graft substitute, and incubated at 37℃ for 3 h to allow attachment. The substitutes with cells were then implanted subcutaneously at the dorsal sides of nude mice (n=4). After 8 weeks, the transplants were harvested and subjected to hematoxylin and eosin staining. The osteoid matrix areas were measured using image pro plus 6.0 software by selecting random five microscopic fields of each sample.

4.2.7 Statistical analysis

Values were presented for each group as means ± SEM. The Student's t-test was used for comparison of mean values between different groups. P value was calculated with SPSS16.0, and $P<0.05$ was considered be statistical significant.

4.3 Results

4.3.1 Overexpression of Sm51 accelerates osteogenic differentiation of rat and human MSCs

MSCs were isolated from rat femora marrow and characterized by using flow cytometry analysis of CD90 (95%), CD44 (98%), CD73 (80%), CD34 (2%) and CD45 (1%), CD31 (2.5%) which were further verified by tri-lineages differentiation assay (data not shown). Considering the limited passage number of normal MSCs and variation of different batches of MSCs, we chose to use the immortalized MSCs by transfection of SV40 as described before (Hamada et al., 2005; Singer et al., 1987). These immortalized MSCs had similar cell surface markers expression pattern and tri-lineage differentiation potential (data not shown). Stable Sm51 overexpressing rat and human MSCs were established by selecting in blasticidin medium for two weeks. The high expression level of Sm51 in Sm51-rMSCs and Sm51-hMSCs were confirmed by qPCR and western blot (Figure 5.1G and 5.1F). We found overexpression of Sm51 in both rat and human MSCs enhanced their osteogenic differentiation after inducing. The extracellular matrix formation was higher in Sm51-rMSCs (Figure 5.1A) shown by alizarin red S staining. Meanwhile, Sm51-rMSCs had higher ALP activity than control (Figure 5.1B). To quantify this on molecular level, we extracted RNA after inducing and detected mRNA expression level of osteogenic markers. The data showed the expression of Runx2, Osteocalcin (OCN), Osteopontin (OPN), ALP, type I collagen significantly increased in Sm51-rMSCs (Figure 5.1C). In particular,

the higher expression of Runx2 in Sm51-rMSCs (Figure 5.1D) were further confirmed at protein level.

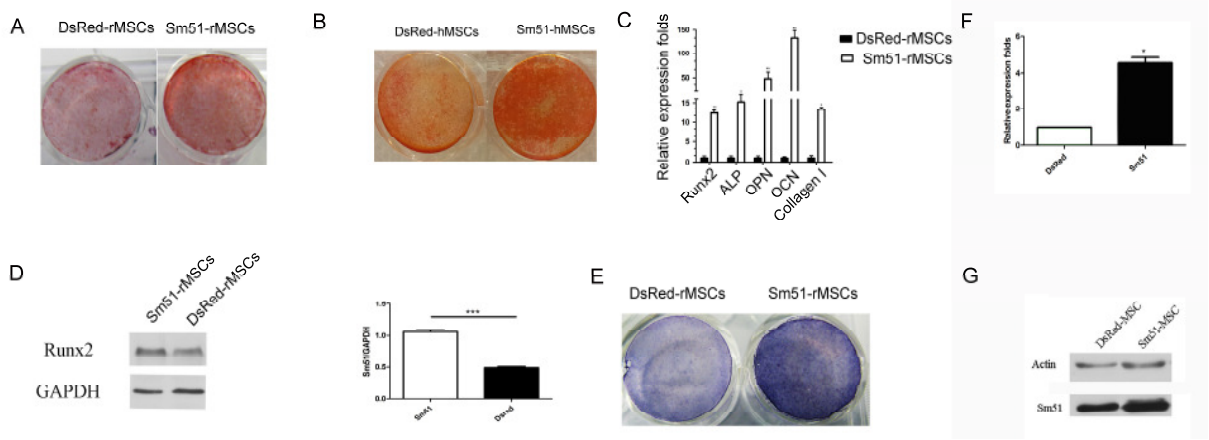

Figure 5.1 Osteogenic differentiation of rat and human MSCs.

A: Alizarin Red S staining of Sm51 overexpressing rat MSCs (Sm51-rMSCs) and DsRed control rat MSCs (DsRed-rMSCs) after osteogenic induction for 4 days. **B:** Alizarin Red S staining of Sm51 overexpressing human MSCs (Sm51-hMSCs) and DsRed control human MSCs (DsRed-hMSCs) after osteogenic induction for 5 days. **C**: Real time analysis of Runx2, ALP, OCN, OPN and type I collagen from Sm51-rMSCs and DsRed-rMSCs after osteogenic induction for 4 days. The relative expression fold was normalized to β-actin and calculated with ddCt methods. Each experiment was performed on 3 independent samples. **D**: Western blot of Runx2 of Sm51-rMSCs and DsRed-rMSCs after osteogenic induction for 4 days. **E:** Sm51-rMSCs and DsRed-rMSCs were fixed after osteogenic induction for 4 days and subjected to NBT/BCIP staining. F: the mRNA level of Sm51 from DsRed-MSCs and Sm51-MSCs was examined by real time PCR. G: the protein level of Sm51 from DsRed-MSCs and Sm51-MSCs was examined by western blot.

4.3.2 Sm51 regulates expression of runx2 in spontaneous osteogenesis

Runx2 was the master regulator in osteogenic differentiation of MSCs, which was regulated on many levels such as transcription, translation, cell signaling and so on. Considering Sm51 was a

RNA spicing associated factor inside the cell nuclear, we tested whether osteogenic induction is indispensable for regulation of Runx2 exerted by Sm51. Interestingly, we found overexpression of Sm51 upregulated expression osteogenic markers like Runx2, ALP, OPN, OCN and VEGF in rat MSCs (Figure 5.2A) and Runx2, ALP and OCN in human MSCs (Figure 5.2C) even without osteogenic induction. Furthermore, the protein level of Runx2 was also upregulated in rat MSCs (Figure 5.2B) and human MSCs (Figure 5.2D) independent of osteogenic induction.

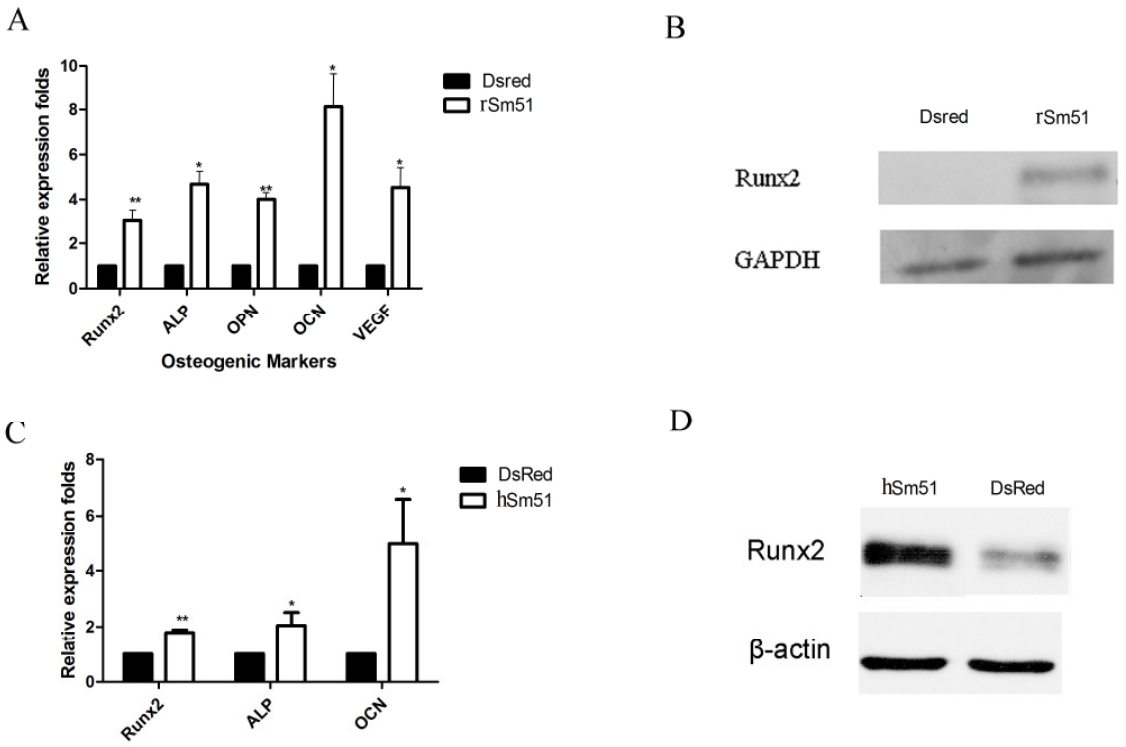

Figure 5.2 Expression osteogenic markers of rat and human MSCs without osteogenic induction.

A: Real time analysis of Runx2, ALP, OCN, OPN and VEGF from Sm51-rMSCs and DsRed-rMSCs without osteogenic induction. The relative expression fold was normalized to β-actin and calculated with ddCt methods. **B**: Western blot of Runx2 of Sm51-rMSCs and DsRed-rMSCs without osteogenic induction. **C**: Real time analysis of

Runx2, ALP, OCN of Sm51-hMSCs and DsRed-hMSCs without osteogenic induction. **D**: Western blot of Runx2 of Sm51-hMSCs and DsRed-hMSCs without osteogenic induction.

4.3.3 Overexpression of Sm51 promotes bone formation *in vivo*

To test the effect of Sm51 in bone formation *in vivo*, we implant Sm51 overexpressing rat MSCs together with HA/TCP material into dorsal side of nude mice for 2 weeks following the protocol reported before (Xu et al., 2012). After 8 weeks, transplants were harvested and prepared for histological analysis. H&E staining showed that Sm51-rMSCs formed more bone tissues than DsRed-rMSCs (Figure 5.3A). Quantitative measurement of mineralized tissue following the instruction published in previous report (Ye et al., 2012) revealed more than twice increase in bone formation by Sm51-rMSCs compared to DsRed-rMSCs (Figure 5.3B).

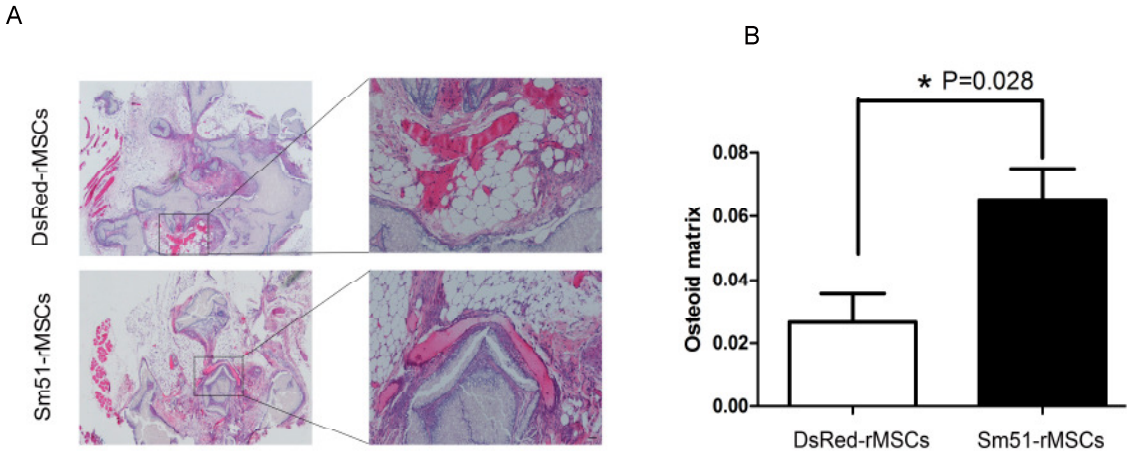

Figure 5.3 Ectopic bone formation of Sm51-rMSCs and DsRed-rMSCs in nude mouse.

A: Sm51-rMSCs and DsRed-rMSCs were implanted into nude mouse dorsal skin with HA/TCP. Samples were harvested and stained with H&E after 8 weeks. **B:** Semi-quantification of osteoid matrix by selecting 5 fields from each sample randomly and quantified with software image pro plus 6.0(n=6).*P=0.028, scale bar: 50μm

4.3.4 Knockdown of Runx2 abolishes osteogenic effect of Sm51 on rat MSCs

To explore whether Sm51 regulated osteogenic differentiation of MSCs through Runx2, Runx2 was silenced in Sm51-rMSCs and DsRed-rMSCs. After osteogenic differentiation inducing, both of Sm51-rMSCs and DsRed-rMSCs could not proceed to osteogenic differentiation although Sm51-rMSCs had higher osteogenic differentiation potential (Figure 5.4A). The data indicated runx2 was indispensable for Sm51 to promote osteogenesis. To further analyze this in detail, we detected mRNA level of some of osteogenic genes such as OCN, OPN, ALP and type I collagen, targets of Runx2 during osteogenesis (Otto et al., 2003; Stein et al., 2004), and found a decrease after silencing Runx2 in Sm51-rMSCs (Figure 5.4B) and DsRed-rMSCs (Figure 5.4C). Together these data demonstrated Runx2 was at least one of downstream targets of Sm51.

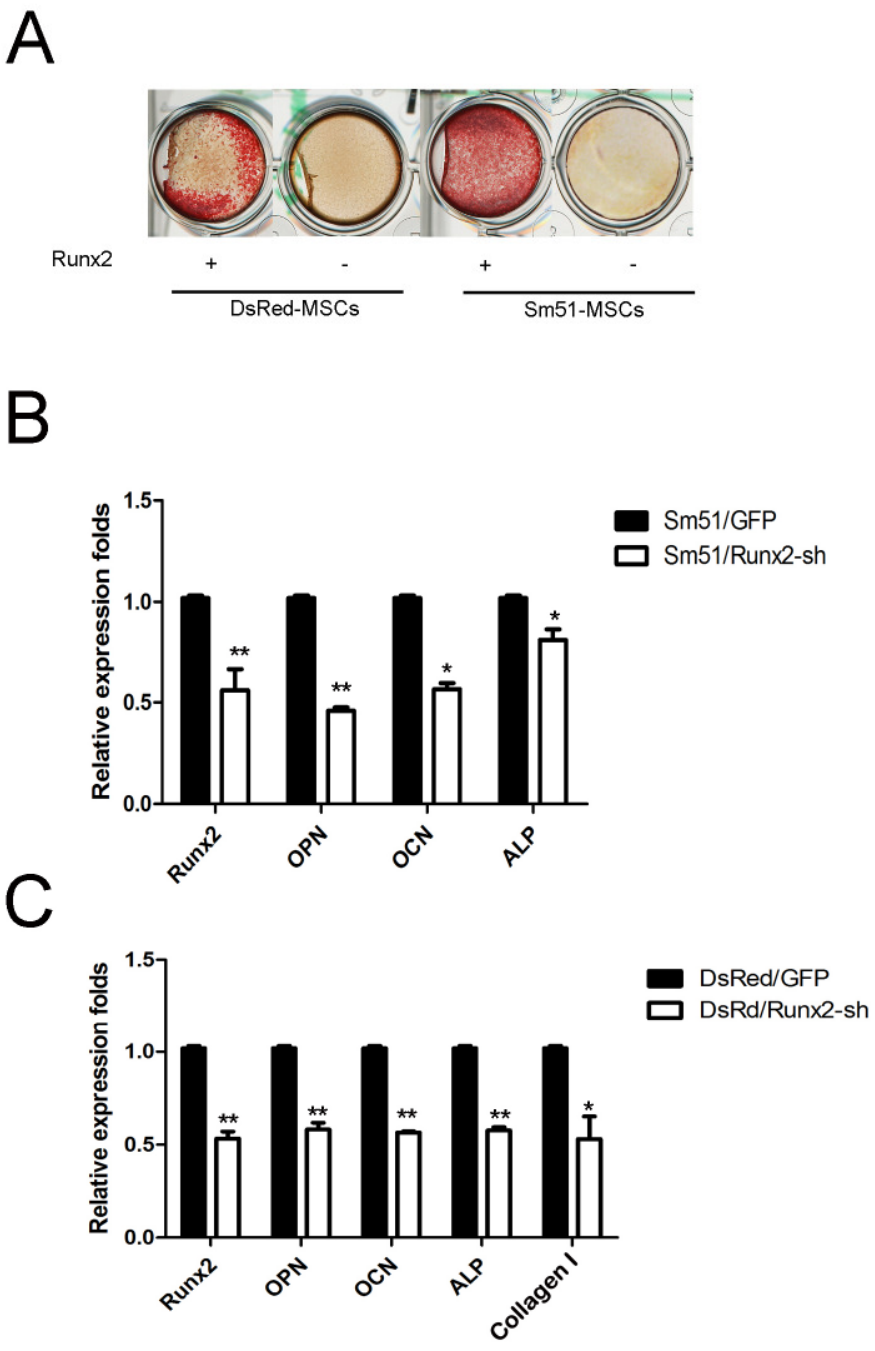

Figure 5.4 Osteogenic differentiation of Runx2 depleted MSCs.

A: Alizarin Red S staining of Sm51-rMSCs and DsRed-rMSCs after osteogenic induction for 4 days with or without expression of Runx2. **B:** Real time analysis of Runx2, ALP, OCN, OPN of Runx2 depleted Sm51-rMSCs. **C:** Real time analysis of Runx2, ALP, OCN, OPN and type I collagen of Runx2 depleted DsRed-rMSCs .

4.3.5 Sm51 binds Runx2 RNA directly

Considering Sm51 was a RNA splice associated molecule, we tested whether Sm51 interact with Runx2 RNA precursor directly by RNA immunoprecipitating method. Sm51 was fused with flag tag and expressed in rat MSCs. The Sm51 and RNA complex were pull down by flag antibody. To analyze the candidate target genes, we designed specific primers in adjacent exons of osteogenic markers Runx2, OCN, OPN, type I collagen and adipogenic markers PPARγ, C/EBP for amplification by RT-PCR. Interestingly, only Runx2 could be amplified specifically rather than other osteogenic markers OCN, OPN, type I collagen (Figure 5.5A), while adipogenic markers PPARγ, C/EBP were not specifically amplified (Figure 5.5B).

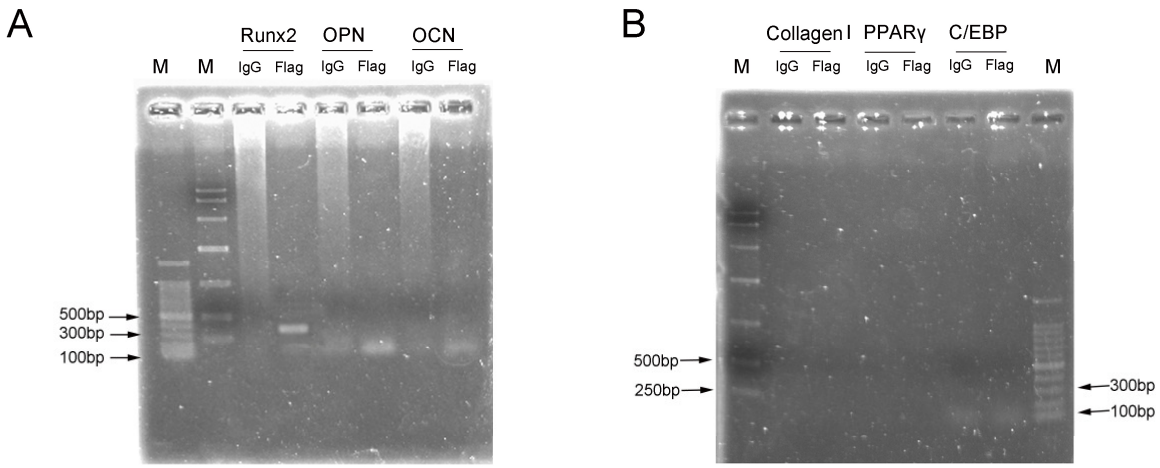

Figure 5.5 RNA immunoprecipitation of Sm51 in rat MSCs.

A: Sm51 binding RNA complex was precipitated with Sm51 conjugated Flag antibody and amplified with specific primers. RT-PCR of Sm51 binding complex with specific primers for Runx2, OPN and OCN (). **B:** RT-PCR of Sm51 binding complex with specific primers for PPARγ, C/EBP and type I collagen.

4.4 Discussion

In this study, we reported that Sm51 promoted osteogenic differentiation of MSCs by upregulating expression of runx2 and other osteogenic genes. Runx2 was responsible for the effect of Sm51 in osteogenesis. Furthermore, Sm51 could bind runx2 RNA precursor directly.

MSCs have multiple differentiation potentials and can be induced into osteoblast, adipocyte, and chondrocyte *et al*. Each differentiation pathway was tightly regulated by external and internal signals. Due to the critical importance of bone formation in fracture healing and osteoporosis, the mechanism of osteogenic differentiation of MSCs was studied extensively, with large number of regulators identified(Long, 2012). Here, we also found a novel factor Sm51, which could enhance osteogenic differentiation of MSCs *in vitro* and ectopic bone formation after implanting into nude mice *in vivo*. For the mechanism study, we found that Sm51 can regulate expression of Runx2 and other osteogenic genes ALP, OPN, OCN, type I collagen even without osteogenic induction, indicating this regulation was independent of external signal. As is known, Runx2 is particularly indispensable for osteoblast commitment, which can regulate and many osteogenic genes including ALP, OPN, OCN, type I collagen(Stein et al., 2004). So, it is reasonable that the expression of ALP, OPN, OCN, type I collagen was upregulated after overexpressing Sm51 through Runx2 , as silencing Runx2 led to downregulation of ALP, OPN, OCN, type I collagen even in Sm51 overexpressing MSCs. Moreover, silencing Runx2 totally abolished the effect of Sm51 in osteogenesis, indicating that runx2 was one of the downstream targets of Sm51.

As a novel component of RNA splice machine, Sm51 is seldom known in regulating biological events. Although it is closely related to another ubiquitous SmB/B' in sequence, Sm51 is expressed only in a limited range of tissues and cell types like brain(Horn et al., 1992), setting it apart from other mammalian snRNP polypeptides. In this study, we found Sm51 was expressed in bone marrow MSCs as it could be cloned from MSCs. Furthermore, the amino acid sequences of human and rat Sm51 are 100% conserved(Schmauss et al., 1989), which implies Sm51 has the conserved function in rat and human. Our study also demonstrated that Sm51 promoted osteogenesis in both rat and human MSCs in the same way. Moreover, we found that sm51 exerted its role by binding runx2 in RNA splicing process, distinguishing with many other factors in regulating expression of Runx2. However, this does not exclude that Sm51 may also bind and regulate some other genes not completely identified in this study. Previous studies show that depletion of Sm51 results in Prader-Willi syndrome, which is characterized by neonatal hypotonia and failure to thrive, mental retardation, hypogonadism, short hands and feet, and hyperphagia resulting in obesity. Although we do not analyze bone formation in Prader-Willi syndrome patient, our results provide an explanation of Sm51 depletion and bone development disorder.

Overall, our study provides a new pathway in regulation osteogenic differentiation of MSCs and expression of Runx2 at RNA splicing process. Based on our study, we can design sm51 agonist or introduce sm51 gene into bone to augment bone formation and skeletal genes expression specifically.

Chapter5 GATA6 promotes osteogenic differentiation of MSCs

The purpose of this chapter is to answer----

What is the role of GATA6 in osteogenic differentiation of BM-MSCs?

5.1 Chapter introduction

Osteoblast differentiated from MSCs is the block of bone. Abnormal osteogenic differentiation of MSCs characterized by osteoblast decrease results in various bone related diseases, such as bone loss in osteoporosis individual and no union in fracture healing. However, osteoblast is not the only cell type from MSCs, which are also capable of differentiating in adipocytes, chondrocytes *et al*. The fate choice of MSCs is tightly regulated, although the mechanisms are not fully understood. As mentioned in the introduction part, various factors and signals are involved in the osteogenesis process. The master transcription factor in osteogenesis is Runx2, loss of which in the mouse results in absence of a mineralized skeleton and perinatal lethality (Romero-Prado et al., 2006). Meanwhile, Runx2 need cooperated with various factors in this process in order to bind specifically and transactivate efficiently target genes.

Previous attempts have identified various partners of Runx2 in osteoblast formation, including TAZ, p300 CBP, MOZ(Schroeder et al., 2005). As a zinc finger transcription factor, GATA6 is expressed in various tissue and organs and plays a role in the embryonic endoderm development of lung, pancreas and skeletal muscle. However, whether GATA6 is involved in osteogenesis still not clarified. An approach of my lab in analyzing the differential gene expression of PB-MSCs and BM-MSCs reveal a higher level of GATA6 in PB-MSCs. So, we hypothesize GATA6 may be involved in osteogenic differentiation of MSCs.

In this chapter, we first established the stable GATA6 overexpressing and depleted MSCs by lentiviral transfection, then assess the osteogenic differentiation of MSCs *in vitro and in vivo*. Given the indispensable role of Runx2 in osteogenesis, we further analyze the relationship of GAAT6 and Runx2 on protein level.

5.2 Methods

5.2.1 Plasmids construction and lentiviral transfection

Rat and human GATA6 gene (GeneBank number: NM_019185.1, NM_005257.4) was amplified from rat bone marrow MSCs cDNA, cloned into pLenti-MCS-DsRed vector. For hGATA6 depleted experiments, 2 pairs of GATA6-shRNA and scramble control were designed and cloned into plentiLox3.7 vector. The correspondent sequences were: GATA6-sh-1 5'-TGGGAATTCAAACCAGGAAA-3', GATA6-sh-2 5'- TGGAATTCAAACCAGGAAAC-3' Scramble-sh 5'-ACTTGCCATACATGACTCT-3', Lentivirus carrying above vectors were produced in 293FT cell line by transient transfected with calcium phosphate transfection method as described before (Song and Li, 2011). Cell supernatants containing lentiviral particles were collected after transfection for 48h and 72h, filtered through 0.45 membrane (Millipore, Billerica, USA) and subject to further concentration using PEG-it Virus Precipitation kit (System Biosciences, Mountain View, USA) following manufacturer's instructions. Rat and human derived MSCs were immortalized by lentiviral transduction of Simian virus 40 plasmid and single colony was selected and amplified for the following experiments. As the amino acide sequence of human Sm51 gene is identical to rat Sm51 gene, we used rat Sm51 gene for human MSCs transduction. For transduction, 1×10^5 MSCs were seeded into 6-well plate and incubated with lentiviruses together with 8μg/ml polybrene in the incubator for 10 h. Stable transfected MSCs cell lines were then established in the presence of blasticidin (10μg/ml) for two weeks. The expression of Sm51 in transfected stable cell lines was examined using quantitative PCR and western blot.

5.2.2 Osteogenic differentiation

MSCs were seeded in 6-well plate at a concentration of 1×10^5 cells per well. After incubating in the α-MEM for two or three days, the medium was changed into osteogenic induction medium (OIM) containing 100 nmol/L dexamethasone, 10 mmol/L beta-glycerophosphate, and 0.05 mmol/L l-ascorbic acid-2-phosphate. The medium refreshed twice a week. The osteogenic differentiation was evaluated by real-time PCR and 2% alizarin red S staining (sigma, St. Louis, USA).

5.2.3 Western blot

Western blot examination was carried out as described previously (Song and Li, 2011). In brief, cells on confluence were scraped and lysed in RIPA buffer (Invitrogen, Grand Island, USA). Total protein concentration was quantified by BCA method (Pierce, Rockford, USA). Equal amount of proteins was run on 10% SDS-PAGE. Proteins were then transferred from gel into PVDF membrane. After blocking in 5% milk, membranes were incubated with primary antibodies overnight at 4℃. After washing three times with TBST buffer, membranes were then incubated with secondary antibodies conjugated with horseradish peroxidase for 1h at room temperature. Proteins were visualized with enhanced chemiluminescence (Pierce, Rockford, USA). The following primary antibodies were used: Runx2 (1:1000, Cell Signaling Technology, Danvers, USA), GAPDH (1:1000, Santa Cruz Biotechnology, Santa Cruz, USA).

5.2.4 Co-immunoprecipatation

Cells at confluence were washed in ice-cold PBS, scraped and re-suspended with 1ml lysis buffer containing 20 mM Tris-HCl (pH 8), 137 mM NaCl, 10% glycerol, 1% Nonidet P-40 (NP-40), 2 mM EDTA. Cell lysate was pre-cleared by incubated with 50μl protein G-agorose slurry (Invitrogen, USA) for 1h at 4℃. After brief centrifuge (2min at 14,000g at 4℃), supernatant was

incubated with 1μg Aqp1 (Santa Cruz, USA) antibody and IgG (Epitomics, Inc., USA) overnight at 4℃, then 50μl protein G-agorose slurry for 4h. The immunoprecipitated samples were recovered after centrifugation, washed three times for 2 minutes at 14,000g at 4℃, each with lysing buffer. The immunoprecipitated samples were boiled 5 min and re-suspended with 2× Laemmli buffer (4% SDS, 10% 2-mercaptoehtanol, 20% glycerol, 0.004% bromophenol blue, 0.125 M Tris-HCl) for SDS/PAGE examination as described previously.

5.2.5 Ectopic bone formation

The protocol followed previous reports with little modification(Xu et al., 2012).Briefly, 1×10^6 MSCs overexpressing Sm51 or DsRed were loaded onto sterilized Skelite® resorbable HA-TCP bone graft substitute, and incubated at 37℃ for 3 h to allow attachment. The substitutes with cells were then implanted subcutaneously at the dorsal sides of nude mice (n=4). After 8 weeks, the transplants were harvested and subjected to hematoxylin and eosin staining. The osteoid matrix areas were measured using image pro plus 6.0 software by selecting random five microscopic fields of each sample.

5.2.6 Statistical analysis

Values were presented for each group as means ± SEM. The Student's t-test was used for comparison of mean values between different groups. P value was calculated with SPSS16.0, and $P<0.05$ was considered be statistical significant.

5.3 Results

5.3.1 Overexpression of GATA6 accelerates osteogenic differentiation of MSCs

Stable GATA6 overexpressing rat and human MSCs were established by selecting in blasticidin containing medium for two weeks, and the level of GATA6 after selection were confirmed by qPCR and western blot. We found overexpression of GATA6 enhanced the osteogenic differentiation of rat and human MSCs shown by alizarin red S staining after osteogenic induction in vitro (Figure 6.1).

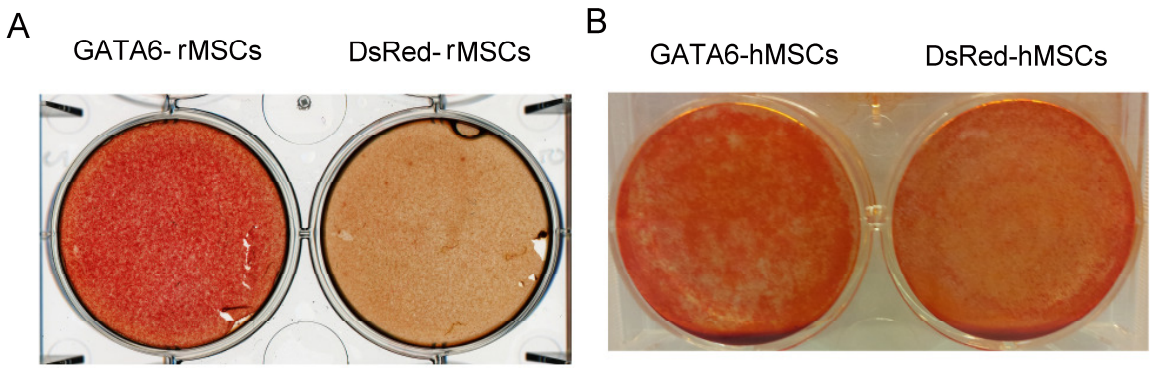

Figure 6.1 Osteogenic differentiation of rat and human MSCs.

A: Alizarin Red S staining of Sm51 overexpressing rat MSCs (Sm51-rMSCs) and DsRed control rat MSCs (DsRed-rMSCs) after osteogenic induction for 4 days. **B**: Alizarin Red S staining of Sm51 overexpressing human MSCs (Sm51-hMSCs) and DsRed control human MSCs (DsRed-hMSCs) after osteogenic induction for 5 days.

5.3.2 Depletion of GATA6 reduces the level of Runx2

To explore the mechanism of GATA6 in osteogenesis, we chose to examine the relationship of GATA6 and Runx2, a master regulator in osteogenesis, by knockdowning GATA6 in human MSCs using shRNA transfection. The level of GATA6 was efficiently depleted (Figure 6.2A), which led to the level of Runx2 decreased on protein level (Figure 6.2B).

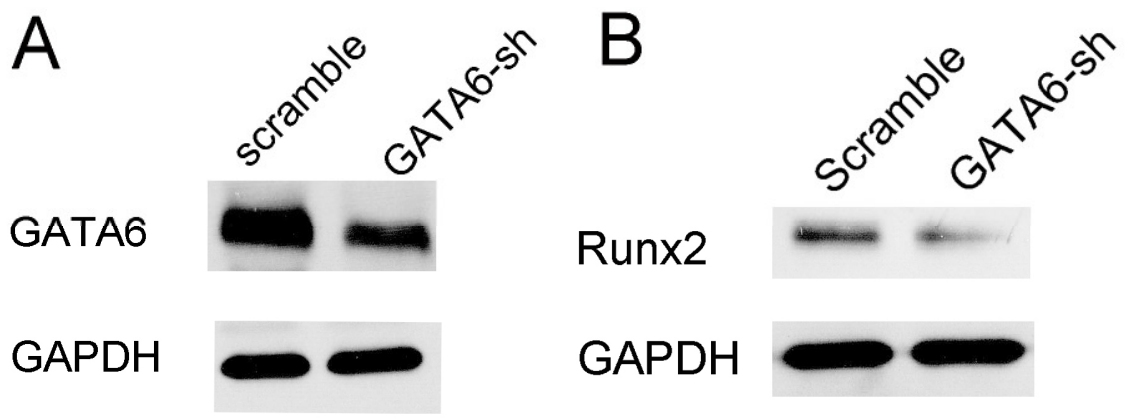

Figure 6.2 Western blot of the level of GATA6 and Runx2 in GATA6-sh human MSCs

A: The protein level of GATA6 was examined by western blot in GATA6 depleted MSCs after stable transfection of GATA6 shRNA with scramble shRNA as a negative control. B: The expression of Runx2 in GATA6-overexpressing MSCs.

5.3.3 GATA6 interacts with Runx2

As a central organizer, Runx2 controls multiple osteogenic gene expression by cooperating various factors. We chose to investigate the role of GATA6 in osteogenic differentiation by testing whether it was capable of binding Runx2 by CoIP method. As positive control, Runx2 was detected in whole protein before immunoprecipitation and in the Runx2 pull down product (Figure 6.3 Input, Runx2 lane). As expected, GATA6 could interact with Runx2, while the negative control IgG lane had no signal (Figure 6.3 GATA6 lane, IgG lane).

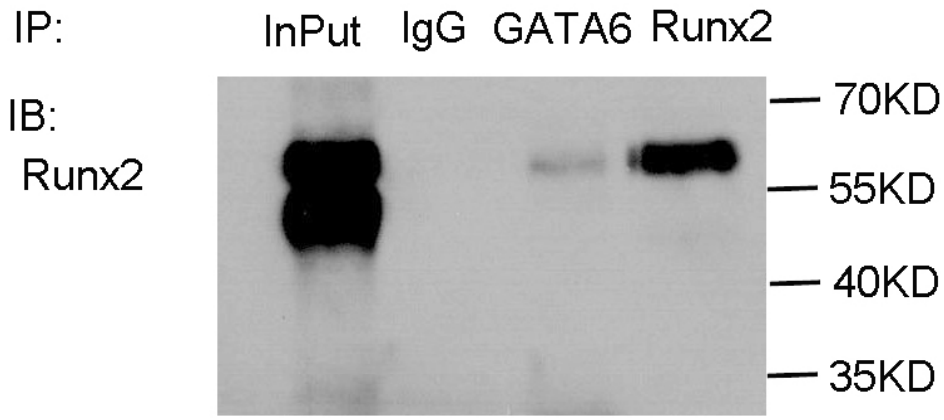

Figure 6.3 CoIP analysis of GATA6 and Runx2

Total protein of MSCs was extracted and pull down with Runx2, IgG and GATA6 antibodies respectively. The precipitation was then blotted with Runx2 antibody. The whole protein was used for positive control.

5.3.4 GATA6 decreases in MSCs from ovariectomised rat

To explore the role of GATA6 in osteoporosis, we examined the level of GATA6 in MSCs from ovaryectomised rat, an animal model to mimic osteoporosis in human. The expression of GATA6 decreased in OVX-MSCs compared to wild type MSCs (Figure 6.4).

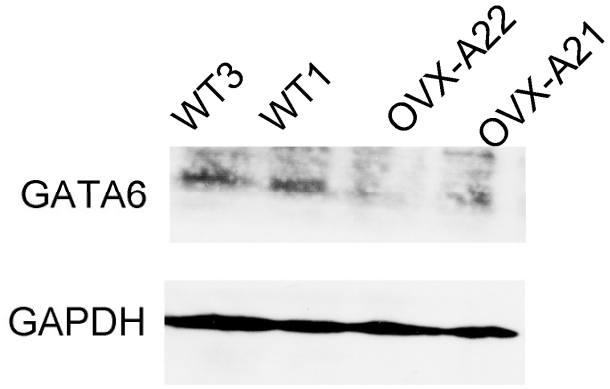

Figure 6.4 Level of GATA6 in MSCs from OVX rats

The protein level of GATA6 from ovariectomised (OVX) rat derived MSCs (OVX-A22, A21) and wild type MSCs was detected by western blot.

5.4 Discussion

In this chapter, we uncovered the novel role of GATA6 in osteogenic differentiation of rat and human MSCs. Forced expression of GATA6 in MSCs promote the osteogenic differentiation of rat and human MSCs in vitro characterized by higher calcium deposit after osteogenic inducement, and the level of Runx2 increase in GATA6 overexpressing MSCs. In addition, GATA6 is associated with Runx2 via directly interaction. Interestingly, the level of GATA6 in MSCs from ovariectomised (OVX) rat was much lower than wild type MSCs.

GATA6 contains a conserved zinc fingers to bind conserved DNA sequence (G/A) GATA (A/T) and transcription activation domain in mammal. Previous studies demonstrated that GATA6 was associated with embryonic development cooperated with partner factors, such as TTF-1 for epithelium of lung, Nkx2.2 for pancreas specification and Nkx3.2 for smooth muscle (Nishida et al., 2002). Bhushan reported one microRNA miR-181a directly controlled receptor of TGFβI signaling pathway Tgfbi and TR-I and mediated the downregulation of GATA6 in osteogenic differentiation (Bhushan et al., 2013), which seems to be inconsistent with our findings. Due to the complexity of miR-181a, it is hard to discriminate which targets possess the major effects on osteogenic differentiation. However, the clear role of GATA6 in embryonic development of bone and postnatal osteogenesis still need investigate further.

In our study, we showed that GATA6 promote osteogenic differentiation of MSCs, and depletion of GATA6 led to the downregulation of Runx2. Furthermore, GATA6 has a directly interaction

with Runx2, implying that GATA6 is one of the partners of Runx2 in osteogenesis. However, the relationship of GATA6 and Runx2 is still required for further study in detail.

Several factors involved in osteogenesis were further proved to decrease in aged osteoporosis individuals like histone demethylases KDM4B and KDM6B (Ye et al., 2012). Consisted with this finding, we also found the level of GATA6 decreased in osteoporosis rat model. The role of GATA6 in the regulation network of osteoporosis remains to elucidate in future study. Taken together, our preliminary data uncover a novel role of GATA6 in osteogenesis and osteoporosis, which not only broaden the understanding of the mechanism but also guide the clinical application in future.

Chapter6 General discussion and future work

In this chapter, we will summarize the work carried out in the past 3 years, highlight the findings in this thesis, and discuss the work in future.

6.1 Summary

By employing the conventional adherent method in isolation and culture BM-MSCs, we successfully isolated and culture MSCs from peripheral blood of normal individual. The culture frequency of PB-MSCs is pretty low compared to BM-MSCs probably due to the low percentage in peripheral blood of normal individual, which is partially proved that high isolation frequency occur in cancer individual, fractured patients and puberty. However, the isolation method should be optimized to allow MSCs to adhere *in vitro* by supplementing extra factors to stimulate the adherence or coating the culture dishes and using the bioreactor to expand the non-adherent PB-MSCs for a while then induce it to attach. Compared to BM-MSCs, the colony of PB-MSCs appeared 8 days after plating in culture, later than BM-MSCs, but it possesses similar properties with BM-MSCs like fibroblast like morphology and high proliferation. When examined the cell surface markers expression pattern, PB-MSCs were shown to positively express CD90, CD44, and negatively express CD34, CD45 and CD31. Meanwhile, PB-MSCs are capable of being induced to osteogenic and adipogenic differentiation *in vitro*.

Previous attempts to identify the origin of PB-MSCs uncovered PB-MSCs were mobilized from bone marrow especially during the bone fracture healing. In order to quantify the number of PB-MSCs, we chose two MSCs cell surface markers CD45 and CD90 to evaluate the relative number of PB-MSCs in mononuclear cell population. CD45, a common antigen in white blood cells, is absent in MSCs, while CD90 is highly expressed in MSCs from various tissue origin. Using CD90+ CD45 – cells from peripheral blood mononuclear cells as a selective gate for PB-MSCs is convenient to quantify by flow cytometry, excluding the contamination of

hematopoietic lineage cells and endothelial cells. We found the number of PB-MSCs started to increase at the initial stage of fracture, from day 3 to day11, reached the maximal level at day 13 and decreased after then. Meanwhile, in the rat fracture healing process, it is in the inflammation stage in the first 7 to 10 days after fracture, indicating the trauma at fracture site recruited the PB-MSCs. Following this finding, we can use PB-MSCs as one biomarker to monitor the fracture healing process and guide the clinical therapy of fracture.

To further clarify the instinct of PB-MSCs on molecular level, we screen the differential genes between PB-MSCs and BM-MSCs using microarray. We choose three genes Aqp1, Sm51 and GATA6 and investigate their roles in biological characters of BM-MSCs. Aqp1, as one major water channel, was shown to promote the endothelial cells migration and angiogenesis in tumor formation. Given the critical role of Aqp1 in migration, we demonstrated that Aqp1 was capable of enhancing the MSCs migration *in vitro* detected by transwell and wound healing assays. In addition, β-catenin and FAK were associated with Aqp1 mediated MSCs migration, as overexpression of Aqp1 upregulated the level of β-catenin and FAK instead of CXCR4, an indispensable factor in MSCs mobilization. As one transmembrane protein, Aqp1 also interacted with β-catenin and FAK physically, which located at the cytoplasm portion of tyrosine receptor. The existence of Aqp1 may contribute the stability of β-catenin and FAK. Furthermore, depletion of FAK abolished the effects of Aqp1 in MSCs migration, suggesting FAK is critical in this process.

The fact that the level of PB-MSCs increase during fracture patients and puberty undergoing rapidly bone remodeling led to the concept some genes should be involved in osteogenesis. We detected the osteogenic differentiation capacity of two selective genes Sm51 and GATA6. Identified as the tissue specific small nuclear ribonucleoprotein-associated polypeptide N

(SNRPN), Sm51 mainly exists in the U-2 snRNP of RNA splicing complex. Overexpression of Sm51 in rat and human MSCs accelerated the osteogenesis process with the elevated mRNA level of osteogenic marker genes Runx2, OPN, OCN, collagen type I and ALP in vitro. When examined by implanting with HA-TCP material into nude mice, Sm51 overexpressing rat MSCs appear to possess higher ectopic bone formation ability. Furthermore, the protein level of Runx2 increased after overexpression of Sm51, while knockdown of Runx2 abolish the effect of Sm51 in osteogenic differentiation of rat MSCs, implying the potential relationship of Runx2 and Sm51. To explore this in detail, we test whether Sm51 is capable of regulation the splice of Runx2 RNA precursor. Expected, Sm51 binds the Runx2 RNA specially rather than osteognenic markers OPN, OCN, collagen type I and adipogenic markers C/EBP and PPARγ. Taken together, Sm51 was shown to be a novel regulator in osteogenesis by playing a role in Runx2 splice.

GATA6, a 45 kDa polypeptide, is first cloned from rat heart cDNA library as well as GATA4 and possesses the common characters of GATA family proteins described in the introduction chapter. The role of GATA6 in osteogenic differentiation of rat and human comes from higher mineralization capacity in vitro after inducing for 4 days. When depleted GATA6, the level of Runx2 decreased, implying the potential relationship of Runx2 and GATA6. In addition, we found GATA6 interacted with Runx2 physically. There are several factors involved in osteogenesis were further proved to decrease in aged osteoporosis individuals like histone demethylases KDM4B and KDM6B. In this study, we also found the level of GATA6 decreased in osteoporosis rat model. Therefore, we demonstrate that GATA6 is associated with osteogenic differentiation of MSCs.

6.2 Future work

Although PB-MSCs are high similar with BM-MSCs, the unique role of PB-MSCs remains to clarify in term of their mobilization, adhere independence and biological role. The efficiency of culture of PB-MSCs is still low, and how to optimize the isolation methods is indispensable for its application in clinical practice as a substitute of BM-MSCs. The study that the change of PB-MSCs during fracture is preliminary, and numerous studies about the recruitment mechanism of PB-MSCs from the source, like bone marrow, should be elucidated in future.

The role of Aqp1 in migration of endothelial cells and MSCs is well known, while the mechanism in regard of the interaction domain or responsible motif of Aqp1and FAK is not clear yet. It also should test whether the finding was applicable for other cell types, and it is even more interesting to investigate the relationship of irons channel besides of Aquaporin and cell migration.

The regulation of osteogenic differentiation of MSCs, albeit complex, is mainly performed by Runx2 and its partners. In this study, we demonstrate Sm51 control the splice event of Runx2 at upstream, and GATA6 seems to cooperate with Runx2 in osteogenic differentiation. However, some questions still be open: Is Sm51 indispensable for Runx2 expression or just as a substitute of SmB/B' in MSCs? How Sm51 contribute to specific splicing of Runx2 mRNA precursor? About the study of GATA6, more strong evidences should be given that the ability of GATA6 in promoting osteogenesis in vivo and how GATA6 interact Runx2. Moreover, the role of GATA6 in osteoporosis needs to study further. According to the literatures, there are still no reports about the link among Aqp1, Sm51 and GATA6. Due to the role of GATA6 and Sm51 in osteogenesis, there might be some interaction of Sm51 and GATA6 on mRNA splicing or gene transcription level.

6.3 Conclusion

In conclusion, the research work of this thesis demonstrates that the PB-MSCs are capable of being isolated and have similar characters with BM-MSCs. The number of PB-MSCs increases at the initial stage of fracture healing and decrease to normal level two weeks after fracture. Aqp1 enhances the migration of MSCs both in vitro and in vivo by interacting with β-catenin and FAK, and depletion of FAK totally abolishes the effect of Aqp1 in MSCs migration. When administrated in vivo, the Aqp1-MSCs group has better outcome of bone healing in rat femoral model. Sm51 promotes the osteogenic differentiation of MSCs and upregulates the level of Runx2 via directing the specific splicing of Runx2 mRNA precursors. Overexpression of GATA6 accelerates the osteogenic differentiation of MSCs, while depletion of GATA6 leads to the reduction of Runx2 level. Moreover, GATA6 is associated with Runx2 by interacting physically. In the osteoporosis rat model, the level of GATA6 is higher in normal individuals.

References

1. Agre, P., Saboori, A.M., Asimos, A., & Smith, B.L. (1987). Purification and partial characterization of the Mr 30,000 integral membrane protein associated with the erythrocyte Rh(D) antigen. *Journal of Biological Chemistry* 262, 17497-17503.

2. Akiyama, T. (2000). Wnt/beta-catenin signaling. *Cytokine Growth Factor Rev* 11, 273-282.

3. Al-azzeh, E.-d., Fegert, P., Blin, N., & Gött, P. (2000). Transcription factor GATA-6 activates expression of gastroprotective trefoil genes TFF1 and TFF2. *Biochimica et Biophysica Acta (BBA) - Gene Structure and Expression* 1490, 324-332.

4. Albers, J., Schulze, J., Beil, F.T., Gebauer, M., Baranowsky, A., Keller, J., Marshall, R.P., Wintges, K., Friedrich, F.W., Priemel, M., Schilling, A.F., Rueger, J.M., Cornils, K., Fehse, B., Streichert, T., Sauter, G., Jakob, F., Insogna, K.L., Pober, B., Knobeloch, K.-P., Francke, U., Amling, M., & Schinke, T. (2011). Control of bone formation by the serpentine receptor Frizzled-9. *The Journal of Cell Biology* 192, 1057-1072.

5. Alm, J.J., Koivu, H.M.A., Heino, T.J., Hentunen, T.A., Laitinen, S., & Aro, H.T. (2010). Circulating plastic adherent mesenchymal stem cells in aged hip fracture patients. *Journal of Orthopaedic Research* 28, 1634-1642.

6. Bangsow, C., Rubins, N., Glusman, G., Bernstein, Y., Negreanu, V., Goldenberg, D., Lotem, J., Ben-Asher, E., Lancet, D., Levanon, D., & Groner, Y. (2001). The RUNX3 gene – sequence, structure and regulated expression. *Gene* 279, 221-232.

7. Baron, R., & Kneissel, M. (2013). WNT signaling in bone homeostasis and disease: from human mutations to treatments. *Nat Med* 19, 179-192.

8. Bhushan, R., Grünhagen, J., Becker, J., Robinson, P.N., Ott, C.-E., & Knaus, P. (2013). miR-181a promotes osteoblastic differentiation through repression of TGF-β signaling molecules. *The International Journal of Biochemistry & Cell Biology* 45, 696-705.

9. Bialek, P., Kern, B., Yang, X., Schrock, M., Sosic, D., Hong, N., Wu, H., Yu, K., Ornitz, D.M., Olson, E.N., Justice, M.J., & Karsenty, G. (2004). A Twist Code Determines the Onset of Osteoblast Differentiation. *Developmental Cell* 6, 423-435.

10. Bienert, G.P., Møller, A.L.B., Kristiansen, K.A., Schulz, A., Møller, I.M., Schjoerring, J.K., & Jahn, T.P. (2007). Specific Aquaporins Facilitate the Diffusion of Hydrogen Peroxide across Membranes. *Journal of Biological Chemistry* 282, 1183-1192.

11. Black, D.L. (2003). MECHANISMS OF ALTERNATIVE PRE-MESSENGER RNA SPLICING. *Annual Review of Biochemistry* 72, 291-336.

12. Borgnia, M., Nielsen, S., Engel, A., & Agre, P. (1999). Cellular and molecular biology of the aquaporin water channels. *Annual Review of Biochemistry* 68, 425-458.

13. Brabletz, T., Jung, A., Dag, S., Hlubek, F., & Kirchner, T. (1999). β-catenin regulates the expression of the matrix metalloproteinase-7 in human colorectal cancer. *The American Journal of Pathology* 155, 1033-1038.

14. Braunschweig, U., Gueroussov, S., Plocik, A.M., Graveley, Brenton R., & Blencowe, Benjamin J. (2013). Dynamic Integration of Splicing within Gene Regulatory Pathways. *Cell* 152, 1252-1269.

15. Bresnick, E.H., Katsumura, K.R., Lee, H.-Y., Johnson, K.D., & Perkins, A.S. (2012). Master regulatory GATA transcription factors: mechanistic principles and emerging links to hematologic malignancies. *Nucleic Acids Research* 40, 5819-5831.

16. Bruno, M.D., Korfhagen, T.R., Liu, C., Morrisey, E.E., & Whitsett, J.A. (2000). GATA-6 Activates Transcription of Surfactant Protein A. *Journal of Biological Chemistry* 275, 1043-1049.

17. Butler, M.G., Haber, L., Mernaugh, R., Carlson, M.G., Price, R., & Feurer, I.D. (2001). Decreased bone mineral density in Prader-Willi syndrome: Comparison with obese subjects. *American Journal of Medical Genetics* 103, 216-222.

18. Campagnoli, C., Roberts, I.A.G., Kumar, S., Bennett, P.R., Bellantuono, I., & Fisk, N.M. (2001). Identification of mesenchymal stem/progenitor cells in human first-trimester fetal blood, liver, and bone marrow. *Blood* 98, 2396-2402.

19. Caplan, A.I. (1994). The mesengenic process. *Clin Plast Surg* 21, 429-435.

20. Carbrey, J.M., Gorelick-Feldman, D.A., Kozono, D., Praetorius, J., Nielsen, S., & Agre, P. (2003). Aquaglyceroporin AQP9: Solute permeation and metabolic control of expression in liver. *Proceedings of the National Academy of Sciences* 100, 2945-2950.

21. Cattanach, B.M., Barr, J.A., Evans, E.P., Burtenshaw, M., Beechey, C.V., Leff, S.E., Brannan, C.I., Copeland, N.G., Jenkins, N.A., & Jones, J. (1992). A candidate mouse model for Prader-Willi syndrome which shows an absence of Snrpn expression. *Nat Genet* 2, 270-274.

22. Chamberlain, G., Fox, J., Ashton, B., & Middleton, J. (2007). Concise review: mesenchymal stem cells: their phenotype, differentiation capacity, immunological features, and potential for homing. *Stem Cells* 25, 2739-2749.

23. Chari, A., Golas, M.M., Klingenhäger, M., Neuenkirchen, N., Sander, B., Englbrecht, C., Sickmann, A., Stark, H., & Fischer, U. (2008). An Assembly Chaperone Collaborates with the SMN Complex to Generate Spliceosomal SnRNPs. *Cell* 135, 497-509.

24. Chen, S.-Y., & Chen, H.-C. (2006). Direct Interaction of Focal Adhesion Kinase (FAK) with Met Is Required for FAK To Promote Hepatocyte Growth Factor-Induced Cell Invasion. *Molecular and Cellular Biology* 26, 5155-5167.

25. Chen, X., McClurg, A., Zhou, G.-Q., McCaigue, M., Armstrong, M.A., & Li, G. (2007). Chondrogenic differentiation alters the immunosuppressive property of bone marrow-derived mesenchymal stem cells, and the effect is partially due to the upregulated expression of B7 molecules. *Stem Cells* 25, 364-370.

26. Cheung, W.-H., Chin, W.-C., Wei, F.-Y., Li, G., & Leung, K.-S. (2013). Applications of Exogenous Mesenchymal Stem Cells and Low Intensity Pulsed Ultrasound Enhance Fracture Healing in Rat Model. *Ultrasound in Medicine & Biology* 39, 117-125.

27. Cory, G.O.C., & Ridley, A.J. (2002). Cell motility: Braking WAVEs. *Nature* 418, 732-733.

28. Crossley, M., & Orkin, S.H. (1994). Phosphorylation of the erythroid transcription factor GATA-1. *Journal of Biological Chemistry* 269, 16589-16596.

29. David, C.J., & Manley, J.L. (2010). Alternative pre-mRNA splicing regulation in cancer: pathways and programs unhinged. *Genes & Development* 24, 2343-2364.

30. Davidson, K.C., Adams, A.M., Goodson, J.M., McDonald, C.E., Potter, J.C., Berndt, J.D., Biechele, T.L., Taylor, R.J., & Moon, R.T. (2012). Wnt/β-catenin signaling promotes differentiation, not self-renewal, of human embryonic stem cells and is repressed by Oct4. *Proceedings of the National Academy of Sciences* 109, 4485-4490.

31. De Becker, A., Van Hummelen, P., Bakkus, M., Vande Broek, I., De Wever, J., De Waele, M., & Van Riet, I. (2007). Migration of culture-expanded human mesenchymal stem cells through bone marrow endothelium is regulated by matrix metalloproteinase-2 and tissue inhibitor of metalloproteinase-3. *Haematologica* 92, 440-449.

32. Decker, K., Goldman, D.C., L. Grasch, C., & Sussel, L. (2006). Gata6 is an important regulator of mouse pancreas development. *Developmental Biology* 298, 415-429.

33. Delsert, C.D., & Rosenfeld, M.G. (1992). A tissue-specific small nuclear ribonucleoprotein and the regulated splicing of the calcitonin/calcitonin gene-related protein transcript. *Journal of Biological Chemistry* 267, 14573-14579.

34. Dennis, J.E., Merriam, A., Awadallah, A., Yoo, J.U., Johnstone, B., & Caplan, A.I. (1999). A Quadripotential Mesenchymal Progenitor Cell Isolated from the Marrow of an Adult Mouse. *Journal of Bone and Mineral Research* 14, 700-709.

35. Dimitriou, R., Jones, E., McGonagle, D., & Giannoudis, P. (2011). Bone regeneration: current concepts and future directions. *BMC Medicine* 9, 66.

36. Dobreva, G., Chahrour, M., Dautzenberg, M., Chirivella, L., Kanzler, B., Fariñas, I., Karsenty, G., & Grosschedl, R. (2006). SATB2 Is a Multifunctional Determinant of Craniofacial Patterning and Osteoblast Differentiation. *Cell* 125, 971-986.

37. Doll, B., Aleef, M., & Hollinger, J.O. (2008). Overview of Fracture Repair Musculoskeletal Tissue Regeneration. W.S. Pietrzak, ed. (Humana Press), pp. 39-61.

38. Dominici, M., Le Blanc, K., Mueller, I., Slaper-Cortenbach, I., Marini, F., Krause, D., Deans, R., Keating, A., Prockop, D., & Horwitz, E. (2006). Minimal criteria for defining multipotent mesenchymal stromal cells. The International Society for Cellular Therapy position statement. *Cytotherapy* 8, 315-317.

39. Drews, K., Jozefczuk, J., Prigione, A., & Adjaye, J. (2012). Human induced pluripotent stem cells—from mechanisms to clinical applications. *J Mol Med* 90, 735-745.

40. Drissi, H., Luc, Q., Shakoori, R., Chuva De Sousa Lopes, S., Choi, J.-Y., Terry, A., Hu, M., Jones, S., Neil, J.C., Lian, J.B., Stein, J.L., Van Wijnen, A.J., & Stein, G.S. (2000). Transcriptional autoregulation of the bone related CBFA1/RUNX2 gene. *Journal of Cellular Physiology* 184, 341-350.

41. Ducy, P., Zhang, R., Geoffroy, V., Ridall, A.L., & Karsenty, G. (1997). Osf2/Cbfa1: A Transcriptional Activator of Osteoblast Differentiation. *Cell* 89, 747-754.

42. Durocher, D., Charron, F., Warren, R., Schwartz, R.J., & Nemer, M. (1997). The cardiac transcription factors Nkx2-5 and GATA-4 are mutual cofactors. *EMBO J* 16, 5687-5696.

43. Eghbali-Fatourechi, G.Z., Lamsam, J., Fraser, D., Nagel, D., Riggs, B.L., & Khosla, S. (2005). Circulating Osteoblast-Lineage Cells in Humans. *New England Journal of Medicine* 352, 1959-1966.

44. Einhorn, T.A. (2005). The science of fracture healing. *J Orthop Trauma* 19, S4-6.

45. Emsley, J., Knight, C.G., Farndale, R.W., Barnes, M.J., & Liddington, R.C. (2000). Structural Basis of Collagen Recognition by Integrin α2β1. *Cell* 101, 47-56.

46. Engel, A., Fujiyoshi, Y., Gonen, T., & Walz, T. (2008). Junction-forming aquaporins. *Current Opinion in Structural Biology* 18, 229-235.

47. Erices, A., Conget, P., & Minguell, J.J. (2000). Mesenchymal progenitor cells in human umbilical cord blood. *British Journal of Haematology* 109, 235-242.

48. Etheridge, S.L., Spencer, G.J., Heath, D.J., & Genever, P.G. (2004). Expression Profiling and Functional Analysis of Wnt Signaling Mechanisms in Mesenchymal Stem Cells. *STEM CELLS* 22, 849-860.

49. Ezquer, F.E., Ezquer, M.E., Parrau, D.B., Carpio, D., Yañez, A.J., & Conget, P.A. (2008). Systemic administration of multipotent mesenchymal stromal cells reverts hyperglycemia and prevents nephropathy in type 1 diabetic mice. *Biology of Blood and Marrow Transplantation* 14, 631-640.

50. Ezura, Y., Sekiya, I., Koga, H., Muneta, T., & Noda, M. (2009). Methylation status of CpG islands in the promoter regions of signature genes during chondrogenesis of human synovium–derived mesenchymal stem cells. *Arthritis & Rheumatism* 60, 1416-1426.

51. Fan, C.G., Tang, F.W., Zhang, Q.J., Lu, S.H., Liu, H.Y., Zhao, Z.M., Liu, B., Han, Z.B., & Han, Z.C. Characterization and Neural Differentiation of Fetal Lung Mesenchymal Stem Cells. *Cell Transplantation* 14, 311-321.

52. Fischer, U., & Luhrmann, R. (1990). An essential signaling role for the m3G cap in the transport of U1 snRNP to the nucleus. *Science* 249, 786-790.

53. Friedenstein, A.J., Gorskaja, J.F., & Kulagina, N.N. (1976). Fibroblast precursors in normal and irradiated mouse hematopoietic organs. *Exp Hematol* 4, 267-274.

54. Gao, H., Priebe, W., Glod, J., & Banerjee, D. (2009). Activation of signal transducers and activators of transcription 3 and focal adhesion kinase by stromal cell-derived factor 1 is required for migration of human mesenchymal stem cells in response to tumor cell-conditioned medium. *Stem Cells* 27, 857-865.

55. Gao, X., Sedgwick, T., Shi, Y.-B., & Evans, T. (1998). Distinct Functions Are Implicated for the GATA-4, -5, and -6 Transcription Factors in the Regulation of Intestine Epithelial Cell Differentiation. *Molecular and Cellular Biology* 18, 2901-2911.

56. Garces, C.A., Kurenova, E.V., Golubovskaya, V.M., & Cance, W.G. (2006). Vascular Endothelial Growth Factor Receptor-3 and Focal Adhesion Kinase Bind and Suppress Apoptosis in Breast Cancer Cells. *Cancer Research* 66, 1446-1454.

57. Gerstenfeld, L.C., Cullinane, D.M., Barnes, G.L., Graves, D.T., & Einhorn, T.A. (2003). Fracture healing as a post-natal developmental process: Molecular, spatial, and temporal aspects of its regulation. *Journal of Cellular Biochemistry* 88, 873-884.

58. Ghosh, M.C., Makena, P.S., Gorantla, V., Sinclair, S.E., & Waters, C.M. (2012). CXCR4 regulates migration of lung alveolar epithelial cells through activation of Rac1 and matrix metalloproteinase-2. *Am J Physiol Lung Cell Mol Physiol* 302, L846-856.

59. Ghozi, M.C., Bernstein, Y., Negreanu, V., Levanon, D., & Groner, Y. (1996). Expression of the human acute myeloid leukemia gene AML1 is regulated by two promoter regions. *Proceedings of the National Academy of Sciences* 93, 1935-1940.

60. Gilles, C., Polette, M., Mestdagt, M., Nawrocki-Raby, B., Ruggeri, P., Birembaut, P., & Foidart, J.-M. (2003). Transactivation of vimentin by β-catenin in human breast cancer cells. *Cancer Research* 63, 2658-2664.

61. Golubovskaya, V., Beviglia, L., Xu, L.-H., Earp, H.S., Craven, R., & Cance, W. (2002). Dual Inhibition of Focal Adhesion Kinase and Epidermal Growth Factor Receptor Pathways Cooperatively Induces Death Receptor-mediated Apoptosis in Human Breast Cancer Cells. *Journal of Biological Chemistry* 277, 38978-38987.

62. Gong, Y., Slee, R.B., Fukai, N., Rawadi, G., Roman-Roman, S., Reginato, A.M., Wang, H., Cundy, T., Glorieux, F.H., Lev, D., Zacharin, M., Oexle, K., Marcelino, J., Suwairi, W., Heeger, S., Sabatakos, G., Apte, S., Adkins, W.N., Allgrove, J., Arslan-Kirchner, M., Batch, J.A., Beighton, P., Black, G.C.M., Boles, R.G., Boon, L.M., Borrone, C., Brunner, H.G., Carle, G.F., Dallapiccola, B., De Paepe, A., Floege, B., Halfhide, M.L., Hall, B., Hennekam, R.C., Hirose, T., Jans, A., Jüppner, H., Kim, C.A., Keppler-Noreuil, K., Kohlschuetter, A., LaCombe, D., Lambert, M., Lemyre, E., Letteboer, T., Peltonen, L., Ramesar, R.S., Romanengo, M., Somer, H., Steichen-Gersdorf, E., Steinmann, B., Sullivan, B., Superti-Furga, A., Swoboda, W., van den Boogaard, M.-J., Van Hul, W., Vikkula, M., Votruba, M., Zabel, B., Garcia, T., Baron, R., Olsen,

B.R., & Warman, M.L. (2001). LDL Receptor-Related Protein 5 (LRP5) Affects Bone Accrual and Eye Development. *Cell* 107, 513-523.

63. Gottschling, S., Saffrich, R., Seckinger, A., Krause, U., Horsch, K., Miesala, K., & Ho, A.D. (2007). Human mesenchymal stromal cells regulate initial self-renewing divisions of hematopoietic progenitor cells by a beta1-integrin-dependent mechanism. *Stem Cells* 25, 798-806.

64. Granero-Moltó, F., Weis, J.A., Miga, M.I., Landis, B., Myers, T.J., O'Rear, L., Longobardi, L., Jansen, E.D., Mortlock, D.P., & Spagnoli, A. (2009). Regenerative effects of transplanted mesenchymal stem cells in fracture healing. *Stem Cells* 27, 1887-1898.

65. Hamada, H., Kobune, M., Nakamura, K., Kawano, Y., Kato, K., Honmou, O., Houkin, K., Matsunaga, T., & Niitsu, Y. (2005). Mesenchymal stem cells (MSC) as therapeutic cytoreagents for gene therapy. *Cancer Science* 96, 149-156.

66. Hamm, J., Darzynkiewicz, E., Tahara, S.M., & Mattaj, I.W. (1990). The trimethylguanosine cap structure of U1 snRNA is a component of a bipartite nuclear targeting signal. *Cell* 62, 569-577.

67. Hara-Chikuma, M., & Verkman, A.S. (2005). Aquaporin-3 functions as a glycerol transporter in mammalian skin. *Biology of the Cell* 97, 479-486.

68. Hara-Chikuma, M., & Verkman, A.S. (2006). Aquaporin-1 Facilitates Epithelial Cell Migration in Kidney Proximal Tubule. *Journal of the American Society of Nephrology* 17, 39-45.

69. Harada, S.-i., & Rodan, G.A. (2003). Control of osteoblast function and regulation of bone mass. *Nature* 423, 349-355.

70. Harris, T.J.C., & Peifer, M. (2005). Decisions, decisions: β-catenin chooses between adhesion and transcription. *Trends in Cell Biology* 15, 234-237.

71. Hatsell, S., Rowlands, T., Hiremath, M., & Cowin, P. (2003). β-catenin and Tcfs in mammary development and cancer. *Journal of Mammary Gland Biology and Neoplasia* 8, 145-158.

72. Hayakawa, F., Towatari, M., Ozawa, Y., Tomita, A., Privalsky, M.L., & Saito, H. (2004). Functional regulation of GATA-2 by acetylation. *Journal of Leukocyte Biology* 75, 529-540.

73. Hayashi, S., Takahashi, N., Kurata, N., Yamaguchi, A., Matsui, H., Kato, S., & Takeuchi, K. (2009). Involvement of aquaporin-1 in gastric epithelial cell migration during wound repair. *Biochemical and Biophysical Research Communications* 386, 483-487.

74. He, Q., Wan, C., & Li, G. (2007). Concise Review: Multipotent Mesenchymal Stromal Cells in Blood. *STEM CELLS* 25, 69-77.

75. He, Q., Wan, C., & Li, G. (2011). Circulating mesenchymal stem cells and their clinical implications. *Journal of Bone & Joint Surgery, British Volume* 93-B, 68.

76. Hernandez-Hernandez, A., Ray, P., Litos, G., Ciro, M., Ottolenghi, S., Beug, H., & Boyes, J. (2006). Acetylation and MAPK phosphorylation cooperate to regulate the degradation of active GATA-1. *EMBO J* 25, 3264-3274.

77. Herrera, M., & Garvin, J.L. (2007). Novel role of AQP-1 in NO-dependent vasorelaxation. *American Journal of Physiology - Renal Physiology* 292, F1443-F1451.

78. Hietakangas, V., Anckar, J., Blomster, H.A., Fujimoto, M., Palvimo, J.J., Nakai, A., & Sistonen, L. (2006). PDSM, a motif for phosphorylation-dependent SUMO modification. *Proceedings of the National Academy of Sciences of the United States of America* 103, 45-50.

79. Ho, P.-J., Yen, M.-L., Yet, S.-F., & Yen, B.L. (2012). Current Applications of Human Pluripotent Stem Cells: Possibilities and Challenges. *Cell Transplantation* 21, 801-814.

80. Holmen, S.L., Giambernardi, T.A., Zylstra, C.R., Buckner-Berghuis, B.D., Resau, J.H., Hess, J.F., Glatt, V., Bouxsein, M.L., Ai, M., Warman, M.L., & Williams, B.O. (2004). Decreased BMD and Limb Deformities in Mice Carrying Mutations in Both Lrp5 and Lrp6. *Journal of Bone and Mineral Research* 19, 2033-2040.

81. Horn, D.A., Suburo, A., Terenghi, G., Hudson, L.D., Polak, J.M., & Latchman, D.S. (1992). Expression of the tissue specific splicing protein SmN in neuronal cell lines and in regions of the brain with different splicing capacities. *Molecular Brain Research* 16, 13-19.

82. Hu, H., Hilton, M.J., Tu, X., Yu, K., Ornitz, D.M., & Long, F. (2005). Sequential roles of Hedgehog and Wnt signaling in osteoblast development. *Development* 132, 49-60.

83. Huang, J., Zhang, Z., Guo, J., Ni, A., Deb, A., Zhang, L., Mirotsou, M., Pratt, R.E., & Dzau, V.J. (2010). Genetic modification of mesenchymal stem cells overexpressing CCR1 increases cell viability, migration, engraftment, and capillary density in the injured myocardium. *Circ Res* 106, 1753-1762.

84. Huntriss, J.D., Latchman, D.S., & Williams, D.G. (1993). The snRNP core protein SmB and tissue-specific SmN protein are differentially distributed between snRNP particles. *Nucleic Acids Research* 21, 4047-4053.

85. in `t Anker, P.S., Scherjon, S.A., Kleijburg-van der Keur, C., Noort, W.A., Claas, F.H.J., Willemze, R., Fibbe, W.E., & Kanhai, H.H.H. (2003). Amniotic fluid as a novel source of mesenchymal stem cells for therapeutic transplantation. *Blood* 102, 1548-1549.

86. Ishibashi, K., Hara, S., & Kondo, S. (2009). Aquaporin water channels in mammals. *Clin Exp Nephrol* 13, 107-117.

87. Ishibashi, K., Morinaga, T., Kuwahara, M., Sasaki, S., & Imai, M. (2002). Cloning and identification of a new member of water channel (AQP10) as an aquaglyceroporin. *Biochimica et Biophysica Acta (BBA) - Gene Structure and Expression* 1576, 335-340.

88. Itoh, T., Rai, T., Kuwahara, M., Ko, S.B.H., Uchida, S., Sasaki, S., & Ishibashi, K. (2005). Identification of a novel aquaporin, AQP12, expressed in pancreatic acinar cells. *Biochemical and Biophysical Research Communications* 330, 832-838.

89. Jones, D.C., Wein, M.N., Oukka, M., Hofstaetter, J.G., Glimcher, M.J., & Glimcher, L.H. (2006). Regulation of Adult Bone Mass by the Zinc Finger Adapter Protein Schnurri-3. *Science* 312, 1223-1227.

90. Juuti-Uusitalo, K., Delporte, C., Gregoire, F., Perret, J., Huhtala, H., Savolainen, V., Nymark, S., Hyttinen, J., Uusitalo, H., Willermain, F., & Skottman, H. (2013). Aquaporin expression and function in human pluripotent stem cell-derived retinal pigmented epithelial cells. *Invest Ophthalmol Vis Sci* 54, 3510-3519.

91. Kamachi, Y., Ogawa, E., Asano, M., Ishida, S., Murakami, Y., Satake, M., Ito, Y., & Shigesada, K. (1990). Purification of a mouse nuclear factor that binds to both the A and B cores of the polyomavirus enhancer. *Journal of Virology* 64, 4808-4819.

92. Kang, M.-I., Kim, H.-S., Jung, Y.-C., Kim, Y.-H., Hong, S.-J., Kim, M.-K., Baek, K.-H., Kim, C.C., & Rhyu, M.-G. (2007). Transitional CpG methylation between promoters and retroelements of tissue-specific genes during human mesenchymal cell differentiation. *Journal of Cellular Biochemistry* 102, 224-239.

93. Kanno, T., Kanno, Y., Chen, L.-F., Ogawa, E., Kim, W.-Y., & Ito, Y. (1998). Intrinsic Transcriptional Activation-Inhibition Domains of the Polyomavirus Enhancer Binding Protein 2/Core Binding Factor α Subunit Revealed in the Presence of the β Subunit. *Molecular and Cellular Biology* 18, 2444-2454.

94. Karis, A., Pata, I., van Doorninck, J.H., Grosveld, F., de Zeeuw, C.I., de Caprona, D., & Fritzsch, B. (2001). Transcription factor GATA-3 alters pathway selection of olivocochlear neurons and affects morphogenesis of the ear. *The Journal of Comparative Neurology* 429, 615-630.

95. Keijzer, R., van Tuyl, M., Meijers, C., Post, M., Tibboel, D., Grosveld, F., & Koutsourakis, M. (2001). The transcription factor GATA6 is essential for branching morphogenesis and epithelial cell differentiation during fetal pulmonary development. *Development* 128, 503-511.

96. Khosla, S., & Eghbali-Fatourechi, G.Z. (2006). Circulating Cells with Osteogenic Potential. *Annals of the New York Academy of Sciences* 1068, 489-497.

97. Kim, M., Carman, C.V., & Springer, T.A. (2003a). Bidirectional Transmembrane Signaling by Cytoplasmic Domain Separation in Integrins. *Science* 301, 1720-1725.

98. Kim, S., Koga, T., Isobe, M., Kern, B.E., Yokochi, T., Chin, Y.E., Karsenty, G., Taniguchi, T., & Takayanagi, H. (2003b). Stat1 functions as a cytoplasmic attenuator of Runx2 in the transcriptional program of osteoblast differentiation. *Genes & Development* 17, 1979-1991.

99. Koga, T., Matsui, Y., Asagiri, M., Kodama, T., de Crombrugghe, B., Nakashima, K., & Takayanagi, H. (2005). NFAT and Osterix cooperatively regulate bone formation. *Nat Med* 11, 880-885.

100. Komori, T., Yagi, H., Nomura, S., Yamaguchi, A., Sasaki, K., Deguchi, K., Shimizu, Y., Bronson, R.T., Gao, Y.H., Inada, M., Sato, M., Okamoto, R., Kitamura, Y., Yoshiki, S., & Kishimoto, T. (1997). Targeted disruption of cbfa1 results in a complete lack of bone formation owing to maturational arrest of osteoblasts. *Cell* 89, 755-764.

101. Kornblihtt, A.R., Schor, I.E., Allo, M., Dujardin, G., Petrillo, E., & Munoz, M.J. (2013). Alternative splicing: a pivotal step between eukaryotic transcription and translation. *Nat Rev Mol Cell Biol* 14, 153-165.

102. Kortesidis, A., Zannettino, A., Isenmann, S., Shi, S., Lapidot, T., & Gronthos, S. (2005). Stromal-derived factor-1 promotes the growth, survival, and development of human bone marrow stromal stem cells. *Blood* 105, 3793-3801.

103. Krampera, M., Pizzolo, G., Aprili, G., & Franchini, M. (2006). Mesenchymal stem cells for bone, cartilage, tendon and skeletal muscle repair. *Bone* 39, 678-683.

104. Kumagai, K., Vasanji, A., Drazba, J.A., Butler, R.S., & Muschler, G.F. (2008). Circulating cells with osteogenic potential are physiologically mobilized into the fracture healing site in the parabiotic mice model. *Journal of Orthopaedic Research* 26, 165-175.

105. Kumar, S., & Ponnazhagan, S. (2012). Mobilization of bone marrow mesenchymal stem cells in vivo augments bone healing in a mouse model of segmental bone defect. *Bone* 50, 1012-1018.

106. Kuslich, C.D., Kobori, J.A., Mohapatra, G., Gregorio-King, C., & Donlon, T.A. (1999). Prader-Willi syndrome is caused by disruption of the SNRPN Gene. *The American Journal of Human Genetics* 64, 70-76.

107. Kuznetsov, S.A., Mankani, M.H., Gronthos, S., Satomura, K., Bianco, P., & Robey, P.G. (2001). Circulating Skeletal Stem Cells. *The Journal of Cell Biology* 153, 1133-1140.

108. Lévesque, J.-P., Hendy, J., Takamatsu, Y., Simmons, P.J., & Bendall, L.J. (2003). Disruption of the CXCR4/CXCL12 chemotactic interaction during hematopoietic stem cell mobilization induced by GCSF or cyclophosphamide. *The Journal of Clinical Investigation* 111, 187-196.

109. Lechertier, T., & Hodivala-Dilke, K. (2012). Focal adhesion kinase and tumour angiogenesis. *The Journal of Pathology* 226, 404-412.

110. Lee, J., Ishihara, A., Oxford, G., Johnson, B., & Jacobson, K. (1999). Regulation of cell movement is mediated by stretch-activated calcium channels. *Nature* 400, 382-386.

111. Lee, R.H., Hsu, S.C., Munoz, J., Jung, J.S., Lee, N.R., Pochampally, R., & Prockop, D.J. (2006). A subset of human rapidly self-renewing marrow stromal cells preferentially engraft in mice. *Blood* 107, 2153-2161.

112. Lerner, M.R., & Steitz, J.A. (1979). Antibodies to small nuclear RNAs complexed with proteins are produced by patients with systemic lupus erythematosus. *Proceedings of the National Academy of Sciences* 76, 5495-5499.

113. Leung, K.S., Shi, H.F., Cheung, W.H., Qin, L., Ng, W.K., Tam, K.F., & Tang, N. (2009). Low-magnitude high-frequency vibration accelerates callus formation, mineralization, and fracture healing in rats. *Journal of Orthopaedic Research* 27, 458-465.

114. Levanon, D., Glusman, G., Bangsow, T., Ben-Asher, E., Male, D.A., Avidan, N., Bangsow, C., Hattori, M., Taylor, T.D., Taudien, S., Blechschmidt, K., Shimizu, N., Rosenthal, A., Sakaki, Y., Lancet, D., & Groner, Y. (2001). Architecture and anatomy of the genomic locus encoding the human leukemia-associated transcription factor RUNX1/AML1. *Gene* 262, 23-33.

115. Li, H., Kamiie, J., Morishita, Y., Yoshida, Y., Yaoita, E., Ishibashi, K., & Yamamoto, T. (2005). Expression and localization of two isoforms of AQP10 in human small intestine. *Biology of the Cell* 97, 823-829.

116. Lietha, D., Cai, X., Ceccarelli, D.F.J., Li, Y., Schaller, M.D., & Eck, M.J. (2007). Structural basis for the autoinhibition of focal adhesion kinase. *Cell* 129, 1177-1187.

117. Liu, H., Liu, S., Li, Y., Wang, X., Xue, W., Ge, G., & Luo, X. (2012). The role of SDF-1-CXCR4/CXCR7 axis in the therapeutic effects of hypoxia-preconditioned mesenchymal stem cells for renal ischemia/reperfusion injury. *PLoS ONE* 7, e34608.

118. Logan, C.Y., & Nusse, R. (2004). The Wnt signaling pathway in development and disease. *Annual Review of Cell and Developmental Biology* 20, 781-810.

119. Long, F. (2012). Building strong bones: molecular regulation of the osteoblast lineage. *Nat Rev Mol Cell Biol* 13, 27-38.

120. Lu, D.C., Zhang, H., Zador, Z., & Verkman, A.S. (2008). Impaired olfaction in mice lacking aquaporin-4 water channels. *The FASEB Journal* 22, 3216-3223.

121. Lu, P., Blesch, A., & Tuszynski, M.H. (2004). Induction of bone marrow stromal cells to neurons: Differentiation, transdifferentiation, or artifact? *Journal of Neuroscience Research* 77, 174-191.

122. Luria, E.A., Panasyuk, A.F., & Friedenstein, A.Y. (1971). Fibroblast Colony Formation from Monolayer Cultures of Blood Cells. *Transfusion* 11, 345-349.

123. Müller, T., Bain, G., Wang, X., & Papkoff, J. (2002). Regulation of Epithelial Cell Migration and Tumor Formation by β-Catenin Signaling. *Experimental Cell Research* 280, 119-133.

124. Müller, T., Choidas, A., Reichmann, E., & Ullrich, A. (1999). Phosphorylation and Free Pool of β-Catenin Are Regulated by Tyrosine Kinases and Tyrosine Phosphatases during Epithelial Cell Migration. *Journal of Biological Chemistry* 274, 10173-10183.

125. Ma, T., Yang, B., & Verkman, A.S. (1997). Cloning of a Novel Water and Urea-Permeable Aquaporin from Mouse Expressed Strongly in Colon, Placenta, Liver, and Heart. *Biochemical and Biophysical Research Communications* 240, 324-328.

126. Maeda, N., Funahashi, T., Hibuse, T., Nagasawa, A., Kishida, K., Kuriyama, H., Nakamura, T., Kihara, S., Shimomura, I., & Matsuzawa, Y. (2004). Adaptation to fasting by glycerol

transport through aquaporin 7 in adipose tissue. *Proceedings of the National Academy of Sciences of the United States of America* 101, 17801-17806.

127. Massagué, J. (1998). TGF-β Signal Transduction. *Annual Review of Biochemistry* 67, 753-791.

128. McAllister, G., Amara, S.G., & Lerner, M.R. (1988). Tissue-specific expression and cDNA cloning of small nuclear ribonucleoprotein-associated polypeptide N. *Proceedings of the National Academy of Sciences* 85, 5296-5300.

129. Menghini, R., Marchetti, V., Cardellini, M., Hribal, M.L., Mauriello, A., Lauro, D., Sbraccia, P., Lauro, R., & Federici, M. (2005). Phosphorylation of GATA2 by Akt Increases Adipose Tissue Differentiation and Reduces Adipose Tissue–Related Inflammation: A Novel Pathway Linking Obesity to Atherosclerosis. *Circulation* 111, 1946-1953.

130. Mirotsou, M., Zhang, Z., Deb, A., Zhang, L., Gnecchi, M., Noiseux, N., Mu, H., Pachori, A., & Dzau, V. (2007). Secreted frizzled related protein 2 (Sfrp2) is the key Akt-mesenchymal stem cell-released paracrine factor mediating myocardial survival and repair. *Proceedings of the National Academy of Sciences* 104, 1643-1648.

131. Mitra, S.K., Hanson, D.A., & Schlaepfer, D.D. (2005). Focal adhesion kinase: in command and control of cell motility. *Nat Rev Mol Cell Biol* 6, 56-68.

132. Mjösberg, J., Bernink, J., Peters, C., & Spits, H. (2012). Transcriptional control of innate lymphoid cells. *European Journal of Immunology* 42, 1916-1923.

133. Molkentin, J.D. (2000). The Zinc Finger-containing Transcription Factors GATA-4, -5, and -6: Ubiquitously expressed regulators of tissue-specific gene expression. *Journal of Biological Chemistry* 275, 38949-38952.

134. Monzani, E., Bazzotti, R., Perego, C., & La Porta, C.A.M. (2009). AQP1 is not only a water channel: It contributes to cell migration through Lin7/Beta-Catenin. *PLoS One* 4, e6167.

135. Morishita, Y., Matsuzaki, T., Hara-chikuma, M., Andoo, A., Shimono, M., Matsuki, A., Kobayashi, K., Ikeda, M., Yamamoto, T., Verkman, A., Kusano, E., Ookawara, S., Takata, K.,

Sasaki, S., & Ishibashi, K. (2005). Disruption of Aquaporin-11 Produces Polycystic Kidneys following Vacuolization of the Proximal Tubule. *Molecular and Cellular Biology* 25, 7770-7779.

136. Morrisey, E.E., Tang, Z., Sigrist, K., Lu, M.M., Jiang, F., Ip, H.S., & Parmacek, M.S. (1998). GATA6 regulates HNF4 and is required for differentiation of visceral endoderm in the mouse embryo. *Genes & Development* 12, 3579-3590.

137. Nakashima, K., Zhou, X., Kunkel, G., Zhang, Z., Deng, J.M., Behringer, R.R., & de Crombrugghe, B. (2002). The Novel Zinc Finger-Containing Transcription Factor Osterix Is Required for Osteoblast Differentiation and Bone Formation. *Cell* 108, 17-29.

138. Nielsen, S., King, L.S., Christensen, B.M., & Agre, P. (1997). Aquaporins in complex tissues. II. Subcellular distribution in respiratory and glandular tissues of rat. *American Journal of Physiology - Cell Physiology* 273, C1549-C1561.

139. Nielsen, S., Smith, B.L., Christensen, E.I., & Agre, P. (1993a). Distribution of the aquaporin CHIP in secretory and resorptive epithelia and capillary endothelia. *Proceedings of the National Academy of Sciences* 90, 7275-7279.

140. Nielsen, S., Smith, B.L., Christensen, E.I., Knepper, M.A., & Agre, P. (1993b). CHIP28 water channels are localized in constitutively water-permeable segments of the nephron. *The Journal of Cell Biology* 120, 371-383.

141. Nishida, W., Nakamura, M., Mori, S., Takahashi, M., Ohkawa, Y., Tadokoro, S., Yoshida, K., Hiwada, K., Hayashi, K.i., & Sobue, K. (2002). A Triad of Serum Response Factor and the GATA and NK Families Governs the Transcription of Smooth and Cardiac Muscle Genes. *Journal of Biological Chemistry* 277, 7308-7317.

142. Nishikawa, K., Nakashima, T., Takeda, S., Isogai, M., Hamada, M., Kimura, A., Kodama, T., Yamaguchi, A., Owen, M.J., Takahashi, S., & Takayanagi, H. (2010). Maf promotes osteoblast differentiation in mice by mediating the age-related switch in mesenchymal cell differentiation. *The Journal of Clinical Investigation* 120, 3455-3465.

143. Obermeyer, T.S., Yonick, D., Lauing, K., Stock, S.R., Nauer, R., Strotman, P., Shankar, R., Gamelli, R., Stover, M., & Callaci, J.J. (2012). Mesenchymal stem cells facilitate fracture repair in an alcohol-induced impaired healing model. *J Orthop Trauma* 26, 712-718.

144. Orkin, S. (1992). GATA-binding transcription factors in hematopoietic cells. *Blood* 80, 575-581.

145. Ortiz, L.A., Gambelli, F., McBride, C., Gaupp, D., Baddoo, M., Kaminski, N., & Phinney, D.G. (2003). Mesenchymal stem cell engraftment in lung is enhanced in response to bleomycin exposure and ameliorates its fibrotic effects. *Proceedings of the National Academy of Sciences* 100, 8407-8411.

146. Otto, F., Lübbert, M., & Stock, M. (2003). Upstream and downstream targets of RUNX proteins. *Journal of Cellular Biochemistry* 89, 9-18.

147. Otto, F., Thornell, A.P., Crompton, T., Denzel, A., Gilmour, K.C., Rosewell, I.R., Stamp, G.W.H., Beddington, R.S.P., Mundlos, S., Olsen, B.R., Selby, P.B., & Owen, M.J. (1997). Cbfa1, a Candidate Gene for Cleidocranial Dysplasia Syndrome, Is Essential for Osteoblast Differentiation and Bone Development. *Cell* 89, 765-771.

148. Oury, F., Sumara, G., Sumara, O., Ferron, M., Chang, H., Smith, Charles E., Hermo, L., Suarez, S., Roth, Bryan L., Ducy, P., & Karsenty, G. (2011). Endocrine Regulation of Male Fertility by the Skeleton. *Cell* 144, 796-809.

149. Ozawa, M., Baribault, H., & Kemler, R. (1989). The cytoplasmic domain of the cell adhesion molecule uvomorulin associates with three independent proteins structurally related in different species. *EMBO J* 8, 1711-1717.

150. Ozturan, K.E., Demir, B., Yucel, I., Cakıcı, H., Yilmaz, F., & Haberal, A. (2011). Effect of strontium ranelate on fracture healing in the osteoporotic rats. *Journal of Orthopaedic Research* 29, 138-142.

151. Peritz, T., Zeng, F., Kannanayakal, T.J., Kilk, K., Eiriksdottir, E., Langel, U., & Eberwine, J. (2006). Immunoprecipitation of mRNA-protein complexes. *Nat. Protocols* 1, 577-580.

152. Phinney, D.G., & Prockop, D.J. (2007). Concise Review: Mesenchymal Stem/Multipotent Stromal Cells: The State of Transdifferentiation and Modes of Tissue Repair—Current Views. *Stem Cells* 25, 2896-2902.

153. Polakis, P. (2000). Wnt signaling and cancer. *Genes & Development* 14, 1837-1851.

154. Polette, M., Mestdagt, M., Bindels, S., Nawrocki-Raby, B., Hunziker, W., Foidart, J.M., Birembaut, P., & Gilles, C. (2007). β-catenin and ZO-1: shuttle molecules involved in tumor invasion-associated epithelial-mesenchymal transition processes. *Cells Tissues Organs* 185, 61-65.

155. Preston, G.M., Carroll, T.P., Guggino, W.B., & Agre, P. (1992). Appearance of water channels in Xenopus oocytes expressing red cell CHIP28 protein. *Science* 256, 385-387.

156. Provenzano, P.P., & Keely, P.J. (2009). The role of focal adhesion kinase in tumor initiation and progression. *Cell Adhesion & Migration* 3, 347-350.

157. Quarto, R., Mastrogiacomo, M., Cancedda, R., Kutepov, S.M., Mukhachev, V., Lavroukov, A., Kon, E., & Marcacci, M. (2001). Repair of large bone defects with the use of autologous bone marrow stromal cells. *New England Journal of Medicine* 344, 385-386.

158. Rüster, B., Göttig, S., Ludwig, R.J., Bistrian, R., Müller, S., Seifried, E., Gille, J., & Henschler, R. (2006). Mesenchymal stem cells display coordinated rolling and adhesion behavior on endothelial cells. *Blood* 108, 3938-3944.

159. Raghunath, J., Sutherland, J., Salih, V., Mordan, N., Butler, P.E., & Seifalian, A.M. (2010). Chondrogenic potential of blood-acquired mesenchymal progenitor cells. *Journal of Plastic, Reconstructive & Aesthetic Surgery* 63, 841-847.

160. Raheja, L.F., Genetos, D.C., Wong, A., & Yellowley, C.E. (2011). Hypoxic regulation of mesenchymal stem cell migration: the role of RhoA and HIF-1alpha. *Cell Biol Int* 35, 981-989.

161. Raker, V.A., Plessel, G., & Luhrmann, R. (1996). The snRNP core assembly pathway: identification of stable core protein heteromeric complexes and an snRNP subcore particle in vitro. *EMBO J* 15, 2256-2269.

162. Ranganath, Sudhir H., Levy, O., Inamdar, Maneesha S., & Karp, Jeffrey M. (2012). Harnessing the mesenchymal stem cell secretome for the treatment of cardiovascular disease. *Cell Stem Cell* 10, 244-258.

163. Ridley, A.J., Schwartz, M.A., Burridge, K., Firtel, R.A., Ginsberg, M.H., Borisy, G., Parsons, J.T., & Horwitz, A.R. (2003). Cell migration: integrating signals from front to back. *Science* 302, 1704-1709.

164. Ries, C., Egea, V., Karow, M., Kolb, H., Jochum, M., & Neth, P. (2007). MMP-2, MT1-MMP, and TIMP-2 are essential for the invasive capacity of human mesenchymal stem cells: differential regulation by inflammatory cytokines. *Blood* 109, 4055-4063.

165. Rochefort, G.Y., Delorme, B., Lopez, A., Herault, O., Bonnet, P., Charbord, P., Eder, V., & Domenech, J. (2006). Multipotential mesenchymal stem cells are mobilized into peripheral blood by hypoxia. *Stem Cells* 24, 2202-2208.

166. Rojek, A.M., Skowronski, M.T., Füchtbauer, E.-M., Füchtbauer, A.C., Fenton, R.A., Agre, P., Frøkiær, J., & Nielsen, S. (2007). Defective glycerol metabolism in aquaporin 9 (AQP9) knockout mice. *Proceedings of the National Academy of Sciences* 104, 3609-3614.

167. Romero-Prado, M., Blázquez, C., Rodríguez-Navas, C., Muñoz, J., Guerrero, I., Delgado-Baeza, E., & García-Ruiz, J.P. (2006). Functional characterization of human mesenchymal stem cells that maintain osteochondral fates. *Journal of Cellular Biochemistry* 98, 1457-1470.

168. Roudier, N., Ripoche, P., Gane, P., Le Pennec, P.Y., Daniels, G., Cartron, J.-P., & Bailly, P. (2002). AQP3 Deficiency in Humans and the Molecular Basis of a Novel Blood Group System, GIL. *Journal of Biological Chemistry* 277, 45854-45859.

169. Saadoun, S., Papadopoulos, M.C., Hara-Chikuma, M., & Verkman, A.S. (2005). Impairment of angiogenesis and cell migration by targeted aquaporin-1 gene disruption. *Nature* 434, 786-792.

170. Satokata, I., Ma, L., Ohshima, H., Bei, M., Woo, I., Nishizawa, K., Maeda, T., Takano, Y., Uchiyama, M., Heaney, S., Peters, H., Tang, Z., Maxson, R., & Maas, R. (2000). Msx2

deficiency in mice causes pleiotropic defects in bone growth and ectodermal organ formation. *Nat Genet* 24, 391-395.

171. Schaller, M.D. (2010). Cellular functions of FAK kinases: insight into molecular mechanisms and novel functions. *Journal of Cell Science* 123, 1007-1013.

172. Schaller, M.D., Otey, C.A., Hildebrand, J.D., & Parsons, J.T. (1995). Focal adhesion kinase and paxillin bind to peptides mimicking beta integrin cytoplasmic domains. *J Cell Biol* 130, 1181-1187.

173. Schindeler, A., McDonald, M.M., Bokko, P., & Little, D.G. (2008). Bone remodeling during fracture repair: The cellular picture. *Seminars in Cell & Developmental Biology* 19, 459-466.

174. Schmauss, C., McAllister, G., Ohosone, Y., Hardin, J.A., & Lerner, M.R. (1989). A comparison of snRNP-associated Sm-autoantigens: human N, rat N and human B/B′. *Nucleic Acids Research* 17, 1733-1743.

175. Schroeder, T.M., Jensen, E.D., & Westendorf, J.J. (2005). Runx2: A master organizer of gene transcription in developing and maturing osteoblasts. *Birth Defects Research Part C: Embryo Today: Reviews* 75, 213-225.

176. Seta, N., & Kuwana, M. (2007). Human circulating monocytes as multipotential progenitors. *Keio J Med* 56, 41-47.

177. Shaw-White, J.R., Bruno, M.D., & Whitsett, J.A. (1999). GATA-6 Activates Transcription of Thyroid Transcription Factor-1. *Journal of Biological Chemistry* 274, 2658-2664.

178. Shimizu, R., Takahashi, S., Ohneda, K., Engel, J.D., & Yamamoto, M. (2001). In vivo requirements for GATA-1 functional domains during primitive and definitive erythropoiesis. *EMBO J* 20, 5250-5260.

179. Shirley, D., Marsh, D., Jordan, G., McQuaid, S., & Li, G. (2005). Systemic recruitment of osteoblastic cells in fracture healing. *Journal of Orthopaedic Research* 23, 1013-1021.

180. Sieg, D.J., Hauck, C.R., Ilic, D., Klingbeil, C.K., Schaefer, E., Damsky, C.H., & Schlaepfer, D.D. (2000). FAK integrates growth-factor and integrin signals to promote cell migration. *Nat Cell Biol* 2, 249-256.

181. Singer, J., Charbord, P., Keating, A., Nemunaitis, J., Raugi, G., Wight, T., Lopez, J., Roth, G., Dow, L., & Fialkow, P. (1987). Simian virus 40-transformed adherent cells from human long-term marrow cultures: cloned cell lines produce cells with stromal and hematopoietic characteristics. *Blood* 70, 464-474.

182. Song, C., & Li, G. (2011). CXCR4 and matrix metalloproteinase-2 are involved in mesenchymal stromal cell homing and engraftment to tumors. *Cytotherapy* 13, 549-561.

183. Song, H., Cha, M.-J., Song, B.-W., Kim, I.-K., Chang, W., Lim, S., Choi, E.J., Ham, O., Lee, S.-Y., Chung, N., Jang, Y., & Hwang, K.-C. (2010). Reactive oxygen species inhibit adhesion of mesenchymal stem cells implanted into ischemic myocardium via interference of focal adhesion complex. *Stem Cells* 28, 555-563.

184. Sordi, V., Malosio, M.L., Marchesi, F., Mercalli, A., Melzi, R., Giordano, T., Belmonte, N., Ferrari, G., Leone, B.E., Bertuzzi, F., Zerbini, G., Allavena, P., Bonifacio, E., & Piemonti, L. (2005). Bone marrow mesenchymal stem cells express a restricted set of functionally active chemokine receptors capable of promoting migration to pancreatic islets. *Blood* 106, 419-427.

185. Splinter, P.L., Masyuk, A.I., & LaRusso, N.F. (2003). Specific inhibition of AQP1 water channels in isolated rat intrahepatic bile duct units by small interfering RNAs. *Journal of Biological Chemistry* 278, 6268-6274.

186. St-Jacques, B., Hammerschmidt, M., & McMahon, A.P. (1999). Indian hedgehog signaling regulates proliferation and differentiation of chondrocytes and is essential for bone formation. *Genes & Development* 13, 2072-2086.

187. Stein, G.S., Lian, J.B., Wijnen, A.J.v., Stein, J.L., Montecino, M., Javed, A., Zaidi, S.K., Young, D.W., Choi, J.-Y., & Pockwinse, S.M. (2004). Runx2 control of organization, assembly and activity of the regulatory machinery for skeletal gene expression. *Oncogene* 23, 4315-4329.

188. Stirling, G.A., & Kakkar, V.V. (1969). Cells in the circulating blood capable of producing connective tissue. *Br J Exp Pathol* 50, 51-55.

189. Taguchi, D., Takeda, T., Kakigi, A., Takumida, M., Nishioka, R., & Kitano, H. (2007). Expressions of Aquaporin-2, Vasopressin Type 2 Receptor, Transient Receptor Potential Channel Vanilloid (TRPV)1, and TRPV4 in the Human Endolymphatic Sac. *The Laryngoscope* 117, 695-698.

190. Tome, M., Lopez-Romero, P., Albo, C., Sepulveda, J.C., Fernandez-Gutierrez, B., Dopazo, A., Bernad, A., & Gonzalez, M.A. (2011). miR-335 orchestrates cell proliferation, migration and differentiation in human mesenchymal stem cells. *Cell Death Differ* 18, 985-995.

191. Tou, L., Quibria, N., & Alexander, J.M. (2001). Regulation of human cbfa1 gene transcription in osteoblasts by selective estrogen receptor modulators (SERMs). *Molecular and Cellular Endocrinology* 183, 71-79.

192. Towatari, M., May, G.E., Marais, R., Perkins, G.R., Marshall, C.J., Cowley, S., & Enver, T. (1995). Regulation of GATA-2 Phosphorylation by Mitogen-activated Protein Kinase and Interleukin-3. *Journal of Biological Chemistry* 270, 4101-4107.

193. Tremblay, J.J., & Viger, R.S. (1999). Transcription Factor GATA-4 Enhances Müllerian Inhibiting Substance Gene Transcription through a Direct Interaction with the Nuclear Receptor SF-1. *Molecular Endocrinology* 13, 1388-1401.

194. Tsuji, K., Bandyopadhyay, A., Harfe, B.D., Cox, K., Kakar, S., Gerstenfeld, L., Einhorn, T., Tabin, C.J., & Rosen, V. (2006). BMP2 activity, although dispensable for bone formation, is required for the initiation of fracture healing. *Nat Genet* 38, 1424-1429.

195. Undale, A., Fraser, D., Hefferan, T., Kopher, R.A., Herrick, J., Evans, G.L., Li, X., Kakar, S., Hayes, M., Atkinson, E., Yaszemski, M.J., Kaufman, D.S., Westendorf, J.J., & Khosla, S. (2011). Induction of fracture repair by mesenchymal cells derived from human embryonic stem cells or bone marrow. *Journal of Orthopaedic Research* 29, 1804-1811.

196. Ussing, H.H. (1965). Transport of electrolytes and water across epithelia. *Harvey Lect* 59, 1-30.

197. Van Esch, H., Groenen, P., Nesbit, M.A., Schuffenhauer, S., Lichtner, P., Vanderlinden, G., Harding, B., Beetz, R., Bilous, R.W., Holdaway, I., Shaw, N.J., Fryns, J.-P., Van de Ven, W., Thakker, R.V., & Devriendt, K. (2000). GATA3 haplo-insufficiency causes human HDR syndrome. *Nature* 406, 419-422.

198. Vasioukhin, V., Bauer, C., Yin, M., & Fuchs, E. (2000). Directed Actin Polymerization Is the Driving Force for Epithelial Cell–Cell Adhesion. *Cell* 100, 209-219.

199. Verkman, A.S., Hara-Chikuma, M., & Papadopoulos, M.C. (2008). Aquaporins--new players in cancer biology. *J Mol Med (Berl)* 86, 523-529.

200. Von Lüttichau, I., Notohamiprodjo, M., Wechselberger, A., Peters, C., Henger, A., Seliger, C., Djafarzadeh, R., Huss, R., & Nelson, P.J. (2005). Human adult CD34- progenitor cells functionally express the chemokine receptors CCR1, CCR4, CCR7, CXCR5, and CCR10 but not CXCR4. *Stem Cells Dev* 14, 329-336.

201. Wada, H., Hasegawa, K., Morimoto, T., Kakita, T., Yanazume, T., Abe, M., & Sasayama, S. (2002). Calcineurin-GATA-6 pathway is involved in smooth muscle–specific transcription. *The Journal of Cell Biology* 156, 983-991.

202. Wan, C., He, Q., McCaigue, M., Marsh, D., & Li, G. (2006). Nonadherent cell population of human marrow culture is a complementary source of mesenchymal stem cells (MSCs). *Journal of Orthopaedic Research* 24, 21-28.

203. Wan, M., & Cao, X. (2005). BMP signaling in skeletal development. *Biochemical and Biophysical Research Communications* 328, 651-657.

204. Wang, X., Kua, H.-Y., Hu, Y., Guo, K., Zeng, Q., Wu, Q., Ng, H.-H., Karsenty, G., de Crombrugghe, B., Yeh, J., & Li, B. (2006). p53 functions as a negative regulator of osteoblastogenesis, osteoblast-dependent osteoclastogenesis, and bone remodeling. *The Journal of Cell Biology* 172, 115-125.

205. Welch, M.D., & Mullins, R.D. (2002). Cellular control of action nucleation. *Annual Review of Cell and Developmental Biology* 18, 247-288.

206. Wendel, C., Hemping-Bovenkerk, A., Krasnyanska, J., Mees, S.T., Kochetkova, M., Stoeppeler, S., & Haier, J. (2012). CXCR4/CXCL12 participate in extravasation of metastasizing breast cancer cells within the liver in a rat model. *PLoS ONE* 7, e30046.

207. Wexler, S.A., Donaldson, C., Denning-Kendall, P., Rice, C., Bradley, B., & Hows, J.M. (2003). Adult bone marrow is a rich source of human mesenchymal 'stem' cells but umbilical cord and mobilized adult blood are not. *Br J Haematol* 121, 368-374.

208. Williams, J.T., Southerland, S.S., Souza, J., Calcutt, A.F., & Cartledge, R.G. (1999). Cells isolated from adult human skeletal muscle capable of differentiating into multiple mesodermal phenotypes. *Am Surg* 65, 22-26.

209. Wozney, J., Rosen, V., Celeste, A., Mitsock, L., Whitters, M., Kriz, R., Hewick, R., & Wang, E. (1988). Novel regulators of bone formation: molecular clones and activities. *Science* 242, 1528-1534.

210. Wu, X., Suetsugu, S., Cooper, L.A., Takenawa, T., & Guan, J.-L. (2004). Focal adhesion kinase regulation of N-WASP subcellular localization and function. *Journal of Biological Chemistry* 279, 9565-9576.

211. Wynn, R.F., Hart, C.A., Corradi-Perini, C., O'Neill, L., Evans, C.A., Wraith, J.E., Fairbairn, L.J., & Bellantuono, I. (2004). A small proportion of mesenchymal stem cells strongly expresses functionally active CXCR4 receptor capable of promoting migration to bone marrow. *Blood* 104, 2643-2645.

212. Xu, L., Song, C., Ni, M., Meng, F., Xie, H., & Li, G. (2012). Cellular retinol-binding protein 1 (CRBP-1) regulates osteogenenesis and adipogenesis of mesenchymal stem cells through inhibiting RXRα-induced β-catenin degradation. *The International Journal of Biochemistry & Cell Biology* 44, 612-619.

213. Yamagata, T., Mitani, K., Oda, H., Suzuki, T., Honda, H., Asai, T., Maki, K., Nakamoto, T., & Hirai, H. (2000). Acetylation of GATA-3 affects T-cell survival and homing to secondary lymphoid organs. *EMBO J* 19, 4676-4687.

214. Yang, S., & Kim, H.-M. (2012). The RhoA-ROCK-PTEN pathway as a molecular switch for anchorage dependent cell behavior. *Biomaterials* 33, 2902-2915.

215. Ye, L., Fan, Z., Yu, B., Chang, J., Al Hezaimi, K., Zhou, X., Park, N.-H., & Wang, C.-Y. (2012). Histone demethylases KDM4B and KDM6B promotes osteogenic differentiation of human MSCs. *Cell Stem Cell* 11, 50-61.

216. Yoshioka, T., Mishima, H., Ohyabu, Y., Sakai, S., Akaogi, H., Ishii, T., Kojima, H., Tanaka, J., Ochiai, N., & Uemura, T. (2007). Repair of large osteochondral defects with allogeneic cartilaginous aggregates formed from bone marrow-derived cells using RWV bioreactor. *J Orthop Res* 25, 1291 - 1298.

217. Yu, X., Chen, D., Zhang, Y., Wu, X., Huang, Z., Zhou, H., & Zhang, Z. (2012). Overexpression of CXCR4 in mesenchymal stem cells promotes migration, neuroprotection and angiogenesis in a rat model of stroke. *J Neurol Sci* 316, 141-149.

218. Zambotti, A., Makhluf, H., Shen, J., & Ducy, P. (2002). Characterization of an Osteoblast-specific Enhancer Element in the CBFA1 Gene. *Journal of Biological Chemistry* 277, 41497-41506.

219. Zhang, D., Fan, G.-C., Zhou, X., Zhao, T., Pasha, Z., Xu, M., Zhu, Y., Ashraf, M., & Wang, Y. (2008). Over-expression of CXCR4 on mesenchymal stem cells augments myoangiogenesis in the infarcted myocardium. *Journal of Molecular and Cellular Cardiology* 44, 281-292.

220. Zhang, J., Niu, C., Ye, L., Huang, H., He, X., Tong, W.-G., Ross, J., Haug, J., Johnson, T., Feng, J.Q., Harris, S., Wiedemann, L.M., Mishina, Y., & Li, L. (2003). Identification of the haematopoietic stem cell niche and control of the niche size. *Nature* 425, 836-841.

221. Zon, L.I., Youssoufian, H., Mather, C., Lodish, H.F., & Orkin, S.H. (1991). Activation of the erythropoietin receptor promoter by transcription factor GATA-1. *Proceedings of the National Academy of Sciences* 88, 10638-10641.

222. Zuk, P.A., Zhu, M., Mizuno, H., Huang, J., Futrell, J.W., Katz, A.J., Benhaim, P., Lorenz, H.P., & Hedrick, M.H. (2001). Multilineage cells from human adipose tissue: implications for cell-based therapies. *Tissue Eng* 7, 211-228.